École Doctorale
d'Informatique,
Télécommunications
et Électronique de Paris

Thèse

présentée pour obtenir le grade de docteur
de l'École Nationale Supérieure des Télécommunications

Spécialité : **Électronique et Communications**

Ghassan KRAIDY

Coded modulations for the multiple-antenna and cooperative fading channels

Soutenue le 9 Juillet 2007 devant le jury composé de :

Philippe Godlewski	Président
Helmut Bölcskei	Rapporteurs
Raymond Knopp	
Inbar Fijalkow	Examinateurs
Dirk Slock	
Nicolas Gresset	
Joseph Boutros	Directeur de thèse

Acknowledgements

This thesis would not have been possible without the role of key people to whom I am grateful.

First, I would like to thank Prof. Helmut Bölcskei and Prof. Raymond Knopp for thoroughly reviewing this manuscript and for raising concerns that largely helped in improving the quality of the work. I am also grateful to Prof. Philippe Godlewski for accepting to serve as a president of the defense jury, and Prof. Inbar Fijalkow and Prof. Dirk Slock for accepting to be members of the jury.

One person has played a major role in this thesis: Nicolas Gresset. From the beginning till the end, Nicolas has spent hours discussing concepts related to my thesis as well as giving insight onto the various results I reached. His maturity, patience, and pedagogical skills have largely contributed to the stable flow of my doctoral studies.

This whole project would not have been possible without the continuous support and commitment of my thesis supervisor, prof. Joseph Boutros. Always available for discussions, his deep scientific knowledge go together with his valuable qualities as a person. I cannot find the words to express how grateful I am for having worked under his supervision.

I am also thankful to Albert Guillén i Fàbregas for hosting me at the Institute of Telecommunications Research, Mawson Lakes, Australia, in October 2006. My collaboration with Albert triggered the second part of my thesis.

I cannot forget my colleagues with whom I spent precious moments in the lab; my office mates Fatma, Sheng, and Souheil, and my fellows Eric, Maya, Marcia, Daniel, Jo|ão, Ioannis, Sylvain, Amira, Qing, Yang, Sami, Korinna, Judson, Rodrigo, David. Thank you all for making my experience at Telecom Paris full of memories.

My local support during my studies was carried out by Tony and my brother Ziad who were always there to motivate me. My brother Marwan was always a phone call away to make me feel by his side. I am very thankful to Astrid who shared my moments of frustration as well as my moments of joy, and who always found the words to help me advance in this project.

Finally, I would like to dedicate this thesis to my parents who did everything, from support to sacrifices, to help me achieve my goals,

For Aïda and Michel

Abstract

This thesis deals with the design of coded modulations for block fading channels with iterative detection and decoding. First, the design of coded modulations for multiple antenna fading channels is discussed. The design consists of choosing a space-time precoding matrix that minimizes the discrete-input outage probability for such systems, while taking into account several parameters that make it suitable for optimized iterative decoding. To conclude this part, the design of turbo codes for multiple-antenna fading systems is proposed based on channel multiplexers. Introducing no additional complexity at the receiver end, these mutliplexers allow to achieve full diversity and high coding gains. Second, coded modulations for cooperative fading channels is proposed, in which relays transmit sequentially to each others. Bounds on the achievable diversity orders are derived, and space-time transmission strategies are proposed to achieve optimal performance. Finally, the design of irregular turbo codes for block-fading channels is presented. Based on the density evolution method, degree profiles that perform very close to the fundamental limits are proposed.

Contents

List of Figures

List of Tables

Résumé de la thèse en Français

Introduction

Depuis une dizaine d'années, les applications de réseaux sans-fil sont devenues très populaires. Ces applications permettent de trouver de nouvelles opportunités au systèmes de communications qui n'étaient pas présentes auparavant. Par contre, de part la nature du canal sans-fil, des effets comme l'évanouissement du signal, l'ombrage et l'interference d'autres transmetteurs font que la qualité de la propagation du signal fluctue durant la transmission. Une approche permettant de combattre ces fluctuations est la conception de systèmes de communication qui assure la diversité du signal en envoyant plusieurs copies du meme signal. La diversité du signal peut se faire dans le temps, l'espace, ou la fréquence. Les systèmes à antennes multiples sont connus pour assurer la diversité spatiale tout en améliorant la capacité d'un système. Cependant, pour des raisons de taille d'un mobile ou de prix, il n'est pas possible d'implémenter plusieurs antennes. Pour cette raison, plusieurs groupes de recherche se sont recemment penchés sur les systèmes de transmission coopératifs, ou des mobiles s'entraident pour envoyer leur information à une station de base. Ceci leur permet de profiter de la diversité spatiale et de transmettre à des débits plus élevés.
Dans cette thèse, des systèmes de modulations codées avec précodage spatio-temporel sont etudiées pour des canaux à évanouissements par blocs sélectifs en fréquence:

- Dans le Chapitre 2, les limites théoriques des canaux à évanouissements par blocs sélectifs en fréquence sont introduites, notamment la probabilité de coupure. Ces concepts seront utilisés dans les chapitres suivant de la thèse. Les modulations codées avec précodage spatio-temporel sont ensuite introduites ainsi que le récepteur itératif qui permet d'atteindre de très bonnes performances a complexité réduite. La fin de ce chapitre est dediée à la borne de Singleton sur l«ordre de diversité qu«une modulation codée peut atteindre sur un canal à évanouissements par blocs.

- Le Chapitre 3 couvre les modulations codées avec précodage spatio-temporel pour

les systèmes à antennes multiples avec décodage itératif. Nous commencons par concevoir des matrices de précodage spatio-temporel qui minimizent la probabilité de coupure à entrée discrète, et nous démontrons les bonnes performances de ces précodeurs dès la première itération du récepteur. Nous considérons par la suite un schema pour quatre antennes en emission basé sur le code d«Alamouti. Nous concluons ce chapitre par la conception de turbo codes pour les canaux á antennes multiples basés sur le multiplexage de canal. Ces codes démontrent des performances à 1 dB de la probabilité de coupure.

- Le Chapitre 4 est dedié à la conception de modulations codées avec précodage spatio-temporel pour un canal coopératif à plusieurs utilisateurs. Des bornes sur la diversité de ce système sont d'abord calculées, et il est demontré que l'introduction d'une matrice de précodage spatio-temporel ne mène à aucune augmentation de la complexité. Des résultats de simulations qui montrent d'importants gains de codage sont ensuite montrées, et la conception de turbo codes pour ce type de canaux conclue ce chapitre.

- Le dernier chapitre de cette thèse montre la conception de turbo codes irreguliers pour les canaux à évanouissements par blocs. En utilisant la méthode de l'évolution de densité, il est démontré que ces codes surclassent les codes à matrices de parité à faible densité (LDPC). En adaptant les multiplexeurs de canal des turbo codes réguliers, ces codes montrent des performances à une moitié de dB de la probabilité de coupure sur un canal à évanouissements par blocs.

La conclusion de ce manuscrit contient les remarques sur les résultats ainsi que les perspectives pour de futures extensions des travaux de ce chapitre, comme notamment un système coopératif où les terminaux sont equippés de plusieurs antennes.

Chapitre 1: Notions de théorie de l'information

Afin de concevoir des modulations codées à précodage spatio-temporel pour les canaux à évanouissements par blocs à antennes multiples ou coopératifs, il s'avère important d'établir les limites theoriques de ces canaux. Pour les canaux bruités en général, Claude Shannon a établi la notion de capacité, qui represente le debit maximal qu'un canal peut soutenir tout en ayant des probabilités d'erreurs négligeables au niveau du récepteur. Cette capacité est donnée par la valeure maximale de l'information mutuelle entre l'entrée et la sortie du canal donnée par une certaine distribution de l'entrée. Pour les canaux à évanouissements, pour calculer la capacité du canal, on distingue deux cas; 1) les évanouissements varient rapidement, définissant un canal ergodique et 2) les évanouissements varient lentement avec le temps, définissant un canal non-ergodique. Dans le premier cas, la limite fondamentale du taux de transmission est donnée par la capacité ergodique du canal, donnée par la moyenne statistique de la capacité avec entrée de canal Gaussienne sur toutes les valeurs des réalisations de l'évanouissement. Dans le deuxième cas, la limite fondamentale est la probabilité de coupure du canal, qui est la probabilité que l'information mutuelle entre l'entrée Gaussienne et la sortie du canal tombe en dessous du rendement de transmission requis. Nous présentons ensuite la probabilité de coupure à entrée discrète qui sera utilisée dans le prochain chapitre afin d'optimiser les matrices de précodage spatio-temporel.
Dans la deuxieme partie de ce chapitre, le concept de modulations codées à décodage itératif est présenté, schéma qui sera utilisé dans la partie restante de ce manuscrit. Dans ce schéma, l'émetteur consiste en un code correcteur d'erreurs, un entrelaceur qui assure l'independance probabilistique au niveau du décodeur, un modulateur, puis finalement en un précodeur spatio-temporel. Le domaine du codage correcteur d'erreurs a été très actif pendant plusieurs décennies, ce qui a donné des codes adaptés à plusieurs conditions de transmision; les code binaires puissants à décodage à faible complexité (codes convolutifs, turbo codes, codes à matrice de parité à faible densité (low density parity-check codes)...) et les codes non-binaires capables de corriger des erreurs en blocs (Reed-Solomon, BCH...). Dans le contexte des transmissions sans-fil, les codes binaires cités ci-dessous sont recommandés pour leur décodage itératif à faible complexité. Pour cette raison les codes convolutifs et les turbo codes on été choisis dans cette thèse. L'entrelaceur, dont le role est de mélanger les bits à la sortie du codeur, joue un role très important sur les canaux à évanouissements par blocs, comme ils permettent de placer les bits d'un évènement d'erreurs sur les différents canaux. Le modulateur, type "Phase Shift-Keying" (PSK) ou "Quadrature Amplitude Modulation" (QAM), permet de grouper plusieurs bits en un symbole. Le bloc principal qui perment d'atteindre de hauts debits de transmis-

sion est le modulateur comme il peut implémenter de larges constellations (ex.: 64-QAM ou plus). Le dernier bloc avant transmission est le précodeur spatio-temporel, qui joue un role majeur dans les performances sur les canaux à évanouissements. Les précodeurs sont généralement classés en deux catégories: 1) les précodeurs orthogonaux (Alamouti, Tarokh...) qui permettent d'atteindre des ordres élevés de diversité tout en minimizant l'interférence entre les différents canaux, et 2) Les précodeurs algébriques qui permettent d'atteindre de bon compromis diversité-débit de transmission. La conception de ce type de précodeurs sera largement traitée dans cette these. Au niveau du récepteur, un décodeur itératif basé sur un démodulateur fournissant des probabilités *a posteriori* sur les bits reçus et un décodeur de canal de type "Forward-Backward" sera consideré. Ce type de récepteurs permet d'avoir les meilleures performances possibles dans le cas itératif.
Dans la dernière partie de ce chapitre, la borne de Singleton sur l'ordre de diversité maximal qu'une modulation codée peut atteindre sur un canal à évanouissements par blocs est presentée. Cette borne, qui peut être atteinte sous la seule condition d'un entrelacement optimal, est une fonction du taux de codage et du nombre de blocs de canal sur lesquels le code est transmis. Cette borne permettra par la suite de concevoir des modulations codées optimales en terme de diversité.

Chapitre 2: Modulations codées pour les systèmes à antennes multiples

Ce chapitre présente les résultats de la première moitié de la thèse consistant en la conception de divers schémas de modulations codées pour les canaux à antennes multiples. Nous commençons par un aperçu historique des codes spatio-temporels qui ont permis aux systèmes à antennes multiples d'atteindre de solides performances. La première famille de codes spatio-temporels est la famille des codes orthogonaux qui permettent, de par leur structure, de supprimer toute - ou une partie de - l'interférence au niveau du récepteur. En partant du fameux code d'Alamouti conçu pour deux antennes et qui est parfaitement orthogonal, d'autres codes ont été proposé pour des terminaux ayant plus d'antennes. Cette généralisation s'est faite aux dépens du rendement du code, comme il a été prouvé qu'aucun code orthogonal n'existe pour des schémas de plus que deux antennes en émission. La deuxième famille de codes spatio-temporels est la famille des codes algébriques: permettant d'atteindre des rendements supérieurs aux codes orthogonaux, ces codes ont par contre une complexité de décodage plus élevée. Un bon exemple de ces codes est le "Golden Code" conçu pour deux antennes en émission et qui permet d'atteindre les bornes du compromis diversité-multiplexage. En présence d'un code correcteur d'erreurs, le gain de codage d'une modulation codée émise sur un canal à antennes multiples est largement dû au code lui-même. Ceci signifie que le rôle du précodeur spatio-temporel n'est plus le même que dans le cas non-codé. En effet, il a été démontré que dans le cas d'une modulation codée, la matrice de précodage spatio-temporel doit avoir deux propriétés pour assurer un décodage itératif optimal, qui sont les suivantes:

- Les sous-parties d'une ligne donnée de la matrice doivent avoir la même norme.
- Les sous-parties d'une ligne donnée de la matrice doivent être orthogonales.

Ces propriétés seront donc les bases de la conception de matrices de précodage spatio-temporel dans cette thèse. Nous enchaînons par la suite avec un calcul démontrant que le taux d'erreur par trame d'un système de transmission non-codé augmente logarithmiquement avec la taille de la trame. Ce comportement a aussi été observé avec des modulations codées basées sur des codes convolutifs.
La deuxième partie de ce chapitre consiste en la conception de matrices de précodage spatio-temporel pour les modulations codées transmises sur des canaux à antennes multiples, où l'évanouissement varie par blocs. Nous commençons cette partie par un rappel de l'ordre de diversité qu'une modulation codée transmise sur un canal à évanouissements par blocs et à antennes multiples peut atteindre: cet ordre dépend du nombre d'antennes en émission, en réception, du rendement du code, et du paramètre d'étalage de la matrice

de précodage spatio-temporel. Comme expliqué dans le chapitre précédent, la limite fondamentale de transmission sur un canal à évanouissements par blocs est la probabilité de coupure, qui consiste ne le fair que certaines "mauvaises" réalisations du canal peuvent causer l'information mutuelle du canal à chuter en dessous du taux de transmission désiré. Dans la plupart des travaux de conception de systèmes de communications pour ces types de canaux, la probabilité de coupure à entrée Gaussienne du canal est considérée. Cette hypothèse suppose qu'un code optimal est utilisé, et donc s'éloigne du cas pratique qui est la modulation codée. Pour un canal à entrée discrète, qui est le vrai canal vu par une modulation codée, l'équation de la probabilité de coupure est bien différente de celle pour une entrée Gaussienne, et elle est bien évidemment supérieure à l'optimale. Pour cette raison, nous avons considéré la combinaison des symboles modulés et de la matrice de précodage spatio-temporel comme une modulation multi-dimensionelle à l'entrée du canal, et le choix de la matrice de précodage est celui qui minimize la valeur de la probabilité de coupure à entrée discrète pour un rapport signal sur bruit donné. Cette méthode s'est avérée efficace comme les matrices obtenues pour différents schémas d'antennes en émission ont mené à des performances plus que satisfaisantes.

La troisième de ce chapitre consiste en la conception d'une modulation codées pour un émetteur à quatre antennes basé sur le code spatio-temporel orthogonal d'Alamouti, initialement conçu pour un émetteur à deux antennes. L'idée est convertir un symbol modulé du schéma initial en une matrice de précodage s'appliquant sur quatre symboles modulés transmis sur un groupe de deux antennes et sur deux temps de symbole. Comme le produit matriciel n'est pas commutatif, le fait d'utiliser les opérations de découplage au niveau du détecteur ne permettent pas de supprimer la totalité de l'interférence (comme dans le cas de deux antennes en émission). Ceci ne représente aucun probléme, comme le décodeur itératif, et après quelques itérations, parvient à supprimer l'interférence résiduelle et donc d'atteindre de bonnes performances.

La dernière partie de ce chapitre consiste en la conception de modulations codées basées sur des turbo codes pour les canaux à évanouissements par blocs. Cette famille de codes, connue pour approcher les limites de Shannon pour différents types de canaux, est utilisée dans plusieurs standards de communications sans-fil. Sur un canal à évanouissements par blocs, le but est de concevoir un schéma de codage qui permet d'atteindre la diversité maximale du canal, et de s'assurer que le gain de codage est optimal. En la présence de turbo codes, ceci est possible grâce à l'utilisation de multiplexeurs qui distribuent les bits codés sur les différents blocs du canal. Le premier type de multiplexeurs est le multiplexeur horizontal, qui envoie toujours le même bit à la sortie du codeur sur la même antenne: il permet d'atteindre la diversité maximale, mais par contre il a un gain de codage faible, comme les bits correspondant à un évènement d'erreurs sont mal distribués sur les blocs

d'évanouissement. Le deuxième types est le multiplexeur dit "h-π-diagonal" qui permet d'atteindre la diversité maximale est en plus d'atteindre de gain de codage élevé. Ceci est dû au fait que les bits correspondant à un évènement d'erreurs sont distribués de façon homogène sur les blocs d'évanouissement.

Chapitre 3: Modulations codées pour les systèmes coopératifs

La conception de modulations codées pour les canaux coopératifs à évanouissements est présentée dans ce chapitre. Les schémas de coopération inter-terminaux a récemment gagné en popularité due au fait que l'installation de plusieurs antennes sur des terminaux de petite taille est impossible comme la séparation entre les antennes doit être de l'ordre de la moitié de la longueur d'onde. Pour cette raison, des terminaux peuvent coopérer entre eux avant de transmettre à une destination dans le but d'augmenter la capacité et d'atteindre des ordres de diversité plus élevés. Les protocoles de coopération consistent en deux types: 1) "Amplifies-et-retransmets" (Amplify-and-Forward) et 2) "Décodes-et-retransmets" (Decode-and-Forward). Le premier consiste à ce que le rôle du terminal agissant comme relais amplifies le signal reçu par la source et retransmets à la destination. Le deuxième consiste à décoder le message reçu par la source, le coder, et puis le retransmettre à la destination.
Dans ce chapitre, le canal "Slotted Amplify-and-Forward" est considéré, qui consiste à ce que les relais retransmettent à tour de rôle à la destination ainsi qu'au prochain relais. Le canal généré par ce protocole est appelé "canal à évanouissements par blocs Matryoshka" comme l'ordre de diversité d'un symbole donné decroît au fur et à mesure qu'on avance dans la trame de transmission, ce qui fait allusion aux fameuses poupées russes qui sont imbriquées l'une dans l'autre. En effet, le degré maximal atteint par le premier symbole transmis est donné par le nombre de relais plus un (donné par le lien direct source-destination), alors que le degré minimal donné par le dernier symbole émis est de un, comme ce symbole est juste transmis sur le lien direct source-destination. Basé sur ce canal, la conception de modulations codées avec précodage spatio-temporel est introduite. Une borne de Singleton sur le l'ordre de diversité que peut atteindre une modulation codée est dérivée en fonction du nombre de relais, du rendement du code correcteur d'erreurs, et du facteur d'étalement de la matrice de précodage spatio-temporel. Il est important de noter que, à l'opposé des canaux à antennes multiples, l'étalement n'est pas toujours nécessaire pour les canaux coopératifs, ce qui permet de réduire de façon drastique la complexité au niveau de la destination.
Dans la deuxième partie de ce chapitre, la conception de modulations codées à base de turbo codes est proposée pour un canal "amplify-and-forward" à un relais. Comme il a été démontré dans le chapitre précédent, placer des multiplexeurs à la sortie du turbo code permettent d'atteindre la diversité maximale du canal ainsi que d'obtenir de bons gains de codage. Par contre, à l'opposé des canaux à antennes multiples, le multiplexage horizontal permet d'obtenir de meilleurs performances comparé au multiplexeur "h-π-diagonal"

sur un canal coopératif. Ceci est dû au fait que les bits d'information sont toujours émis au début de la trame de transmission, ce qui leur permet d'atteindre le maximum de diversité en étant systématiquement relayés. Par contre, le multiplexeur "h-π-diagonal" alterne les bits d'information et les bits de parité en première position, ce qui a comme effet de dégrader le gain de codage.

Chapitre 4: Conception de turbo codes irréguliers pour les canaux à évanouissements par blocs

Dans ce dernier chapitre, la conception de turbo codes irréguliers pour les canaux à évanouissements par blocs est présentée. Les turbo codes parallèles proposés initialement consistent en deux codes convolutifs récursifs sytématiques séparés par un entrelaceur. Ces codes sont parmis les plus puissants comme ils permettent d'approcher la limite de Shannon pour différents types de canaux. Du point de vue du graphe du code, chaque bit d'information a un degré de deux, comme il est lié aux deux codes constituants. Dans un but d'améliorer les performances des turbo codes, il est possible de créer une irrégularité de degré à travers les bits d' information du code, méthode qui a fait ses preuves avec notamment les codes à matrice de parité à faible densité, ou "low density parity-check (LDPC) codes". Pour ce faire, il faut modifier la structure du code: au lieu de codes constituants en parallèle séparés par un entrelaceur, un répétiteur de bits est placé avant l'entrelaceur, qui est à son tour suivi d'un seul code constituant. Dans ce cas, si la répétition est régulière de degré deux, les code sera exactement comme le turbo code parallèle initial. Par contre, en variant le degré de répétition des bits d'information, on crée une irrégularité qui pourra améliorer la performance du code. Il est à noter que plus les bits sont répétés à l'entrée du code convolutifs, plus il faut perforer les bits de parité à la sortie du codeur, de façon à ne pas affecter le rendement de codage. La conception de turbo codes irréguliers consiste donc à trouver le profil de degrés des bits d'information qui permet de donner les meilleures performances sur un canal donné pour un rendement donné. Cette recherche de profil se fait en général à travers la méthode de l'évolution de densité, qui sera expliquée par la suite.
Pour ce qui est de la conception de turbo codes irréguliers pour les canaux à évanouissements par blocs, le processus consiste en deux étapes:

- S'assurer que le code atteint la borne de Singleton sur l'ordre de diversité
- Trouver le profil de degrés qui a le meilleur seuil de décodage sur le canal à bruit additif blanc Gaussien, ce qui permet d'assurer un gain de codage optimal sur le canal à évanouissements par blocs

Pour la premiére étape, c'est-à-dire pour atteindre la diversité maximale du canal, il suffit d'utiliser les multiplexeurs décrits précédement (horizontal et h-*pi*-diagonal). Pour la deuxième étape, la méthode de l'évolution de densité est utilisée: on considère un mot de code infini, et on traque l'évolution de la densité de probabilité à la sortie du décodeur à chaque itération de décodage, ce qui permet de savoir si le processus de décodage converge, c'est-à-dire si la probabilité d'erreurs par bit tend vers zero pour un

rapport signal-sur-bruit donné. En appliquant cette méthode, la valeur minimale (ou seuil) du rapport signal-sur-bruit pour laquelle le décodeur converge est révélée. Une autre méthode, appelée “approximation Gaussienne”, consiste à simuler une distribution Gaussienne à l’entrée du code, tout en traquant l’évolution à la sortie du code. En utilisant ces méthodes, un turbo code irrégulier avec un multiplexeur h-*pi*-diagonal atteint un taux d’erreurs par trame de moins d’une moitié de decibel de la probabilité de coupure du canal à évanouissements par blocs, ce qui représente les meilleures performances jamais atteintes sur ce type de canaux.

Introduction

Over the past few years, wireless networks applications have gained ever-increasing popularity. They provide novel opportunities for increased reliability that are non-existent in point to point communications. However, due to the nature of the wireless channel, effects such as fading, shadowing, and interference from other transmitters can cause the channel quality to fluctuate during transmission. One approach to combat such channel fluctuations is to design a communication system that provides some sort of diversity, i.e. provides many replicas of the signal to the receiver. Diversity can be temporal, spatial, or frequential [1]. Multiple-antenna systems (also called Multiple-Input Multiple-Ouput (MIMO) systems)have been shown to provide spatial diversity that boosts the performance in fading environments. In addition, the need to transmit at high data rates is fulfilled with such systems as they allow the simultaneous transmission of multiple streams (spatial multiplexing). However, in some cases, due to space or cost limitations, the implementation of more than one antenna on the same terminal is impossible. For this reason, the concept of cooperative communications was proposed, which means that terminals can cooperate between each others to provide spatial diversity in a distributed configuration, thus forming a virtual antenna array.
In this report, we study the design of space-time bit-interleaved coded modulations (ST-BICM) suited for frequency non-selective single-user block-fading channels. The outline of the manuscript is as follows:

- In Chapter 2, we first introduce the fundamental information theoretical limits of block-fading channels in general (namely the outage probability), limits that are used throughout the report for the analysis of coded modulations. We then describe the ST-BICM transmitter model, before describing the iterative receiver that can lead to quasi-maximum likelihood (ML) performance with reasonably low complexity. We end up this chapter by recalling the Singleton bound on the diversity order of coded systems for a given coding rate.

- In Chapter 3, we propose ST-BICM schemes suited for the multiple-input multiple-output (MIMO) channel with iterative decoding. First, we design space-time pre-

coding matrices that minimize the discrete input outage probability, and we show the good performance of these precoders since the first iteration of an iterative receiver. Second, we investigate a low-complexity coded scheme for a four-transmit antenna configuration based on the Alamouti scheme. Finally, we propose the design of turbo codes for MIMO channels, and we will show that this scheme dramatically approaches the outage probability limit with relatively low decoding complexity using intelligent switches (called "code multiplexers") at the output of the turbo encoder.

- In Chapter 4, the design of ST-BICM for the amplify-and-forward cooperative protocol with multiple relays is considered. We derive bounds on the diversity order for this protocol, and we show that precoders that do not entail an increase in the detection complexity are optimal diversity-wise. We next discuss coding gain issues for this protocol, and show simulation results for various coding rates and network configurations. We finally show the performance of code multiplexers with turbo codes over this protocol.

- In Chapter 5, in a goal to achieve optimal coding gain over block-fading channels, a new method for the design of irregular turbo codes is proposed. We first show that irregular turbo codes outperform LDPC codes for the AWGN channel, and then we show they outperform the regular turbo codes on block-fading channels using density evolution methods.

We end up this manuscript by the concluding remarks and some future perspectives.

Chapter 1

Generalities

1.1 Introduction

In this manuscript, we deal with wireless block-fading channels, that were introduced in [2] to model slowly varying fading channels. In this model, a frame (or a codeword) sent over the wireless channel sees a fixed number of fading coefficients. Standards such as Global System for Mobile Communications (GSM) or the promising Orthogonal Frequency Division Multiplexing (OFDM) that involve slow time-frequency hopping are well represented by this channel model. The block-fading channel model leads to a null capacity, as the capacity depends on the instantaneous channel instance. In this chapter, we will start by introducing the information theoretical limit of block-fading channels, that is outage probability. We will then present the general communication system we will use throughout this report; a transmitter consisting of a space-time precoded coded modulation, and a receiver consisting of an iterative detection and decoding blocks. The last part of this chapter presents the bound on the diversity order of coded systems on block-fading channels.

1.2 Information theory of fading channels

Back in 1948, Claude E. Shannon established the definition of channel capacity through the noisy-channel coding theorem [3] as the maximum theoretical rate at which we can reliably transmit data (i.e. with a vanishing error rate) over a channel with a specified bandwidth and at a particular noise level. Channel capacity is a deterministic bound that takes different expressions depending on the channel type. Now suppose that the input and the output of the channel are given by the two random variables X and Y

respectively. The channel capacity is by definition given by:

$$C = \max_{p(x)} \mathcal{I}(X;Y) \tag{1.1}$$

where $p(x)$ is the input distribution and the mutual information $\mathcal{I}(X;Y)$ between X and Y is given by:

$$\mathcal{I}(X;Y) = H(X) + H(Y) - H(Y,X) = H(Y) - H(Y/X) = H(X) - H(X/Y) \tag{1.2}$$

and the entropy function H gives the average amount of bits one needs to represent a random process. For the additive white Gaussian noise (AWGN) channel for instance, the channel capacity for a Gaussian input is given by:

$$C_{AWGN} = \log_2\left(1 + R\frac{E_b}{N_0}\right) \text{ bits/s/Hz} \tag{1.3}$$

It is thus possible to reliably transmit information on an AWGN channel at a rate $R < C_{AWGN}$ through an infinite length codeword. Now for wireless channels, the channel input-output model is given by:

$$\mathbf{y} = \mathbf{x}\mathbf{H} + \mathbf{w} \tag{1.4}$$

where $\mathbf{x}$ is the input vector, $\mathbf{y}$ is the output vector, $\mathbf{H}$ is the channel matrix with complex Gaussian fading coefficients, and $\mathbf{w}$ is the AWGN vector. In the presence of ergodic Rayleigh fading, it was shown in [4] [5] that the channel capacity for a Gaussian input without side information at the transmitter is given by:

$$C = \mathbb{E}_H\left[C_H\right] = \mathbb{E}_H\left[\log_2 \det\left(I + \mathcal{P}\mathbf{H}^\dagger\mathbf{H}\right)\right] \tag{1.5}$$

where $\mathcal{P}$ is a function of the signal-to-noise ratio. For single-antenna quasi-static fading channels, $\mathbf{H} = h$ has a single entry. For multiple-antenna and amplify-and-forward cooperative channels, the complex channel matrix $\mathbf{H}$ takes different forms that will be discussed in the next chapters. Now as the channel gain process is ergodic, i.e. the time average is equal to the ensemble average, the channel changes at each realization. In other words, the randomness of the channel coefficients can be averaged out (removed) over time as shown in (1.5). This results in the fact that the capacity of an ergodic channel is information stable as it tends to a deterministic value and long-term constant bit rates can be supported.

Now for non-ergodic fading channels, the channel gain is a random variable and does not change with time (at least for the duration of a codeword). The channel gain process is stationary but not ergodic, i.e. the time average is not equal to the ensemble average. This means that certain "weak" realizations of the channel coefficients can cause the capacity of

the channel to fall below the transmission rate we want to maintain. Non-ergodic channels are information unstable [6] as channel capacity is not deterministic. The expression for the channel capacity is a random variable with probability density function $p_{C_H}(i)$ that defines the "outage" probability [2][7]:

$$P_o = P\left(C_H < R\right) = \int_0^R p_{C_H}(i)di \tag{1.6}$$

For block-fading channels, we suppose that a codeword sees n_c different realizations of the channel matrix, and this gives the following expression for the Gaussian input outage probability:

$$P_{o,n_c} = P\left(\frac{1}{n_c}\sum_{j=1}^{n_c}\log_2\det\left(I+\mathcal{P}\mathbf{H}_j^{\dagger}\mathbf{H}_j\right) < \ R\right) \tag{1.7}$$

Note that when $D \to \infty$, the averaging over the channel realizations leads to the ergodic channel capacity as in (1.5). It is clear that area under the tail of the capacity given the channel distribution $p_{C_H}(i)$ in (1.6) is a cumulative distribution function $F_I(R)$. The outage capacity can be seen as the ϵ-capacity [6] [8] [9] of the channel as:

$$C_\epsilon = \sup_{p(x)} \ \sup \ \{R : F_I(R) \leq \epsilon\} \ \ 0 \leq \epsilon \leq 1 \tag{1.8}$$

The ϵ-capacity C_ϵ is the optimum asymptotic rate at which information can be encoded over the channel via a sequence of channel codes that yield a maximal probability of decoding error of ϵ. Note that:

$$C_{\epsilon\downarrow 0} = C \tag{1.9}$$

which gives the Shannon capacity. The ϵ-capacity approach for outage capacity suits the convention of "x percent outage" followed by certain papers (see [10] for example). However, in this report, we will use the outage measure as a probability as in (1.6) to be able to compare it with word error rate performance of coded modulations.
As proved in [4], maximum capacity over ergodic fading channels (consequently minimum outage probability over block-fading channels) is achieved with Gaussian inputs, i.e. when $p(x)$ follows the normal distribution. However, with practical communication systems, we always deal with discrete input constellations. For this reason, the expression in (1.5) for Gaussian inputs does not hold anymore. From (1.2), we have:

$$\mathcal{I}(X;Y) = H(Y) - H(Y/X) \tag{1.10}$$

Now let $X \in \Omega$, a discrete alphabet of 2^n vectors. The entropies from (1.10) can be expressed as [11]:

$$\begin{aligned} H(Y) &= -\int_y p(y) log_2(p(y)) dy \\ &= -\int_y \sum_x p(y/x)p(x) log_2 \left(\sum_{x'} p(y/x')p(x') \right) dy \qquad (1.11) \\ H(Y/X) &= -\sum_x p(x) \int_y p(y/x) log_2(p(y/x)) dy \qquad (1.12) \end{aligned}$$

This gives the expression of the mutual information as:

$$\begin{aligned} \mathcal{I}_H &= n - \frac{1}{2^n} \sum_x \int_y p(y/x) log_2 (\frac{\sum_{x'} p(y/x')}{p(y/x)}) dy \qquad (1.13) \\ &= n - \frac{1}{n_c} \sum_{j=1}^{n_c} \mathbb{E}_{\mathbf{x},\mathbf{y}|\mathbf{H}_j} \left[\log_2 \left(\frac{\sum_{\mathbf{x}'} p(\mathbf{y}|\mathbf{x}', \mathbf{H}_j)}{p(\mathbf{y}|\mathbf{x}, \mathbf{H}_j)} \right) \right] \qquad (1.14) \end{aligned}$$

Fig. 1.1 shows the outage probabilities of a quasi-static fading channel for different inputs and half-rate channel coding. As mentioned earlier, Gaussian inputs outperform all other distributions at the same spectral efficiency. We also notice that with half-rate coding, the 16-QAM constellation outage probability is closer to the Gaussian input outage probability than the BPSK modulation. As the outage probability reflects the variations of the mutual information function depending on the channel realizations, this behavior is explained by the fact that the mutual information curve of the 16-QAM constellation at half-rate coding is closer to the Gaussian mutual information line than the BPSK constellation at the same coding rate (see [12, Fig. 2]). Fig. 1.2 shows the outage probabilities for different MIMO channel antenna configurations, half-rate channel coding and Gaussian input. The diversity order is given by $n_t \times n_r$, but the coding gain differs for the same diversity order depending on the configuration.

1.3 Bit-interleaved coded modulation (BICM) with iterative decoding

In 1992, it was shown in [13] that by cascading an error correcting code, a random interleaver and a modulator, a communication system achieves very high gains. Later,

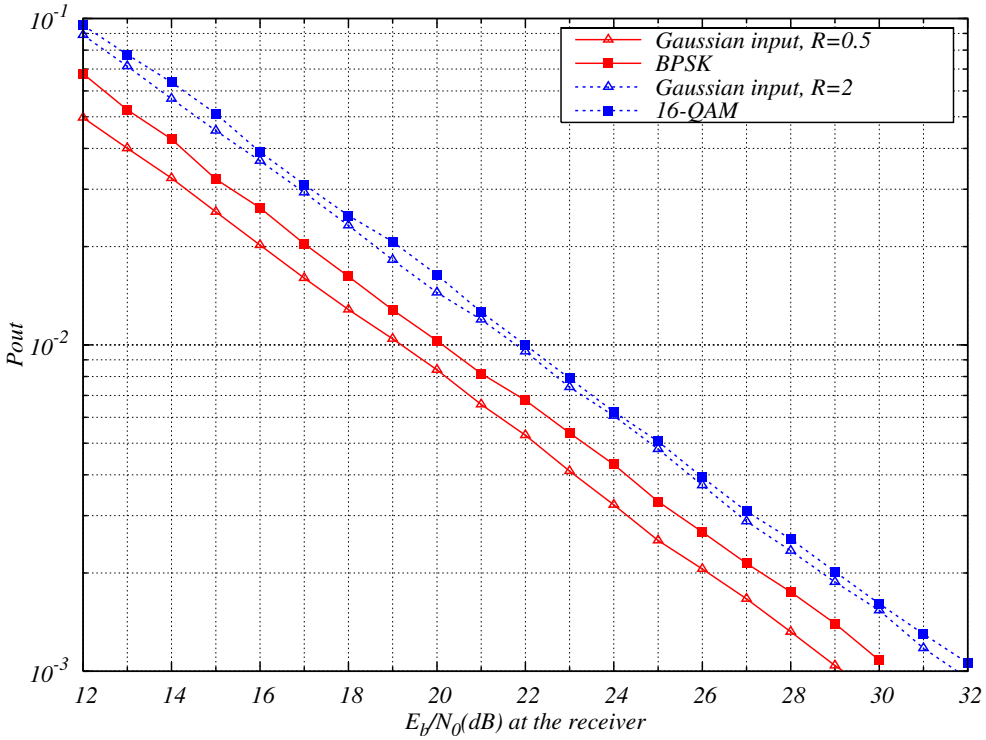

Figure 1.1: Outage limits for quasi-static channel, BPSK, 16QAM, and Gaussian input, half-rate channel coding.

the authors in [14] established a framework for the analysis and design of the so-called "Bit-interleaved coded modulation" (BICM), and showed that this structure allows to approach the information theoretical limits of the channel, for the AWGN case as well as for the ergodic fading case. Since then, this structure has been widely studied for different scenarios. In [15] [16] [17] among others, the authors studied BICM for non-ergodic fading channels, and it was proved that this scheme can also approach the outage limit of the channel. In this report, the BICM model for block-fading channels (i.e. non-ergodic channels) will be considered.

1.3.1 Structure of the BICM transmitter

The general structure of a BICM is shown in Fig. 1.3. It consists of an error correcting code $\mathcal{C}$ of rate R_c, a deterministic interleaver Π, a symbol mapper, and a space-time precoder. We will now describe each block and give historical notes and classifications that justify our choices.

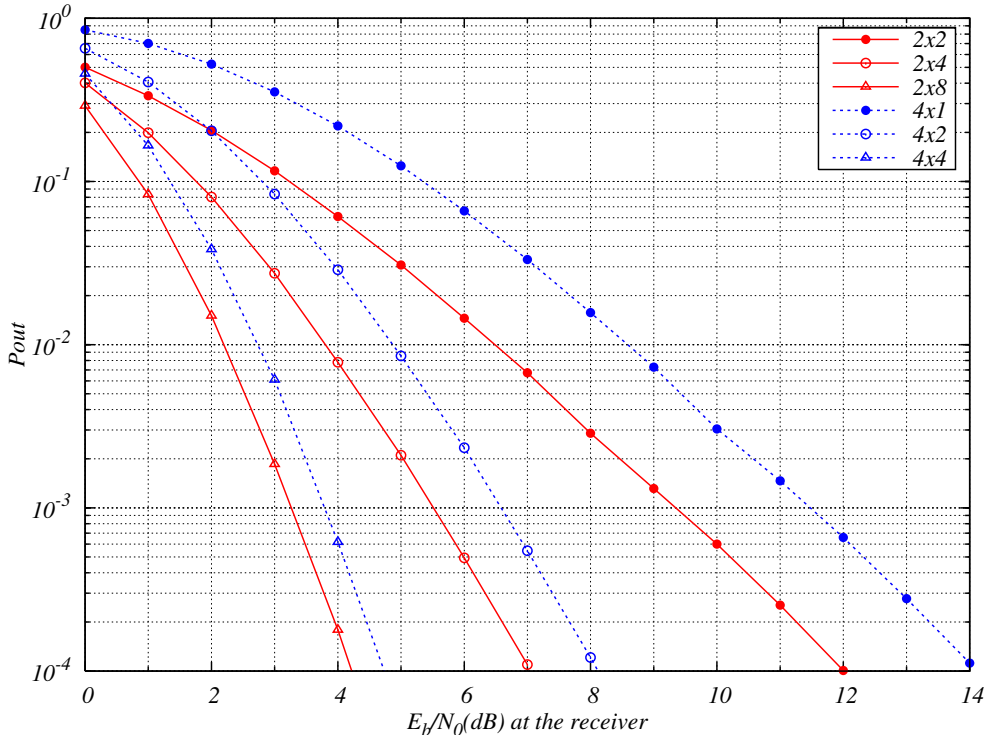

Figure 1.2: Outage limits for different MIMO configurations, Gaussian input, half-rate channel coding.

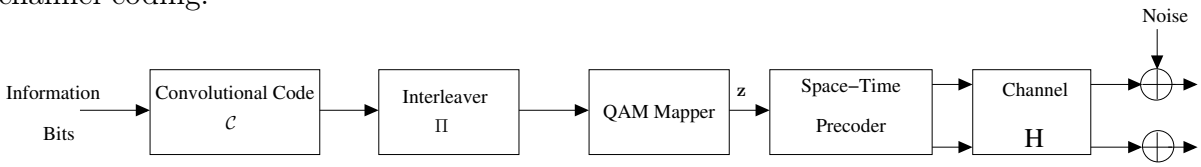

Figure 1.3: ST-BICM transmitter scheme.

The error correcting code

The field of channel coding started with Shannon's landmark paper in 1948 [3]. The idea is to protect data sent through a channel by adding some redundancy to the transmitted signal in way to ensure reliable communication. The encoder is a bijection between the information sequence $\mathbf{b}$ of length K and the coded sequence $\mathbf{c}$ of length N. The coding rate is $R_c = K/N$. There are different types of error correcting codes, and they can be classified into two major categories [18]:

- Algebraic linear block codes: Hamming, Golay, Reed-Muller, BCH, and Reed-Solomon codes among others. Algebraic coding theory dominated the first decades of channel coding history. The main objective of this design theory is to maximize

the minimum distance d (also called Hamming distance (d_{min})) between any two distinct codewords, that is the minimum number of bits in which they differ. They are mostly used for high data rates, but fail to approach fundamental limits. In particular, Reed-Solomon codes are efficient in applications that suffer from bursty errors, such as magnetic tape and disk storage for instance. They can provide high error-correction power with relatively small redundancy at very high data rates.

- Probabilistic codes: in [18], it is stated that "*probabilistic coding is more concerned with finding classes of codes that optimize average performance as a function of coding and decoding complexity*". This class includes convolutional codes, product codes, concatenated codes, and trellis decoding of block codes. Convolutional codes were invented in [19]. They can be grouped into two major categories: non-recursive non-systematic convolutional (NRNSC) codes, where all information bits are encoded through shift registers, and recursive systematic convolutional (RSC) where the uncoded information sequence is sent through the channel and at the same time is encoded through a feedback register. As a result, the code can be represented by a trellis, which allows for low complexity decoders. Although they have infinite length, convolutional codewords can be made finite by proper trellis termination. In this report, we will mainly use NRNSC codes with BICM due to their flexibility. Product codes and compound codes were proposed in [20] and [21] respectively. They consist of a serial concatenation of two or more codes at the transmitter, and by individual decoding of every code at the receiver. Their concept lead to the invention of "Turbo-codes" that will be discussed in chapter 4. Another example of concatenated codes are "low-density parity-check" (LDPC) codes [22]. They are based on sparse generator matrices that allow for probabilistic iterative decoding under the message-passing algorithm. Both LDPC and turbo codes have been proved to be capacity approaching codes for the AWGN channel. However, in this report, we will only deal with trellis codes (NRNSC convolutional and turbo codes).

The interleaver

The role of an interleaver is to scramble the bits of a codeword. It is a very important block in a BICM under iterative decoding, as it ensures independance between the extrinsic probabilities and the *a priori* probabilities exchanged by the nodes in a graph. In addition, if maximum-likelihood (ML) decoding is possible, an interleaver spreads the consecutive bits of an error events thus it limits their interference. There are different types of interleavers: pseudo-random, S-random [23], where two

consecutive bits at the input of the interleaver will be placed a distance S away from each other at the output. In [17], a class of optimized interleavers for block-fading channels was proposed, class that respects the "ideal interleaving" conditions. These conditions are summarized as (see proposition 5, chapter 3 in [17]), : "*...the interleaver should uniformly place consecutive bits on all the channel time realizations, transmit antennas, and bit positions of the mapping and prohibit the interference of these consecutive bits in the mapping*". This class of interleavers will be frequently employed throughout this report.

The modulator

This block converts m coded bits into a constellation symbol at each channel use. The bijection from bits to symbols is called mapping (or labeling) The cardinality of the constellation Ω is given by $|\Omega| = M = 2^m$. Now in the case of MIMO systems with $n_t \geq 2$ transmit antennas for instance, the mapper takes $m \times n_t$ bits at each channel use and converts them into a vector of n_t modulation symbols. There exist different types of mappings, each suited for certain applications or specific channel types. Gray mapping, the most widely used, allows for only one bit to change between any two neighbors of the constellation, but it only exists for square constellations (i.e. $|\Omega| = 2^{2u}$). The mapping presented in [12] known as "Ungerboeck mapping" maximizes the Euclidean distance between neighbor constellation symbols and is suited for trellis-coded modulations. Mapping issues will not be treated in this report, and only Quadrature Amplitude Modulations (QAM) will be considered. The energy per M-QAM symbol is given by:

$$E_s = \frac{2(M-1)}{3} \tag{1.15}$$

The space-time precoder

The precoder $\mathbf{S}$ spreads the QAM symbols over s time periods. In most cases, the precoder is linear, i.e. it maps the QAM vector onto a linear combination of the constellation symbols. However, in some cases, the space-time precoder is not linear, as is the case for orthogonal designs [24] [25] and the scheme presented in section 2.7.

1.3.2 The BICM iterative receiver

The codewords at the output of the concatenation of a space-time precoder and a BICM can be seen as global Euclidean codes [17]. Ideally, such codes should be decoded with a maximum-likelihood (ML) decoding algorithm, but an exhaustive search over all the codewords is unfeasible in practice as the codeword size increases. For this reason, the receiver for such systems is at the image of the transmitter, whereas corresponding blocks iteratively exchange soft information. Thus the receiver of a space-time (ST) BICM consists of two main nodes: a soft-input soft-output (SISO) *a posteriori* probability (APP) QAM detector, that converts the information carried by the constellation mapper and the space-time precoder as soft information on the coded bits, and a SISO decoder that takes the information from the detector as *a priori* and generates more reliable soft information (extrinsic probabilities) on coded bits. The final decision is made on the APP on information bits at the output of the SISO decoder.
Ideally, the optimal SISO detector computes the channel realizations over all possible "space-time codewords". This operation might be too complex for high data rates (large constellation size, large number of antennas, large number of relays...). A complexity reduction method called "List sphere decoding" [26] reduces the exhaustive list of candidates to a smaller list without degrading the overall system performance. There also exist sub-optimal detectors such as SISO Minimum Mean-Square Error (MMSE) detectors or Serial/Parallel Interference Cancellation (SIC/PIC) detectors developed in multi-user detection theory (see [27] and references therein).
As for the channel decoders, there exist hard output decoders and soft output decoders. For algebraic codes, there only exist hard output decoders [28] [29]. For convolutional codes, the most famous hard output decoder is the "Viterbi algorithm" [30] (also known as Maximum-Likelihood Sequence Estimator (MLSE)), that is optimal in the ML sense. The first soft-output decoding algorithm was proposed back in the 1950s [31]. In 1963, Gallager proposed what is known as the "sum-product algorithm" (or also "belief propagation") for the iterative decoding of LDPC codes. Later, in the 1970s, the "forward-backward algorithm" (or BCJR, following the initials of the authors) was proposed as a SISO trellis decoder that gives the APP on information bits. Due to its additional complexity and to its sub-optimality codeword-wise, this algorithm did not replace the Viterbi algorithm until the invention of turbo codes, where the exchange of soft information was mandatory (see chapter 4). In the late 1980s, the "soft-output Viterbi algorithm" was proposed in [32] as a Viterbi algorithm that gives soft information on coded bits, but this algorithm is sub-optimal compared to the BCJR for iterative processing. Throughout this report, the BCJR algorithm will be used for the decoding of error correcting codes, due to its optimality in generating soft information on messages.

As mentioned previously, the optimum decoding of a ST-BICM is to compute a ML decoding algorithm over the global code. This means that the separation between detection and decoding is largely sub-optimal; an exhaustive ML search of the transmitted vector at the detector level can provide information that can mislead the decoder in choosing the probable codeword. For this reason, in a way to approach the optimality of the global ML detection, we will use an iterative detection and decoding receiver throughout this manuscript.
Fig. 1.4 shows the general structure of an iterative receiver suited for fading channels. The two major blocks represent the SISO detector and the SISO decoder, that are separated by interleaving blocks (the block Π^{-1} is a de-interleaver). The iterative process consists of exchanging soft information between the two blocks.

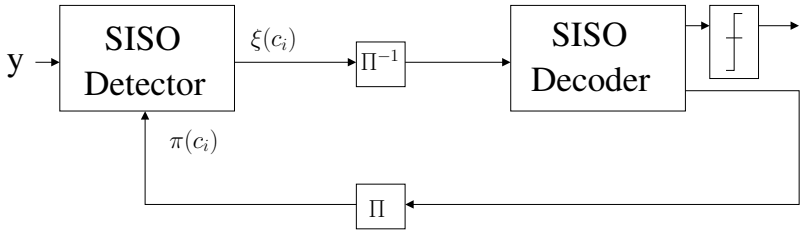

Figure 1.4: ST-BICM iterative receiver.

The SISO detector receives a complex vector $\mathbf{y} \in \mathbb{C}^{N_r}$ given by:

$$\mathbf{y} = \mathbf{zSH} + \mathbf{w} = \mathbf{xH} + \mathbf{w} \tag{1.16}$$

where $\mathbf{z} \in \mathbb{C}^{N_t}$ is the vector of QAM symbols, $\mathbf{S}$ is a $N_t \times N_t$ space-time precoder, $\mathbf{H}$ is the complex channel matrix, and $\mathbf{w}$ is a circularly symmetric zero-mean complex Gaussian noise vector with variance N_0. For a MIMO system with n_r receive antennas, $N_r = s.n_r$, while for a cooperative system with β single-antenna relays, $N_r = \beta + 1$. In addition, $N_t = s.n_t$ for a MIMO system with n_t transmit antennas, and $N_t = \beta + 1$ for a cooperative system, all employing $2^m - QAM$ modulations. The detector first computes the channel likelihoods $p(\mathbf{y}/\mathbf{x})$ over $\mathbb{C}^{N_r}$, then it generates the extrinsic probabilities on coded bits $\xi(c_i)$ based on the channel likelihoods and the *a priori* probabilities $\pi(c_i)$ fed from the SISO decoder. At the first iteration, all the *a priori* probabilities are unbiased. Throughout the iterative process, the exchange of probabilities on coded bits between the two blocks should give more reliable soft information on the information bits. An ideal convergence of the process would lead to near-ML performance.

In the following we will describe the optimal APP detector based on a marginalization over an exhaustive list. Note that complexity reduction for such detectors was proposed in [26]. By definition, the APP of a coded bit c_i is the probability to detect c_i when $\mathbf{y}$ is received:

$$APP(c_i) = p(c_i/\mathbf{y}) = \frac{p(\mathbf{y}/c_i)p(c_i)}{p(\mathbf{y})} \qquad i = 1, ..., mN_t \tag{1.17}$$

where $N_t = s.n_t$ for a MIMO system with n_t transmit antennas, and $N_t = \beta + 1$ for a cooperative system, all employing $2^m - QAM$ modulations. In this expression of the APP on coded bits at the detector, it is obvious that the probability on coded bits $p(c_i)$ is nothing but the *a priori* probability fed from the SISO decoder, thus $p(c_i) = \pi(c_i)$. Now the conditional probability density function $p(\mathbf{y}/c_i)p(c_i)$ is obtained by the marginalization of the joint probability density function of the channel likelihood and the coded bits as follows:

$$p(\mathbf{y}/c_i) = \sum_{j \neq i,\ j \leq mN_t} p(\mathbf{y}, c_j/c_i) \tag{1.18}$$

$$= \sum_{j \neq i,\ j \leq mN_t} p(\mathbf{y}/c_j) \prod_{u \neq i} \pi(c_u) \tag{1.19}$$

Here we suppose that the coded bits transmitted during the same time period are independent. Now as the noise is AWGN and by supposing that the receive antennas are independent we can write:

$$p(\mathbf{y}/c_1, ..., c_{mN_t}) = \frac{1}{2\pi N_0} e^{-\|\mathbf{y} - \mathbf{xH}\|^2/2N_0} \tag{1.20}$$

Now in an iterative process in general, a block (i.e. a detector or a decoder) should not give information on a bit to the other block that is known to this block. The APP on a coded bit computed by the detector can be written as the product of two independent probabilities:

$$APP(c_i) = \xi(c_i)\pi(c_i) \tag{1.21}$$

As $\pi(c_i)$ is computed by the SISO decoder, giving back $APP(c_i)$ to the SISO decoder is not appropriate. For this reason, the extrinsic probability $\xi(c_i)$ is given to the SISO decoder. Now let us define $c_1, ..., c_i, ..., c_{mN_t} \in \Omega(c_i)$ as the set of the mN_t bits in $\mathbf{y}$ having the i^{th} bit equal to c_i, we can write the following normalized expression for the extrinsic

probabilities [17]:

$$\xi(c_i) = \frac{p(\mathbf{y}/c_i=1)}{p(\mathbf{y}/c_i=0)+p(\mathbf{y}/c_i=1)} \quad (1.22)$$

$$= \frac{\sum_{x'\in\Omega(c_i=1)}\left[\left(e^{-\|\mathbf{y}-\mathbf{x}'\mathbf{H}\|^2/2N_0}\right)\prod_{u\neq i}\pi(c_u)\right]}{\sum_{x\in\Omega(c_i=1)}\left[(e^{-\|\mathbf{y}-\mathbf{x}\mathbf{H}\|^2/2N_0})\prod_{u\neq i}\pi(c_u)\right]} \quad (1.23)$$

Note that, luckily enough, the expression for $p(\mathbf{y})$ from (1.17) is cancelled through the normalization. Indeed, the computation of this quantity that depends on the transmitted signal and the noise is tedious.

1.4 Bounds on diversity for coded systems on non-ergodic channels

On a single-antenna ergodic fading channel, a frame sees different channel realizations at each time epoch. This gives a Nakagami distribution of high order (represented by the sum of the $\|h_j\|^2$) at the output of the detector and thus gives a high order of diversity. The diversity order that can be achieved by a ST-BICM on such channels is thus mainly limited by the minimum Hamming distance d_{min} of the channel code. Over block-fading channels with a limited number of states, the situation is different. In the sequel, we will call *BO-channel* the binary-oriented channel with input c_i and output $\xi(c_i)$ as observed by the channel encoder and the channel decoder.

Definition 1. *Under the genie condition (i.e. perfect* a priori *information) in the BO-channel, the number of independent binary-input non-ergodic fading sub-channels is denoted by D_{st} and called the* state diversity.

As an example, in the single-input single-output block-fading channel where a codeword spans n_c channel realizations, we have that $D_{st} = n_c$. Now let $\omega_H(c)$ denote the Hamming weight of a codeword c of length L_c generated by a linear binary code. We write $\omega_H(c) = \sum_{i=1}^{D_{st}} \omega_i$, where ω_i is the partial Hamming weight transmitted on the binary-input sub-channel i within the BO-channel. The state diversity $d_{st}(c)$ achieved by the codeword c is the number of non-zero partial weights. For a given transmitter structure, the achievable state diversity is $d_{st} = \min_{c\neq 0} d_{st}(c)$. Now suppose that each L_c/D_{st} bits are transmitted over one channel state. By grouping all the bits transmitted over one channel state into

one symbol, we get a non-binary code of length $N_s = D_{st}$ built on an alphabet of size $2^{L_c/D_{st}}$. The Singleton bound on the Hamming distance of the non-binary code (K_s, N_s) is thus given by:

$$d_{st} \leq N_s - K_s + 1 = N_s - N_s.R_c + 1 \tag{1.24}$$

Finally, state diversity is upper-bounded by [33][34]

$$d_{st} \leq \lfloor D_{st}(1 - R_c) + 1 \rfloor \leq D_{st} \tag{1.25}$$

Note that the maximal diversity given by the outage limit under a finite size QAM alphabet also achieves the above Singleton bound [9]. We can notice from (1.25) that full diversity is attained only if $R_c \leq 1/D_{st}$. As D_{st} grows to infinity (i.e. tends to an ergodic fading channel), the diversity order of a coded system is limited by $\omega_H(c)$.

1.5 Conclusions

We discussed the outage probability for block-fading channels, that represents the fundamental lower-bound on the performance of coded modulations for long enough codewords on this type of channels. We then presented our system model, that will be used throughout this manuscript to design schemes that approach the outage probability limit. We finally explained the bounds on the diversity order of a binary code over block-fading channels, bound that will be elaborated further to fit to specific types of block-fading channels, namely the multiple-input multiple-output (MIMO) channel and amplify-and-forward cooperative fading channel.

Chapter 2

Coded modulations for the multiple-antenna channel

2.1 Introduction

Since the late nineties, employing multiple-antennas on a communicating terminal has been of great interest as a result of the dramatic increase in capacity these systems can provide [4][5]. Moreover, for block-fading channels, multiple-antennas are a mean to provide spatial diversity that allows to combat the fluctuations of the quality of the channel. Since then, researchers in the wireless communication community studied and designed efficient schemes for such systems that allow for maximal diversity orders and high performance. With the exception of few works that will be mentioned in this chapter, most designs only considered the protection of constellation symbols under ML decoding, without taking into account the presence of an error correcting code. In this chapter, we will propose coded modulation schemes for the multiple-antenna channel that perform close to channel limits. We will start by a state-of-the-art of coding schemes for the MIMO channel in section 2.2. We will then show the frame error rate of uncoded space-time rotations as a function of the frame length (that constitutes the motivation behind our work), the general system model, and the bounds on the diversity order achieved by multiple-antenna systems. Next we will discuss our three proposed schemes; the first one consists of designing space-time precoders that minimize the discrete-input outage probability (section 2.6), the second consists of the extension of the Alamouti scheme to a system with $n_t = 4$ transmit antennas (section 2.7), and the third considers code multiplexer design for turbo codes (section 2.8).

2.2 A brief historical note

After the pioneering works in [4][5] on multiple-antenna channels, the author in [35] proposed the Bell-Labs Layered Space Time codes (BLAST), that demultiplex the symbol stream over n_t transmit antennas, while the receiver recovers the transmitted symbols through n_r receive antennas. This scheme was capable of achieving high data rates through spatial multiplexing, but it was not capable of recovering the diversity provided by the transmit antennas as no "smart" processing was performed at the transmitter level. For that reason, the authors in [25][36] proposed design criteria for "space-time codes", in a goal to make benefit from the transmit diversity at the receiver. These criteria consisted of minimizing the pairwise error probability of a pair of space-time codewords by maximizing both the determinant and the rank of the codeword matrix. The codes proposed at first were constructed following orthogonal designs, from the famous Alamouti code for $n_t = 2$ [24] to the generalization for any number of transmit antennas in [25]. In the same paper [25], the authors proposed the "space-time trellis codes"; these codes follow the concept of convolutional codes as they are encoded via a trellis. They have better error rate performance than orthogonal space-time block codes, but they require a viterbi decoder thus an increase in decoding complexity. The problem with these codes is that they severely degrade the information rate by introducing redundancy, and this degradation is proportional to the number of transmit antennas. Indeed, for an orthogonal complex space-time block code employing n_t antennas, the maximal achievable rate is:

$$R_p = \frac{1 + \log_2 n_t}{2.\log_2 n_t} \tag{2.1}$$

As a nresult of this limitation of orthogonal designs, the use of algebraic tools to build space-time rotations that attain full diversity and full spatial multiplexing was considered. Indeed, precoding signals for fading channels, which is well-known in single antenna transmissions, has been rediscovered for multiple-antenna channels. In fact, Battail was the first to suggest rotations to combat channel fluctuations in [37]. The pioneering work on multi-dimensional rotated modulations achieved in the nineties, such as [38][39][40], opened the way for the study of multi-dimensional rotations (i.e. linear unitary precoders) in MIMO channels. Rotations in single antenna systems have been designed by classical algebraic criteria, except for orthogonal transforms proposed by Rainish which are based on the minimization of the cut-off rate [41]. Also, it has been shown in [42] that random rotations perform as good as algebraic rotations in a high-diversity high-dimensional environment. In [43] [44] [45] among others, the authors proposed then algebraic constructions of space-time codes for uncoded multiple-antenna systems, and they outperformed orthogonal designs as they were full-rate, i.e. one symbol is sent per transmit antenna per

symbol time. However, new problems have arisen with these designs, as the determinant of the codeword matrix vanishes with an increase in the constellation size. The race to the optimal space-time code for uncoded systems was ended by the works in [46] [47] [48] for $n_t = 2$ and by [49] for $n_t = 3, 4, 6$. Indeed, these works provide space-time codes that have non-vanishing determinants, thus they yield optimal performance with uncoded systems under maximum-likelihood detection. As an example, the Golden code [46] is an algebraic precoder optimized for $n_t = n_r = 2$, its precoding matrix is:

$$\mathbf{S_{GC}} = \begin{bmatrix} 0.52e^{-j0.55} & 0 & 0 & 0.85e^{+j1.01} \\ 0.85e^{-j0.55} & 0 & 0 & 0.52e^{-j2.12} \\ 0 & 0.85e^{+j2.58} & 0.52e^{-j0.55} & 0 \\ 0 & 0.52e^{-j0.55} & 0.85e^{-j0.55} & 0 \end{bmatrix} \tag{2.2}$$

As an alternative to the design criteria proposed in [25][36], linear dispersion (LD) codes [50] were designed for multiple antenna channels by a search that maximizes the ergodic capacity of the channel under a Gaussian channel input. Such a design is not necessarily suitable for a non-ergodic channel with a finite number of states, as these channels are information unstable [6]. Also, the type of input alphabet is not considered in the search for linear dispersion codes.

The major drawback of the aforementioned design criteria is that they do not take into account the concatenation with an error correcting code in the system. Furthermore, space-time signal modulations must be combined to error-correcting codes in order to achieve optimal performance in the information theoretical sense.

For this reason, the authors in [16][17] considered bit-interleaved coded modulations for space-time coding (ST-BICM). They showed that quasi-optimal global ML performance of the coded modulation is achieved by imposing specific constraints (called *genie conditions*) on the structure of the space-time precoder under ideal interleaving. In fact, in order to guarantee maximum diversity order and maximum coding gain at the output of the detector, the design must guarantee two conditions:

- Orthogonal sub-rows in the linear precoding matrix.
- Equal norm sub-rows in the linear precoding matrix.

If these conditions are met, perfect *a priori* probability feedback will be assumed in the iterative joint detection and decoding of ST-BICM, hence quasi-ML performance will be attained in practice after some iterations at a high signal-to-noise ratio. As an example, the cyclotomic rotation given below is an algebraic precoder satisfying the genie conditions

for ST-BICM with $n_t = 2$:

$$\mathbf{S_{Cyclo}} = [\phi_{ij}] = \frac{1}{2}\begin{bmatrix} 1 & 1 & e^{j6\pi/15} & -e^{j6\pi/15} \\ e^{j2\pi/15} & je^{j2\pi/15} & -e^{j8\pi/15} & je^{j8\pi/15} \\ e^{j4\pi/15} & -e^{j4\pi/15} & e^{j10\pi/15} & e^{j10\pi/15} \\ e^{j6\pi/15} & -je^{j6\pi/15} & -e^{j12\pi/15} & -je^{j12\pi/15} \end{bmatrix} \tag{2.3}$$

where we have the following:

- Vector $(\phi_{i,1}, \phi_{i,2})$ is orthogonal to vector $(\phi_{i,3}, \phi_{i,4})$ on any row i, $i = 1 \dots 4$.
- Vectors $(\phi_{i,1}, \phi_{i,2})$ and $(\phi_{i,3}, \phi_{i,4})$ have equal norms.

Note that most of the algebraic space-time rotations designed for uncoded systems guarantee at least one of the above conditions. The precoding matrix $\mathbf{S_{GC}}$ of the Golden code from (2.2) for instance guarantees the first genie condition, and the second condition can be compensated by an error correcting code with high coding gain [17].
In this chapter, we will propose space-time precoders suited for the ST-BICM scheme whose design is mostly based on the conditions established in [16][17] for optimal performance. Before doing so, we will show the behavior of the frame error rate performance of uncoded space-time rotations and recall the bounds on the diversity orders that can be attained by a ST-BICM on MIMO block-fading channels under ideal interleaving.

2.3 Upper bound on the frame error rate for uncoded space-time signaling

Suppose that we concatenate N_f space-time precoded blocks forming a frame to be transmitted on a block-fading channel with a probability of error $P_f(N_f)$. Suppose now that each block has diversity order d, so the probability of error P_c of each independent code is a function of the signal-to-noise ratio γ and a chi-square random variable y given by:

$$y = \sum_{i=1}^{2d} y_i^2 \quad y_i \sim \mathcal{N}_f\left(0, \sigma^2\right) \tag{2.4}$$

$$p(y) = \frac{y^{d-1} e^{-y/2\sigma^2}}{(d-1)!} \tag{2.5}$$

Now let $P_f(N_f)$ denote the frame error rate as a function of N_f:

$$P_f(N_f) = \int_0^{+\infty} \left[1 - (1 - P_c(\gamma, y))^{N_f}\right] p(y) dy \tag{2.6}$$

We can write that [33]:

$$P_f(N_f) \leq 1 - (1 - P_c(\gamma, y))^{N_f} \leq N_f.P_c(\gamma, y) \tag{2.7}$$

which gives the upper bound on $P_f(N_f)$ as N_f goes to infinity as [17, Appendix A]:

$$\begin{aligned} P_f(N_f) &\leq \int_0^{+\infty} min\left[1, N_f.P_c(\gamma, y)\right] p(y)dy & (2.8)\\ &= \int_0^{\alpha} p(y)dy + \int_{\alpha}^{+\infty} N_f.P_c(\gamma, y)p(y)dy & (2.9)\end{aligned}$$

where α is given by:

$$P_c(\gamma, \alpha) = \frac{1}{N_f} \tag{2.10}$$

Now let us suppose that when γ goes to infinity we get:

$$P_c(\gamma, y) \cong e^{-y\gamma/2} \tag{2.11}$$

which gives the value for α as:

$$\alpha = \frac{2}{\gamma}\log(\frac{N_f}{2}) \tag{2.12}$$

Now we can write the first term of (2.9) as:

$$P_{f1}(N_f) = \int_0^{\alpha} p(y)dy = 1 - e^{-\alpha}\sum_{k=0}^{d-1}\frac{\alpha^k}{k!} = e^{-\alpha}\sum_{k=d}^{+\infty}\frac{\alpha^k}{k!} \tag{2.13}$$

Then we can write:

$$\lim_{\gamma\to+\infty, N_f\to+\infty,} P_{f1}(N_f) = \frac{\left[\frac{2}{\gamma}\log(\frac{N_f}{2})\right]^d}{d!} \tag{2.14}$$

Finally we can write the second term of (2.9) as:

$$P_{f2}(N_f) = \int_{\alpha}^{+\infty} N_f.P_c(\gamma, y)p(y)dy \tag{2.15}$$

and:

$$\begin{aligned} \lim_{\gamma\to+\infty} P_{f2}(N_f) &= \lim_{\gamma\to+\infty}\int_{\alpha}^{+\infty} N\frac{y^{m-1}e^{-(1+\frac{\gamma}{2})y}}{(m-1)!}dy & (2.16)\\ &= \lim_{\gamma\to+\infty} N\frac{e^{-\gamma(1+\frac{\gamma}{2})}}{(1+\frac{\gamma}{2})^d}\sum_{k=0}^{d-1}\frac{\left[\gamma(1+\frac{\gamma}{2})\right]^k}{k!} & (2.17)\\ &= \lim_{\gamma\to+\infty}\frac{1}{(1+\frac{\gamma}{2})^d} & (2.18)\end{aligned}$$

We can notice from equation (2.14) that the frame error rate of an uncoded system degrades as $\log(N_f)^d$ where d is the diversity order. Hence, it is impossible to approach outage probability with uncoded systems, as a coding scheme that approaches outage probability has to be insensitive (or slightly sensitive) to block length. For the Alamouti scheme for instance, the frame error rate is upper-bounded by:

$$P_f(N_f) \leq \frac{2\log^2(\frac{N_f}{2}) + 4\log(\frac{N_f}{2}) + 4}{\gamma^2} \tag{2.19}$$

In a similar way, it was found in [51] that the frame error rate obtained by concatenating N_f $(8, 4, 4)$ block codes is upper-bounded by:

$$P_f(N_f) \leq \frac{2\log^2(2N_f) + 3/7\log(7N_f) + 2\log(2N_f) + 24/7}{(2R_c\gamma)^2} \tag{2.20}$$

In addition, it was observed in [52] that the frame error rate of convolutional codes varies logarithmically with N_f on block-fading channels.

2.4 System model and notations

In this chapter, we consider the BICM scheme as presented in section 1.3 concatenated with a space-time precoder as shown in Fig. 1.3.

The channel model for a precoded ST-BICM is given by:

$$\mathbf{y} = \mathbf{zSH} + \mathbf{w} = \mathbf{xH} + \mathbf{w} \tag{2.21}$$

where $\mathbf{z} \in \Omega = (M\text{-QAM})^{N_t}$ and $N_t = R_p \cdot s \cdot n_t$, the parameter s being the time spreading of a precoding matrix $\mathbf{S}$ of dimensions $N_t \times N_t/R_p$, where R_p is the rate of the precoder. In general, $\mathbf{S}$ is a full-rate unitary matrix (i.e. $R_p = 1$) whose structure is matched to iterative detection as the class of cyclotomic rotations proposed in [16][17]. The MIMO channel matrix has dimensions $N_t/R_p \times N_r/R_p$, and assuming that the number of independent channel realizations observed during one codeword transmission is n_c, we get:

$$\mathbf{H} = diag\left(\overbrace{\underbrace{\mathbf{H}_1, \ldots, \mathbf{H}_1}_{s.R_p/n_c}, \ldots, \mathbf{H}_{n_c}, \ldots, \mathbf{H}_{n_c}, \ldots, \underbrace{\mathbf{H}_1, \ldots, \mathbf{H}_1}_{s.R_p/n_c}, \ldots, \mathbf{H}_{n_c}, \ldots, \mathbf{H}_{n_c}}^{1/R_p}\right) \tag{2.22}$$

the additive white Gaussian noise vector $\mathbf{w}$ of dimension N_r/R_p is assumed to be circularly symmetric with zero mean and mean N_0. The Rayleigh fading channel is quasi-static frequency non-selective, i.e. the whole transmitted frame undergoes one channel realization.

The channel coefficients are supposed to be perfectly known (perfect CSI) to the receiver, but not to the transmitter. We make the assumption of perfect channel estimation and perfect synchronization. Digital transmission is made as follows: uniformly distributed information bits are fed to a binary convolutional encoder $\mathcal{C}$. Coded bits $\{c_i\}$ are then interleaved through Π, Gray mapped into QAM symbols, precoded through $\mathbf{S}$ and transmitted on the MIMO channel given by (2.22). The coherent MIMO detector computes an extrinsic information $\xi(c_i)$ based on the knowledge of $\mathbf{H}$, the received vector $\mathbf{y}$, and independent *a priori* information $\pi(c_j)$ for all coded bits. The coding rate is $R_c \in [0, 1]$. The transmitted information rate is equal to $R = R_p R_c n_t \log_2 M$ bits per channel use, where M is the cardinality of the bi-dimensional QAM constellation. An interleaver $\mathbf{\Pi}$ enables iterative probabilistic MIMO detection [53][54] of the binary-oriented channel.

2.5 Diversity bounds for coded multiple-antenna systems

In ST-BICM, there exists a strong interaction between the error correcting code with interleaving and the linear precoder, both in terms of diversity and coding gain maximization [17]. Complexity can be controlled by the choice of a space-time rotation $\mathbf{S}$ with minimal time spreading factor s that guarantees full diversity [55]. In other terms, the lowest complexity solution would be to first let the channel decoder recover the highest amount of diversity possible, then the detector recovers the remaining diversity through time spreading. For a MIMO channel, the *channel diversity* is defined as $D_{ch} = n_t n_c n_r$, which is equal to the intrinsic diversity order of the physical channel. For a given transmitter structure, the achievable channel diversity is $d_{ch} = \lim_{SNR \to +\infty} -\log(P_e)/\log(SNR)$, where SNR is the signal-to-noise ratio and P_e is the error probability.

When $\mathbf{S}$ is the identity matrix, the ST-BICM diversity order is upper-bounded by [34]:

$$d_{ch} \leq \min\left(n_r \left\lfloor n_t n_c (1 - R_c) + 1 \right\rfloor,\ D_{ch}\right) \tag{2.23}$$

With a vanishing coding rate, i.e. $R_c \to 0$, it is possible to attain the overall system diversity order $n_r n_c n_t$ produced by the receive antennas, the transmit antennas and the distinct channel states. Unfortunately, this is unacceptable due to the vanishing transmitted information rate. Precoding is one means to achieve maximum diversity with a non-vanishing coding rate. Under linear precoding that spreads QAM symbols over s time periods, the Singleton bound becomes [55]:

$$d_{ch} \leq \min\left(s n_r \left\lfloor \lfloor \frac{n_t n_c}{s} \rfloor (1 - R_c) + 1 \right\rfloor,\ D_{ch}\right) \tag{2.24}$$

Now if $s = n_t.n_c$, from the above inequality, we observe that precoding may achieve maximal diversity $n_t n_c$ without the use of error-correcting codes. Unfortunately, near-outage performance is impossible in this case due to the weak coding gain of all kinds of space-time precoders, as was discussed in section 2.3. The near-outage performance of ST-BICM is a judicious trade-off between error-control coding and linear QAM precoding. The genie conditions are optimal, in terms of ML performance, when all diversity given by the transmit antennas is collected at the detector (i.e. $s = n_t$). A supplementary condition (that will be discussed later) called "Dispersive Nucleo Algebraic" (DNA) has been proposed in [17] to keep optimality when $s < n_t$ while having the genie conditions on sub-groups of transmit antennas.

With a judicious choice of an error-correcting code and a linear precoder, maximum diversity is easily attained ($d_{ch} = D_{ch}$). In general, a Nakagami distribution of order D_{ch}/D_{st} is associated to each binary-input sub-channel embedded within the BO-channel. Recall that D_{st} is the state diversity seen by the binary code. To illustrate the above definitions, we list the following examples:

- For $n_t = 2$, $n_r = 1$, $D_{ch} = 2$, and without rotation ($s = 1$). We get $D_{st} = 2$.
- For $n_t = 2$, $n_r = 2$, $D_{ch} = 4$. Without rotation ($s = 1$), we have $D_{st} = 2$. With a cyclotomic rotation ($s = 2$), we get $D_{st} = 1$.
- For $n_t = 4$, $n_r = 2$, $D_{ch} = 8$. Without rotation ($s = 1$), we have $D_{st} = 4$. With a cyclotomic DNA rotation ($s = 2$), we get $D_{st} = 2$.

2.6 Space-time precoders based on information outage minimization

2.6.1 Introduction

At that stage, in the existing works, the authors achieved optimal (quasi-ML) performance with a space-time precoded BICM under iterative detection and decoding. The genie conditions ensure that *a priori* information fed back from the decoder becomes perfect after a certain number of iterations. However, in some practical receivers, an iterative algorithm might not be possible due to resource limitations. The high data rates and the high processing speed required in a communication system can put strict constraints on the number of iterations. For this reason, we will present full-rate space-time precoders that lead the ST-BICM to perform well since the first iteration. Hence, we propose a simple

information theoretical design of multi-dimensional rotations that take into account the interaction between channel coding and symbol space-time spreading.

2.6.2 Linear precoding designs

For a fixed rotation $\mathbf{S}$ and n_c fixed MIMO channel matrices $\mathbf{H}_i$, $i = 1 \dots n_c$, defined by the n_c fading blocks, let $\mathcal{I}_{SH} = \mathcal{I}(\mathbf{z}; \mathbf{y})$ denote the average mutual information of the equivalent channel with QAM input $\mathbf{z}$ and complex output $\mathbf{y}$ as in (2.21). The expression of $\mathcal{I}_{SH}$ is a slight modification of (1.14) that gives:

$$\mathcal{I}_{SH} = s.m.n_t - \frac{1}{n_c} \sum_{i=1}^{n_c} E_{\mathbf{z},\mathbf{y}|\mathbf{SH}_i} \left[\log_2 \left(\frac{\sum_{\mathbf{z}'} p(\mathbf{y}|\mathbf{z}', \mathbf{SH}_i)}{p(\mathbf{y}|\mathbf{z}, \mathbf{SH}_i)} \right) \right] \tag{2.25}$$

where $E_{\mathbf{z},\mathbf{y}|\mathbf{SH}_i}$ is the conditional mathematical expectation over $\mathbf{z}$ and $\mathbf{y}$. The channel likelihood is written in its classical form

$$p(\mathbf{y}|\mathbf{z}, \mathbf{SH}) \propto \exp\left(-\frac{\|\mathbf{y} - \mathbf{zSH}\|^2}{2\sigma^2} \right) \tag{2.26}$$

Expression (2.25) assumes that the precoder $\mathbf{S}$ does space-time spreading within the same fading block $\mathbf{H}_i$. Its main role is to collect transmit diversity. Time diversity n_c is collected by the convolutional code whereas receive diversity is naturally collected by the detector. The information rate transmitted by the space-time BICM is $R = s.m.n_t.R_c$ bits per s time periods (with $R_p = 1$ for full-rate precoders). An outage occurs if the instantaneous capacity, i.e. $\mathcal{I}_{SH}$ in our case, is less than R (see section 1.2). The outage probability associated to the rotation $\mathbf{S}$ at a given signal-to-noise ratio is

$$P_{out}(\mathbf{S}) = P\left(\mathcal{I}_{SH} < s.m.n_t.R_c\right) \tag{2.27}$$

The new design, called IOM (Information Outage Minimization), selects a matrix $\mathbf{S_{IOM}}$ within the ensemble $\aleph$ of random unitary matrices such that

$$\mathbf{S_{IOM}} = \arg \min_{\mathbf{S} \in \aleph} P_{out}(\mathbf{S}) \tag{2.28}$$

As an example, choosing the best rotation within an ensemble $\aleph$ limited to 2000 matrices yields the matrix written below, for QPSK alphabet with $n_t = s = 2$ and coding rate $R_c = 1/2$

$$\mathbf{S_{IOM}} = \begin{bmatrix} 0.57e^{+j1.71} & 0.64e^{+j1.55} & 0.14e^{-j1.89} & 0.49e^{+j1.22} \\ 0.34e^{-j0.94} & 0.51e^{+j2.82} & 0.57e^{+j1.26} & 0.54e^{+j0.27} \\ 0.59e^{-j1.38} & 0.04e^{-j0.04} & 0.61e^{-j1.46} & 0.52e^{+j1.25} \\ 0.46e^{-j0.84} & 0.57e^{+j1.74} & 0.53e^{+j3.05} & 0.43e^{-j2.66} \end{bmatrix}$$

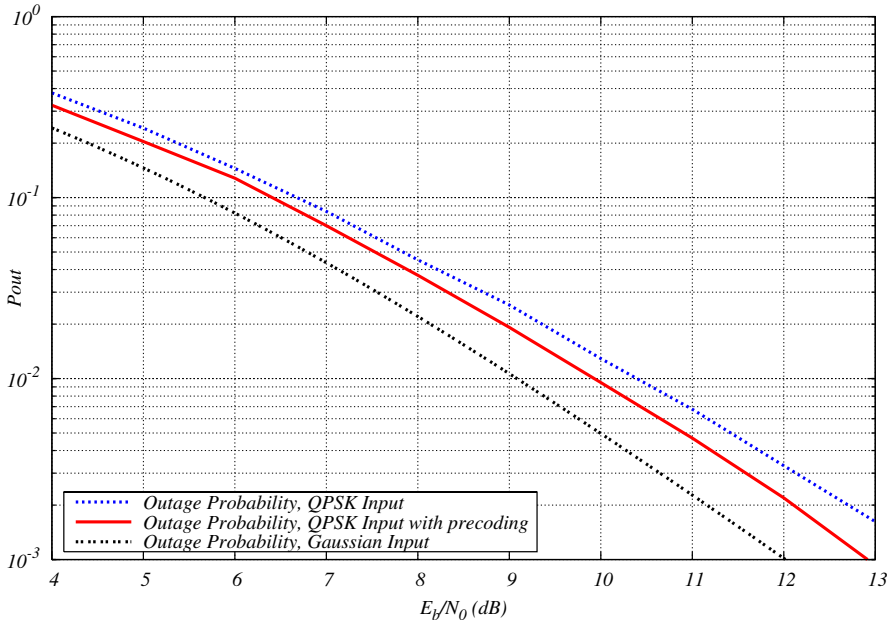

Figure 2.1: Outage limits for $n_t = n_c = s = 2$, $n_r = 1$, and $R_c = 1/2$.

By minimizing the discrete-input outage probability, the random rotation makes the distribution of the input vector $\mathbf{x} = \mathbf{zS}$ to the channel look like a Gaussian distribution. Fig. 2.2 shows the distribution of the vector $\mathbf{zS_{IOM}}$ for a BPSK modulation, the bell shape of the curve is flagrant. The problem with the matrix $\mathbf{S_{IOM}}$ is that it does not satisfy

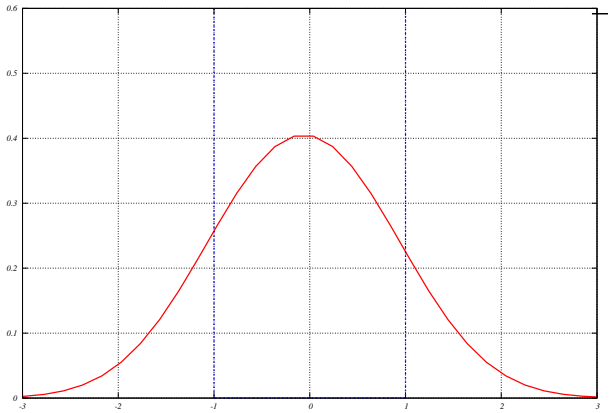

Figure 2.2: Distribution of $\mathbf{zS_{IOM}}$ for a BPSK modulation.

the genie conditions. Although it boosts the performance after a "one-shot" detection and decoding process, it does not guarantee optimal convergence of the iterative process. To make our design suited for both "one-shot" detection and iterative decoding, a smaller

set $\aleph_G$ of random unitary matrices is obtained by adding to $\aleph$ the first genie constraint, i.e. orthogonal sub-rows in $\mathbf{S}$. This condition is much more important than the second genie constraint (i.e. equal-norm sub-rows) as it gives independent extrinsic probabilities at the output of the SISO detector. This second design, called G-IOM, selects a matrix $\mathbf{S_{G-IOM}}$ satisfying

$$\mathbf{S_{G-IOM}} = \arg \min_{S \in \aleph_G} P_{out}(\mathbf{S}) \tag{2.29}$$

As an example, choosing the best rotation within an ensemble $\aleph_G$ limited to 2000 matrices yields the matrix written below, for QPSK alphabet with $n_t = s = 2$ and coding rate $R_c = 1/2$

$$\mathbf{S_{G-IOM}} = \begin{bmatrix} 0.88e^{-j0.30} & 0 & 0 & 0.48e^{-j0.55} \\ 0.48e^{-j0.33} & 0 & 0 & 0.88e^{+j2.57} \\ 0 & 0.47e^{-j2.12} & 0.88e^{+j2.85} & 0 \\ 0 & 0.88e^{+j2.96} & 0.47e^{-j1.49} & 0 \end{bmatrix}$$

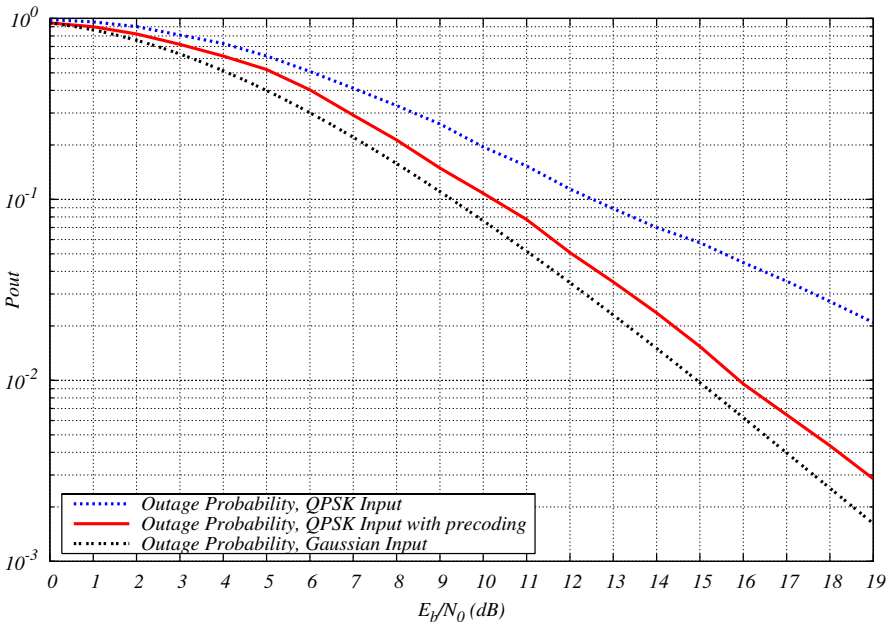

Figure 2.3: Outage limits for $n_t = n_c = s = 2$, $n_r = 1$, and $R_c = 3/4$.

Now for the case of $n_t = 4$, using a half-rate convolutional code allows us to employ a DNA precoder with $s = 2$ as it ensures maximal diversity through (2.24). We thus design a DNA-IOM precoder that minimizes and satisfies DNA constraints [17]; the first step is to pick a 4×4 rotation from the ensemble $\aleph_{DNA}$ of random rotation, and the second step is to place the orthogonal nucleotides inside an 8×8 matrix and separate them with null

nucleotides. We obtain the following rotation for $n_t = 4$ and $s = 2$ (see proposition (2), page 54, in [17]):

$$\mathbf{S_{DNA}} = \begin{bmatrix} \phi_{11} & \phi_{12} & 0 & 0 & \phi_{13} & \phi_{14} & 0 & 0 \\ 0 & 0 & \phi_{11} & \phi_{12} & 0 & 0 & \phi_{13} & \phi_{14} \\ \phi_{21} & \phi_{22} & 0 & 0 & \phi_{23} & \phi_{24} & 0 & 0 \\ 0 & 0 & \phi_{21} & \phi_{22} & 0 & 0 & \phi_{23} & \phi_{24} \\ \phi_{31} & \phi_{32} & 0 & 0 & \phi_{33} & \phi_{34} & 0 & 0 \\ 0 & 0 & \phi_{31} & \phi_{32} & 0 & 0 & \phi_{33} & \phi_{34} \\ \phi_{41} & \phi_{42} & 0 & 0 & \phi_{43} & \phi_{44} & 0 & 0 \\ 0 & 0 & \phi_{41} & \phi_{42} & 0 & 0 & \phi_{43} & \phi_{44} \end{bmatrix} \tag{2.30}$$

with:

$$\mathbf{\Phi_{DNA-IOM}} = \begin{bmatrix} 0.73e^{-j0.81} & 0.22e^{+j4.62} & 0.15e^{+j0.60} & 0.61e^{+j2.59} \\ 0.21e^{+j3.99} & 0.56e^{+j4.44} & 0.62e^{+j0.25} & 0.50e^{-j1.29} \\ 0.57e^{+j0.79} & 0.13e^{-j1.28} & 0.57e^{-j0.63} & 0.57e^{+j0.90} \\ 0.29e^{+j1.01} & 0.78e^{+j3.49} & 0.51e^{+j2.27} & 0.20e^{+j0.91} \end{bmatrix}$$

The DNA-IOM precoder is thus obtained by combining $\mathbf{S_{DNA}}$ with $\mathbf{\Phi_{DNA-IOM}}$. Also, the DNA-cyclotomic precoder is constructed by combining $\mathbf{S_{DNA}}$ to $\mathbf{\Phi_{DNA-Cyclo}} = \mathbf{S_{Cyclo}}$ given previously in (2.3).

Fig. 2.1 and 2.3 show the outage limit for different type of precoders in terms of Word Error Rate versus signal-to-noise ratio. The outage probability has been also evaluated for other system parameters. In fig. 2.1, the precoding matrix enhances the coding gain of the discrete-input outage curve. In fig. 2.3, following the expression in (2.24), a precoding matrix with $s = 2$ is mandatory to recover the diversity at the receiver, as illustrated by the discrete-input outage curves of the unrotated case (that does not achieve diversity), and the rotated case. All outage evaluations have been made by (2.25) and (3.13), without Gaussian and analytical approximations when the channel input is a Gaussian alphabet as in [56][10].

2.6.3 Simulation results

In order to emphasize the diversity order created by coding at the transmitter side, all computer simulations have been conducted with the number of receive antennas $n_r = 1$. Fig. 2.4 and 2.5 illustrate the word error rate performance of a space-time BICM for $n_t = 2$ transmit antennas, $n_c = 2$ channel states, $s = 2$ time period spreading and a coding rate $R_c = 1/2$. Fig. 2.6 illustrates the case with $n_t = 4$ transmit antennas and a precoding spread factor $s = 2$. At the first iteration, for $n_t = 2$, IOM precoding slightly outperforms

other rotations. After 10 detection/decoding iterations, IOM is outperformed by G-IOM and other algebraic rotations. The slight difference in performance is still apparent for $n_t = 4$.

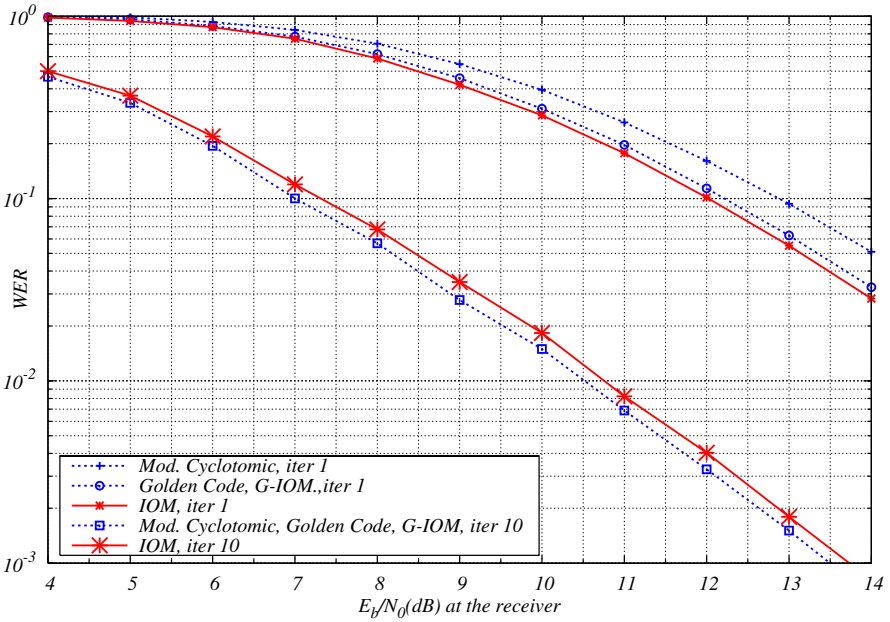

Figure 2.4: QPSK modulation, $n_t = s = n_c = 2$, $n_r = 1$, rate 1/2 16-state $(23, 35)$ convolutional code, interleaver size $N = 2048$ bits, 1 and 10 iterations.

2.7 Space-time precoders based on the Alamouti scheme

2.7.1 Introduction

One orthogonal design that highly caught the attention of the wireless communications community is the Alamouti code [24] with $R_p = 1/2$ for $n_t = 2$. This pragmatic orthogonal scheme allows to convert a 2×1 ($n_t \times n_r$) antenna configuration onto a 1×2 configuration, by creating two independent parallel channels. Many attempts have tried to generalize the Alamouti scheme to systems with larger antenna configurations, among them the ABBA code [57], but in all cases the optimization was done by trading one parameter (diversity order, rate of the precoder $R_p < 1/2$...). In this section, we present a ST-BICM design suited for a MIMO system with $n_t = 4$, design that uses the Alamouti structure to separate blocks of space-time rotated symbols. In our case, the rate of the precoder is still $R_p = 1/2$ even though we have more than two transmit antennas. However, the difference

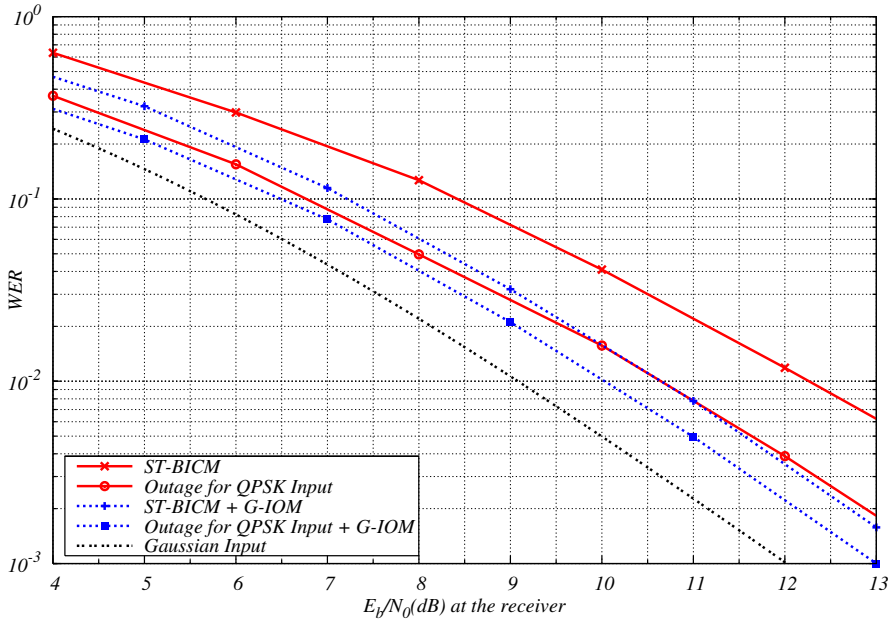

Figure 2.5: QPSK modulation, $n_t = s = n_c = 2$, $n_r = 1$, rate 1/2 16-state $(23, 35)$ convolutional code, interleaver size $N = 2048$ bits.

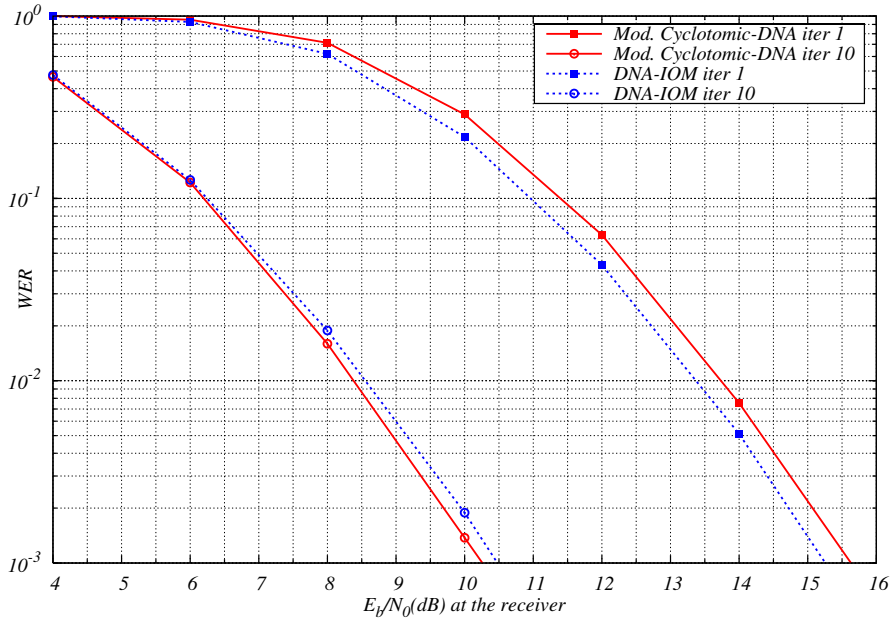

Figure 2.6: BPSK modulation, $n_t = 4$, $s = n_c = 2$, $n_r = 1$, rate 1/2 16-state $(23, 35)$ convolutional code, interleaver size $N = 2048$ bits.

with the $n_t = 2$ case is that interference among blocks is introduced. For this reason, we

look at the problem as if we had a Code-Division Multiple Access (CDMA) system with two users (represented by the two blocks), and inter-block interference becomes similar to inter-user interference in CDMA. There exists several methods to remove the inter-user interference in a CDMA system, and the most efficient algorithms are those that use soft information from a channel decoder [27][58]. In our case, we chose to remove the inter-block interference using the parallel interference cancellation (PIC) algorithm, that proves to be optimal in computer simulations in our context. The performance of this system under quasi-static fading and iterative detection and decoding proved to be close to system limits. All these points will be clarified in the sequel.

2.7.2 Matrix-Alamouti scheme

In a ST-BICM, the cardinality of the generated set of vectors is given by $|\Omega| = 2^{mN_t}$, m being the number of bits per bi-dimensional QAM constellation symbol. The cardinality increases exponentially with n_t thus leading to a high decoding complexity at the receiver. If $n_t = 4$, $m = 2$, and $R_p \cdot s = 2$ for instance, $|\Omega| = 2^{16} = 65536$, which is intractable for practical applications. In the sequel, we investigate a non-linear space-time precoding scheme that combines the symbols in a matrix-Alamouti form [24]. Let us first define the operators $mat(.)$ and $vec(.)$: $mat(.)$ transforms a vector into a matrix by putting its last sub-part beneath its first sub-part, while $vec(.)$ performs exactly the inverse task. Let us also define the operator ‡ where:

$$\mathbf{u}^{\ddagger} = vec(\mathbf{U}^{\dagger}) \tag{2.31}$$

where $\mathbf{u}$ is a complex vector and $\mathbf{U}$ is any complex matrix. In the new model, $\mathbf{x}$ is rewritten as a 1×16 row vector:

$$\mathbf{x} = \begin{bmatrix} \mathbf{x}_1 & \mathbf{x}_2 & -\mathbf{x}_2^{\ddagger} & \mathbf{x}_1^{\ddagger} \end{bmatrix} \tag{2.32}$$

where $\mathbf{x}_1 = \mathbf{z}_1\mathbf{S}$ and $\mathbf{x}_2 = \mathbf{z}_2\mathbf{S}$ are space-time vectors in $\mathbb{C}^4$, obtained by multiplying a QAM symbol vector $\mathbf{z}_i \in (\text{M-QAM})^4$ with a 4×4 space-time rotation $\mathbf{S}$. Many design criteria for $n_t = 2$ antennas lead to different classes of rotations $\mathbf{S}$ as found in [16][43][46], or IOM and G-IOM rotations presented in section 2.6. Although the rate of the precoder in (2.32) is $R_p = \frac{1}{2}$, it is capable of converting the set of cardinality $|\Omega| = 2^{mN_t}$ onto a smaller set Ω_c of cardinality $|\Omega_c| = 2^{\frac{mN_t}{2}}$, and this is due to the orthogonality inherent to the Alamouti structure. In addition, the bound on the diversity of this scheme is exactly that of a system with $n_t = 2$, as it creates two "parallel" streams via $\mathbf{x}_1$ and $\mathbf{x}_2$ that have a diversity order of $2 \times n_r$ each, independently from the coding rate R_c in (2.24). With a conventional $4 \times n_r$ system, when $R_c \to 1$, full spreading with $s = 4$ is mandatory to recover full channel diversity, yielding an exponential increase in detection complexity.

With the scheme proposed in this section, full spreading means $s = 2$. The purpose is then to drastically reduce the complexity at the detector while recovering maximum diversity with high coding rates.

By replacing $\mathbf{x}$ in (2.21) by its form in (2.32), we get a slightly different channel model than the one of (2.21) and (2.22) as follows:

$$\begin{bmatrix} \mathbf{y}_1 & \mathbf{y}_2 \end{bmatrix} = \begin{bmatrix} \mathbf{x}_1 & \mathbf{x}_2 & -\mathbf{x}_2^{\ddagger} & \mathbf{x}_1^{\ddagger} \end{bmatrix} \begin{bmatrix} \mathbf{H}_{b1} & 0 \\ \mathbf{H}_{b2} & 0 \\ 0 & \mathbf{H}_{b1} \\ 0 & \mathbf{H}_{b2} \end{bmatrix} + \begin{bmatrix} \mathbf{w}_1 & \mathbf{w}_2 \end{bmatrix} \tag{2.33}$$

where all vectors $\mathbf{y}_1$, $\mathbf{y}_2$, $\mathbf{w}_1$ and $\mathbf{w}_2$ are in $\mathbb{C}^{2n_r}$, and:

$$\mathbf{H}_{b1} = \begin{bmatrix} \mathbf{H}_1 & 0 \\ 0 & \mathbf{H}_1 \end{bmatrix} \; ; \; \mathbf{H}_{b2} = \begin{bmatrix} \mathbf{H}_2 & 0 \\ 0 & \mathbf{H}_2 \end{bmatrix}$$

where $\mathbf{H}_1$ and $\mathbf{H}_2$ are $2 \times n_r$ channel coefficients matrices. We can write the received signal vectors from (2.33) as follows:

$$\mathbf{y}_1 = \mathbf{x}_1\mathbf{H}_{b1} + \mathbf{x}_2\mathbf{H}_{b2} + \mathbf{w}_1 \tag{2.34}$$

$$\mathbf{y}_2 = -\mathbf{x}_2^{\ddagger}\mathbf{H}_{b1} + \mathbf{x}_1^{\ddagger}\mathbf{H}_{b2} + \mathbf{w}_2 \tag{2.35}$$

The new expressions for $\mathbf{y}_1$ and $\mathbf{y}_2$ from (2.34) and (2.35) become:

$$\begin{aligned} \mathbf{Y}_1 = mat(\mathbf{y}_1) &= mat(\mathbf{x}_1)\mathbf{H}_1 + mat(\mathbf{x}_2)\mathbf{H}_2 + mat(\mathbf{w}_1) \\ &= \mathbf{G}_1\mathbf{H}_1 + \mathbf{G}_2\mathbf{H}_2 + \mathbf{W}_1 \end{aligned} \tag{2.36}$$

$$\begin{aligned} \mathbf{Y}_2 = mat(\mathbf{y}_2) &= mat\left(-\mathbf{x}_2^{\ddagger}\right)\mathbf{H}_1 + mat\left(\mathbf{x}_1^{\ddagger}\right)\mathbf{H}_2 + mat(\mathbf{w}_2) \\ &= -\mathbf{G}_2^{\dagger}\mathbf{H}_1 + \mathbf{G}_1^{\dagger}\mathbf{H}_1 + \mathbf{W}_2 \end{aligned} \tag{2.37}$$

where $\mathbf{G}_1$ and $\mathbf{G}_1$ are 2×2 matrices, and $\mathbf{W}_1$ and $\mathbf{W}_2$ are $2 \times n_r$ matrices.
In order to recover the transmit diversity, the combining scheme in [24] has to be performed on (2.36) and (2.37). However, as matrix multiplication is not commutative, two combining schemes can be implemented.

First combining scheme - FCS

We can write the combined versions of $\mathbf{G}_1$ and $\mathbf{G}_2$ as follows:

$$\begin{aligned}\mathbf{\Gamma}_1 &= \mathbf{H}_1^\dagger \mathbf{Y}_1 + \mathbf{Y}_2^\dagger \mathbf{H}_2 \\ &= \mathbf{H}_1^\dagger \mathbf{G}_1 \mathbf{H}_1 + \mathbf{H}_2^\dagger \mathbf{G}_1 \mathbf{H}_2 + \mathbf{H}_1^\dagger \mathbf{W}_1 + \mathbf{W}_2^\dagger \mathbf{H}_2 \end{aligned} \tag{2.38}$$

$$\begin{aligned}\mathbf{\Gamma}_2 &= \mathbf{H}_2^\dagger \mathbf{Y}_1 - \mathbf{Y}_2^\dagger \mathbf{H}_1 \\ &= \mathbf{H}_1^\dagger \mathbf{G}_2 \mathbf{H}_1 + \mathbf{H}_2^\dagger \mathbf{G}_2 \mathbf{H}_2 + \mathbf{H}_2^\dagger \mathbf{W}_1 - \mathbf{W}_2^\dagger \mathbf{H}_1 \end{aligned} \tag{2.39}$$

Although this combining scheme introduces colored noise, it is capable of totally removing the inter-block interference. However, it gives an estimate of the signal as $\mathbf{H}_i^\dagger \mathbf{G}_j \mathbf{H}_i$ that is not of the form of the matched filter (i.e. $\mathbf{H}_i^\dagger \mathbf{H}_i$), thus it does not recover all the transmit diversity. Indeed, for $n_r = 2$ for instance, the equivalent channel matrix after combining is given by:

$$vec(\mathbf{H}_1^\dagger \mathbf{G}_1 \mathbf{H}_1 + \mathbf{H}_2^\dagger \mathbf{G}_1 \mathbf{H}_2) \triangleq$$

$$\mathbf{z}_1\mathbf{S} \begin{bmatrix} |h_{11}|^2 + |h_{31}|^2 & h_{12}^* h_{11} + h_{32}^* h_{31} & h_{11}^* h_{12} + h_{31}^* h_{32} & |h_{12}|^2 + |h_{32}|^2 \\ h_{21}^* h_{11} + h_{41}^* h_{31} & h_{22}^* h_{11} + h_{42}^* h_{31} & h_{21}^* h_{12} + h_{41}^* h_{32} & h_{22}^* h_{12} + h_{42}^* h_{32} \\ h_{11}^* h_{21} + h_{31}^* h_{41} & h_{12}^* h_{21} + h_{32}^* h_{41} & h_{11}^* h_{22} + h_{31}^* h_{42} & h_{12}^* h_{22} + h_{32}^* h_{42} \\ |h_{21}|^2 + |h_{41}|^2 & h_{22}^* h_{21} + h_{42}^* h_{41} & h_{21}^* h_{22} + h_{41}^* h_{42} & |h_{22}|^2 + |h_{42}|^2 \end{bmatrix} \tag{2.40}$$

We observe from (2.40) that only 2 of the 4 symbols of $\mathbf{z}_1\mathbf{S}$ are multiplied by Nakagami distributed random variables of order 4, thus the overall system diversity is limited to 4. The same reasoning applies to $\mathbf{\Gamma}_2$.

Second combining scheme - SCS

By permuting the matrix product of the first combining scheme, we get other versions of $\mathbf{\Gamma}_1$ and $\mathbf{\Gamma}_2$ denoted by $\mathbf{G}_{c1}$ and $\mathbf{G}_{c2}$ in the sequel:

$$\begin{aligned}\mathbf{G}_{c1} &= \mathbf{Y}_1 \mathbf{H}_1^\dagger + \mathbf{H}_2 \mathbf{Y}_2^\dagger \\ &= \mathbf{G}_1 \mathbf{H}_1 \mathbf{H}_1^\dagger + \mathbf{H}_2^\dagger \mathbf{H}_2 \mathbf{G}_1 + \mathbf{G}_2 \mathbf{H}_2 \mathbf{H}_1^\dagger - \mathbf{H}_2 \mathbf{H}_1^\dagger \mathbf{G}_2 + \mathbf{W}_1 \mathbf{H}_1^\dagger + \mathbf{H}_2 \mathbf{W}_2^\dagger \end{aligned} \tag{2.41}$$

$$\begin{aligned}\mathbf{G}_{c2} &= \mathbf{Y}_1 \mathbf{H}_2^\dagger - \mathbf{H}_1 \mathbf{Y}_2^\dagger \\ &= \mathbf{H}_1 \mathbf{H}_1^\dagger \mathbf{G}_2 + \mathbf{G}_2 \mathbf{H}_2 \mathbf{H}_2^\dagger + \mathbf{G}_1 \mathbf{H}_1 \mathbf{H}_2^\dagger - \mathbf{H}_1 \mathbf{H}_2^\dagger \mathbf{G}_1 + \mathbf{W}_1 \mathbf{H}_2^\dagger - \mathbf{H}_1 \mathbf{W}_2^\dagger \end{aligned} \tag{2.42}$$

The first two terms of (2.41) and (2.42) are the desired signal estimates. The second two terms are the interference introduced by the combining scheme, and the last two terms are the colored noise components. In this scheme we are able to recover the transmit diversity via the first two terms of (2.41) and (2.42), as shown in the following equation for $n_r = 2$:

$$vec(\mathbf{G}_1\mathbf{H}_1\mathbf{H}_1^{\dagger} + \mathbf{H}_2\mathbf{H}_2^{\dagger}\mathbf{G}_1) \triangleq \mathbf{z}_1\mathbf{S}\mathbf{H}_{S_1} \tag{2.43}$$

where

$$\mathbf{H}_{S_1} = \begin{bmatrix} A_1 + A_3 & h_{31}^* h_{41} + h_{32}^* h_{42} & h_{11}h_{21}^* + h_{12}h_{22}^* & 0 \\ h_{31}h_{41}^* + h_{32}h_{42}^* & A_1 + A_4 & 0 & h_{11}h_{21}^* + h_{12}h_{22}^* \\ h_{11}^* h_{21} + h_{12}^* h_{22} & 0 & A_2 + A_3 & h_{31}^* h_{41} + h_{32}^* h_{42} \\ 0 & h_{11}^* h_{21} + h_{12}^* h_{22} & h_{31}h_{41}^* + h_{32}h_{42}^* & A_2 + A_4 \end{bmatrix} \tag{2.44}$$

and

$$A_1 = |h_{11}|^2 + |h_{12}|^2, \quad A_2 = |h_{21}|^2 + |h_{22}|^2, \quad A_3 = |h_{31}|^2 + |h_{32}|^2, \quad A_4 = |h_{41}|^2 + |h_{42}|^2$$

By symmetry, we get:

$$\mathbf{H}_{S_2} = \mathbf{H}_{S_1}^{\dagger} = \begin{bmatrix} A_1 + A_3 & h_{31}h_{41}^* + h_{32}h_{42}^* & h_{11}^* h_{21} + h_{12}^* h_{22} & 0 \\ h_{31}^* h_{41} + h_{32}^* h_{42} & A_1 + A_4 & 0 & h_{11}^* h_{21} + h_{12}^* h_{22} \\ h_{11}h_{21}^* + h_{12}h_{22}^* & 0 & A_2 + A_3 & h_{31}h_{41}^* + h_{32}h_{42}^* \\ 0 & h_{11}h_{21}^* + h_{12}h_{22}^* & h_{31}^* h_{41} + h_{32}^* h_{42} & A_2 + A_4 \end{bmatrix} \tag{2.45}$$

As shown in (2.43), every symbol in $\mathbf{z}_1\mathbf{S}$ and $\mathbf{z}_2\mathbf{S}$ undergoes Nakagami distributed random variables of order 4, which leads to an overall system diversity of 8.

However, this combining scheme introduces considerable interference along with colored noise. In an uncoded system, this combining scheme does not converge as the received signal constellation is not clearly delimited within distinct Voronoï regions, even for significantly high signal-to-noise ratios. This scenario is similar to that of multi-user detection (MUD) in heavily loaded CDMA systems, where users introduce interference to each others. Hence, we can use detection techniques known for coded MUD-CDMA as in [27][58] and their references to get reliable estimates of the signals. Therefore, we choose to map one interleaved codeword through $\mathbf{z}_1$, and another interleaved codeword using $\mathbf{z}_2$, as if we had two "virtual" users. This results in sending a frame that has the length of two codewords. The transmitter for the proposed system is shown in Fig. 2.7.

In our case, as convolutional codes are employed, one can send a unique codeword instead of two. However, we have to make sure that the coded bits that are mapped onto

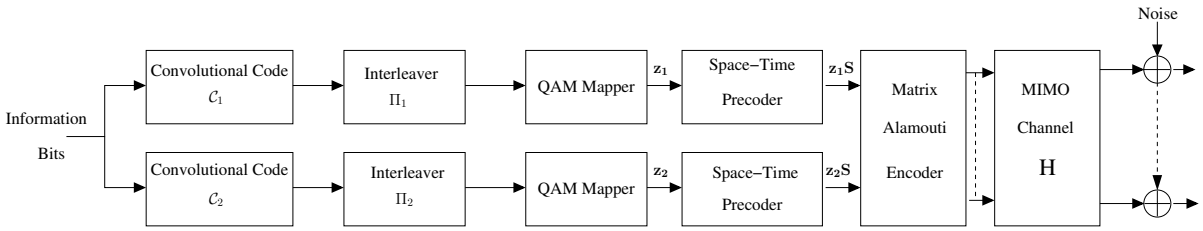

Figure 2.7: Transmitter model for matrix-Alamouti encoded ST-BICM.

$\mathbf{z}_1$ are far from the coded bits that are mapped onto $\mathbf{z}_2$ in the trellis of the code, and the two parts of the code should be interleaved separately. In this way we avoid introducing inter-block interference at the transmitter.

2.7.3 Iterative joint detection and decoding

Let us write (2.41) and (2.42) as:

$$\mathbf{g}_{c1} = vec(\mathbf{G}_{c1}) = \mathbf{z}_1\mathbf{S}\mathbf{H}_{S_1} + \mathbf{z}_2\mathbf{S}\mathbf{H}_{I_1} + vec(\mathbf{W}_1\mathbf{H}_1^\dagger + \mathbf{H}_2\mathbf{W}_2^\dagger) \tag{2.46}$$

$$\mathbf{g}_{c2} = vec(\mathbf{G}_{c2}) = \mathbf{z}_2\mathbf{S}\mathbf{H}_{S_2} + \mathbf{z}_1\mathbf{S}\mathbf{H}_{I_2} + vec(\mathbf{W}_1\mathbf{H}_2^\dagger - \mathbf{H}_1\mathbf{W}_2^\dagger) \tag{2.47}$$

where $\mathbf{H}_{S_1}$ and $\mathbf{H}_{S_2}$ are taken from (2.44) and (2.45). In addition, we have:

$$\mathbf{H}_{I_1} = \begin{bmatrix} 0 & -h_{41}h_{11}^* - h_{42}h_{22}^* & h_{31}h_{21}^* + h_{32}h_{22}^* & 0 \\ -h_{31}h_{21}^* - h_{32}h_{22}^* & B & 0 & h_{31}h_{21}^* + h_{32}h_{22}^* \\ h_{41}h_{11}^* + h_{42}h_{22}^* & 0 & -B & -h_{41}h_{11}^* - h_{42}h_{22}^* \\ 0 & h_{41}h_{11}^* + h_{42}h_{22}^* & -h_{31}h_{21}^* - h_{32}h_{22}^* & 0 \end{bmatrix}$$

where

$$B = h_{31}h_{11}^* + h_{32}h_{12}^* - h_{41}h_{21}^* - h_{42}h_{22}^*$$

and $\mathbf{H}_{I_2} = \mathbf{H}_{I_1}^\dagger$ by symmetry.

Now let N denote the number of M-QAM symbols in one convolutional codeword (i.e. there are $2N$ M-QAM symbols in a frame for both convolutional codes). In order to get reliable estimates of the combined signals, one has to efficiently remove interference from (2.46) and (2.47). This gives us:

$$\begin{aligned} \widetilde{\mathbf{g}_{c1}} &= \mathbf{g}_{c1} - \widetilde{\mathbf{z}_2}\mathbf{S}\mathbf{H}_{I_1} \\ &= \mathbf{z}_1\mathbf{S}\mathbf{H}_{S_1} + (\mathbf{z}_2 - \widetilde{\mathbf{z}_2})\mathbf{S}\mathbf{H}_{I_1} + vec(\mathbf{W}_1\mathbf{H}_1^\dagger + \mathbf{H}_2\mathbf{W}_2^\dagger) \end{aligned} \tag{2.48}$$

$$\begin{aligned}\widetilde{\mathbf{g}_{c2}} &= \mathbf{g}_{c2} - \widetilde{\mathbf{z}_1}\mathbf{S}\mathbf{H}_{I_2} \\ &= \mathbf{z}_2\mathbf{S}\mathbf{H}_{S_2} + (\mathbf{z}_1 - \widetilde{\mathbf{z}_1})\mathbf{S}\mathbf{H}_{I_2} + vec(\mathbf{W}_2\mathbf{H}_2^{\dagger} - \mathbf{H}_1\mathbf{W}_1^{\dagger}) \end{aligned} \quad (2.49)$$

The first term in (2.48) and (2.49) is the desired signal part, and the other two are the residual interference and colored noise terms. In this case, the likelihoods of $\widetilde{\mathbf{g}_{c1}}$ and $\widetilde{\mathbf{g}_{c2}}$ follow the multivariate Gaussian distribution as:

$$p\left(\widetilde{\mathbf{g}_{c1}} \mid \mathbf{z}_1, \mathbf{S}\mathbf{H}_{S_1}\right) \sim \mathcal{N}\left(\mathbf{z}_1\mathbf{S}\mathbf{H}_{S_1}, \mathbf{\Sigma}_1\right); \quad p\left(\widetilde{\mathbf{g}_{c2}} \mid \mathbf{z}_2, \mathbf{S}\mathbf{H}_{S_2}\right) \sim \mathcal{N}\left(\mathbf{z}_2\mathbf{S}\mathbf{H}_{S_2}, \mathbf{\Sigma}_2\right)$$

where

$$\mathbf{\Sigma}_1 = \mathbb{E}\left[\left(\widetilde{\mathbf{g}_{c1}} - \mathbf{z}_1\mathbf{S}\mathbf{H}_{S_1}\right)^{\dagger}\left(\widetilde{\mathbf{g}_{c1}} - \mathbf{z}_1\mathbf{S}\mathbf{H}_{S_1}\right)\right] \quad (2.50)$$

$$\mathbf{\Sigma}_2 = \mathbb{E}\left[\left(\widetilde{\mathbf{g}_{c2}} - \mathbf{z}_2\mathbf{S}\mathbf{H}_{S_2}\right)^{\dagger}\left(\widetilde{\mathbf{g}_{c2}} - \mathbf{z}_2\mathbf{S}\mathbf{H}_{S_2}\right)\right] \quad (2.51)$$

Let us define:

$$V_1\left(\mathbf{z}_1\right) = \widetilde{\mathbf{g}_{c1}} - \mathbf{z}_1\mathbf{S}\mathbf{H}_{S_1} \quad (2.52)$$

$$V_2\left(\mathbf{z}_2\right) = \widetilde{\mathbf{g}_{c2}} - \mathbf{z}_2\mathbf{S}\mathbf{H}_{S_2} \quad (2.53)$$

After the interference and colored noise covariance matrices $\mathbf{\Sigma}_i$ are computed, the soft-input soft-output (SISO) detector computes the extrinsic probabilities $\xi_i\left(c_j\right)$ that the j^{th} bit of codeword i is equal to 1, as given by the slight modification of (1.23) as:

$$\xi_1\left(c_\ell\right) = \frac{\sum_{\mathbf{z}_1' \in \Omega_c(c_\ell=1)} exp\left[-V_1\left(\mathbf{z}'_1\right)\mathbf{\Sigma}_1^{-1}V_1\left(\mathbf{z}_1'\right)^{\dagger}\right]\prod_{r\neq\ell}\pi_1\left(c_r\right)}{\sum_{\mathbf{z}_1 \in \Omega_c} exp\left[-V_1\left(\mathbf{z}_1\right)\mathbf{\Sigma}_1^{-1}V_1\left(\mathbf{z}_1\right)^{\dagger}\right]\prod_{r\neq\ell}\pi_1\left(c_r\right)} \quad (2.54)$$

and

$$\xi_2\left(c_\ell\right) = \frac{\sum_{\mathbf{z}_2' \in \Omega_c(c_\ell=1)} exp\left[-V_2\left(\mathbf{z}_2'\right)\mathbf{\Sigma}_2^{-1}V_2\left(\mathbf{z}_2'\right)^{\dagger}\right]\prod_{r\neq\ell}\pi_2\left(c_r\right)}{\sum_{\mathbf{z}_2 \in \Omega_c} exp\left[-V_2\left(\mathbf{z}_2\right)\mathbf{\Sigma}_2^{-1}V_2\left(\mathbf{z}_2\right)^{\dagger}\right]\prod_{r\neq\ell}\pi_2\left(c_r\right)} \quad (2.55)$$

Where $\pi_1\left(c_r\right)$ and $\pi_2\left(c_r\right)$ are *a priori* probabilities generated by soft-input soft-output (SISO) decoders for the 1^{st} and the 2^{nd} convolutional codes respectively. As shown in Fig. 2.8 below, the extrinsic probabilities are then fed back from the SISO detectors to their respective SISO decoders that use the forward-backward (BCJR) algorithm to give *a posteriori* probabilities of the coded bits. In addition, the decoders give back *a priori* $\pi_1\left(c_r\right)$ and $\pi_2\left(c_r\right)$ probabilities to their respective SISO detectors as in the classical receiver, and also to the detectors of different indices in order to compute the covariance

matrices $\mathbf{\Sigma}_i$ and better remove the interference at each iteration. Unlike the conventional receiver where the extrinsic probabilities generated by the detector are computed once at the first iteration using (1.23), the extrinsic probabilities (2.54) and (2.55) in this case are computed at each iteration as the $\mathbf{\Sigma}_i$ matrices change. However, in most cases, this linear increase in complexity is negligible compared to the exponential increase in complexity introduced by a signal set of higher cardinality. Let us take the following example: suppose we have a conventional ST-BICM with $R_c = 3/4$ and $n_t = 4$ transmit antennas. In order to recover maximal diversity, we need to use a space-time precoder with $s = 4$. This gives a cardinality of the space-time signal vector as $|\Omega| = 2^{mN_t} = 2^{16m}$, over which the exhaustive search to compute the extrinsic information in (1.23) is performed. However, with the matrix-Alamouti scheme, $s = 2$ is sufficient to recover the diversity. This gives $|\Omega_c| = 2^{8m}$, using a higher order M-QAM constellation to compensate $R_p = 1/2$. So even if we need t iterations for the receiver to converge, we still have a drastic complexity reduction, as $2 \times t \times 2^{8m} \ll 2^{16m}$.

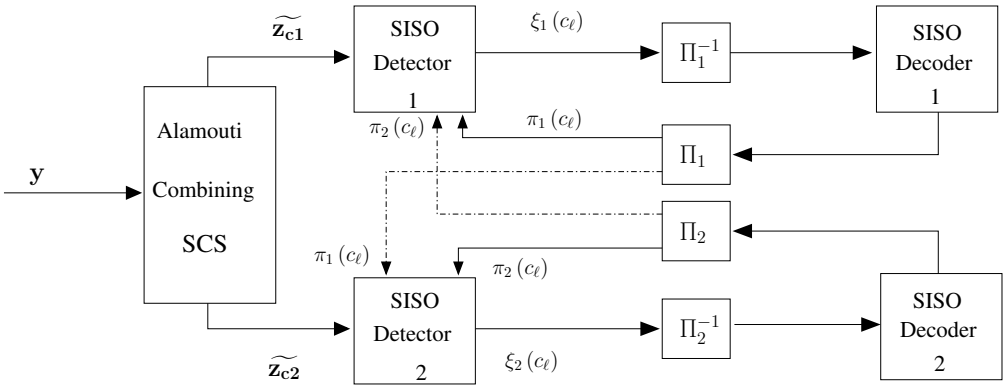

Figure 2.8: Iterative receiver model for matrix-Alamouti encoded ST-BICM

In computer simulations presented in the next section, vectors $\mathbf{z}_1$ and $\mathbf{z}_2$ in (2.50) – (2.53) were replaced by their soft estimates. Thus, we have:

$$\mathbf{\Sigma}_1 \backsimeq \frac{1}{N} \sum_{i=1}^{\frac{N}{4}} \left[(\widetilde{\mathbf{g}_{c1i}} - \mathbf{z}_{1i}\mathbf{S}\mathbf{H}_{S_1})^\dagger (\widetilde{\mathbf{g}_{c1i}} - \mathbf{z}_{1i}\mathbf{S}\mathbf{H}_{S_1}) \right] \tag{2.56}$$

$$\mathbf{\Sigma}_2 \backsimeq \frac{1}{N} \sum_{i=1}^{\frac{N}{4}} \left[(\widetilde{\mathbf{g}_{c2i}} - \mathbf{z}_{2i}\mathbf{S}\mathbf{H}_{S_2})^\dagger (\widetilde{\mathbf{g}_{c2i}} - \mathbf{z}_{2i}\mathbf{S}\mathbf{H}_{S_2}) \right] \tag{2.57}$$

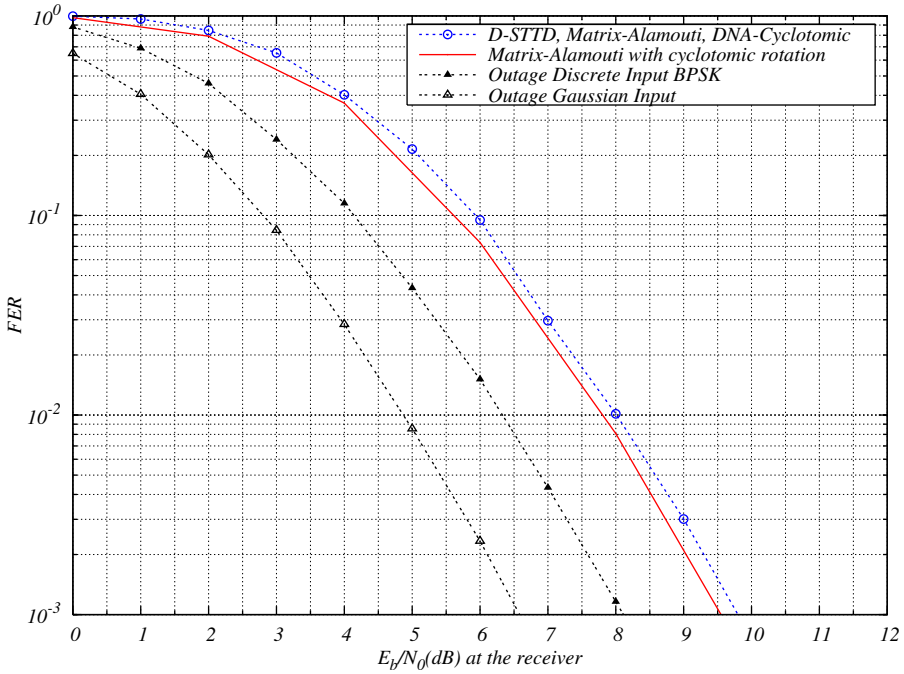

Figure 2.9: Performance for a frame size of 4096 coded bits (2×2048 for matrix-Alamouti), $R_c = 1/2$, $n_t = 4$ and $n_r = 2$ antennas.

2.7.4 Simulation results

In this section, frame error probabilities are illustrated versus signal-to-noise ratios and frame size for $n_t = 4$ and $n_r = 2$. Comparisons are done with respect to discrete input and Gaussian input outage probabilities. The convolutional code is the half-rate 16-state $(23, 35)_8$ non-recursive non-systematic code (NRNSC) and the interleavers are the optimized interleavers from [17]. Fig. 2.9 shows the frame error rate performance for different a frame sizes of 4096 coded bits. The matrix-Alamouti scheme is compared to the DNA-cyclotomic rotations and the D-STTD scheme first proposed in [59] and included in the IEEE802.11n standard, all at a coding rate $R_c = 1/2$. As DNA-cyclotomic rotations are full-rate (i.e. $R_p = 1$), it was simulated with BPSK modulation in order to preserve the same spectral efficiency with the other two schemes that are simulated with QPSK modulations. In fact, with half-rate coding, the matrix $\mathbf{S}$ of matrix-Alamouti scheme does not need to spread the symbol vectors, as diversity can be ensured with $s = 1$. In this case, our scheme performs equally with the two others. However, by setting $\mathbf{S} = \mathbf{S_{Cyclo}}$ from (2.3), we observe a gain with respect to the other schemes. This for sure is at the cost of a slight additional complexity, as $s = 2$ in this case. Fig. 2.10 shows the performance

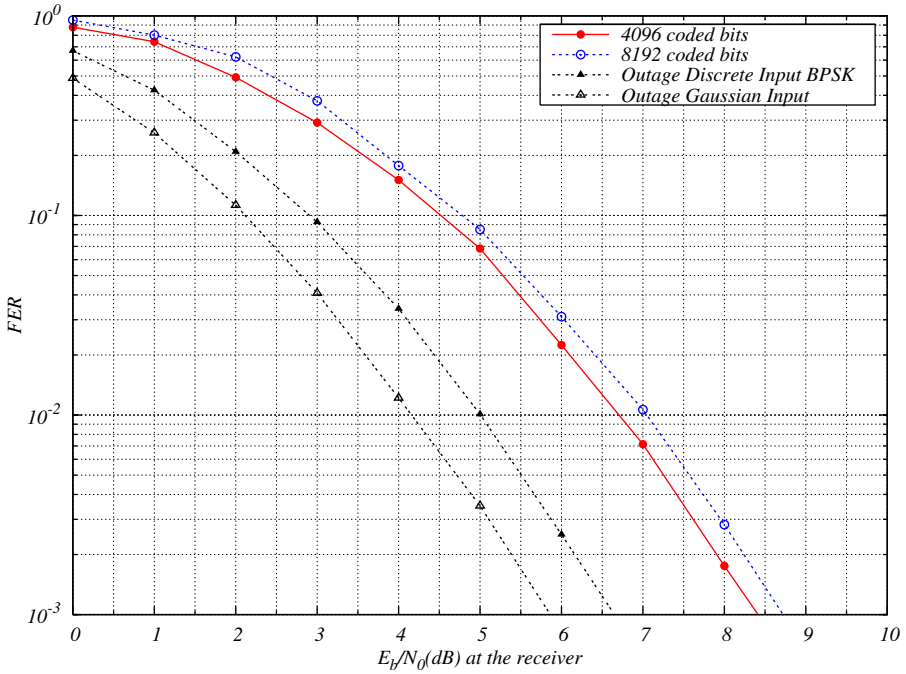

Figure 2.10: Performance for $R_c = 2/3$, BPSK modulation, $n_t = 4$ and $n_r = 2$ antennas.

Alamouti scheme with $R_c = 2/3$, that is the half-rate 16-state $(23, 35)_8$ NRNSC code with puncturing, with BPSK modulation. When $\mathbf{S} = \mathbf{S_{Cyclo}}$, the coded modulation achieves full diversity with $s = 2$ as explained in section 2.7.2. With this coding rate, the D-STTD scheme does not ensure maximum diversity, and the standard ST-BICM requires a spreading factor of $s = 4$ as defined in 2.24 to achieve maximum diversity. Finally, Fig. 2.11 compares the performance of the matrix-Alamouti scheme with the DNA-cyclotomic scheme for different frame sizes at a signal-to-noise ratio of 9dB. We can see that our scheme is more robust to an increase in the frame size than the conventional scheme.

2.8 Outage-approaching turbo codes for the multiple-antenna channels

2.8.1 Introduction

As shown in section 2.3, the frame error rate of uncoded space-time signaling is upper-bounded by a quantity that varies as $\log^d(n)$, where d is the diversity order. In order to approach the outage probability limit, the frame error rate of any given coding scheme

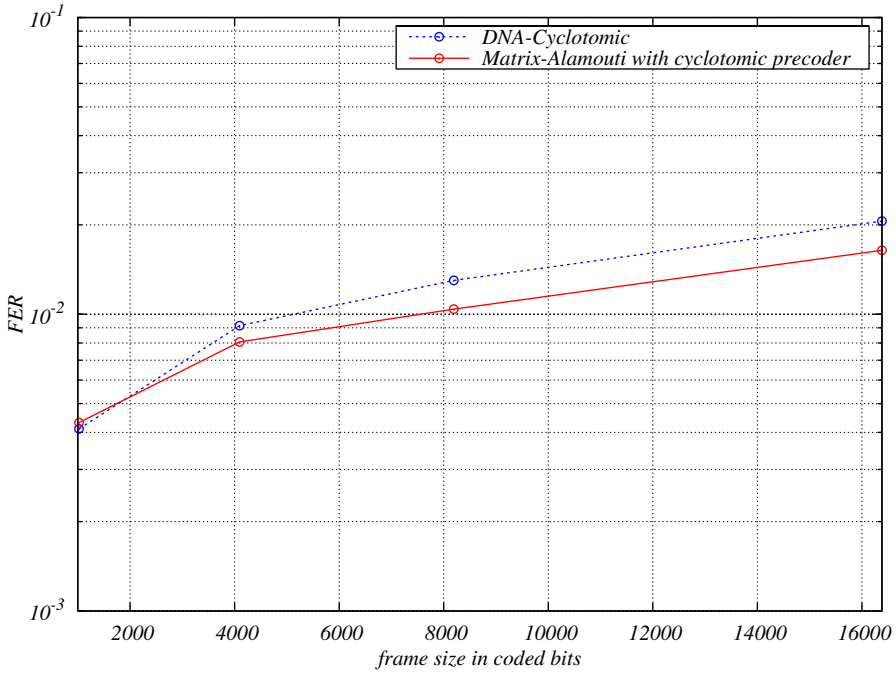

Figure 2.11: Frame error rate versus frame size, $R_c = 1/2$, $E_b/N_0 = 9$ dB, $n_t = 4$ and $n_r = 2$ antennas.

should be independent of the block length [9, 15]. Therefore, such space-time coding techniques will fail in approaching the outage capacity limit of the quasi-static MIMO channel. Algebraic space-time codes described in section 2.2 and any convolutionally/algebraically coded STBC also fail in approaching the outage limit. Hence, our objectives are

- Design a space-time code based on state multiplexing [52] and turbo encoding [60][61] in order to achieve near outage limit performance.
- Control the detection/decoding complexity and propose relatively low complexity schemes.
- Make the word error probability insensitive to the block length. This is the interleaving gain of turbo codes translated to the field of non-ergodic fading channels as discovered in [15][9].

2.8.2 Code multiplexing over channel states

The physical channel we consider is a quasi-static frequency non-selective MIMO channel with n_t transmit antennas and n_r receive antennas. On a Gaussian channel, the pairwise

error probability supposing the zero codeword is emitted by a linear encoder is given by:

$$P(0 \to c) = Q\left(\sqrt{\frac{2R_cE_b}{N_0}\omega_H(c)}\right) \tag{2.58}$$

where $\omega_H(c)$ is the Hamming weight of the codeword and E_b/N_0 is the signal-to-noise ratio. Now, on a Rayleigh fading channel with D_{st} states, the conditional pairwise error probability becomes:

$$P(0 \to c) = Q\left(\sqrt{\frac{2R_cE_b}{N_0}\sum_{i=0}^{D_{st}}\omega_i(c)|h_i|^2}\right) \tag{2.59}$$

where $\omega_i(c)$ represents the partial weight of the codeword c undergoing fading h_i, and $\sum_i \omega_i(c) = \omega_H(c)$. After performing a mathematical expectation over the channel states, we can upper-bound the pairwise error probability as:

$$P(0 \to c) \leq \frac{1}{2}\prod_{i=1}^{D_{st}}\frac{1}{1+\omega_i(c)\frac{RE_b}{N_0}} \tag{2.60}$$

Hence the diversity order $d(c)$ that can be achieved by the code is given by the number of non-zero partial weights $\omega_i(c)$. In addition, for high signal-to-noise ratios, the pairwise error probability behaves like:

$$P(0 \to c) \propto \frac{1}{\prod_{i=1}^{D_{st}}\omega_i(c)} \times \frac{1}{(E_b/N_0)^{d(c)}} \tag{2.61}$$

So our objectives are to first guarantee that $\forall i,\ \omega_i(c) \neq 0$, to attain maximum diversity, second to maximize the product $\prod_{i=1}^{D_{st}}\omega_i(c)$ and hence the coding gain. For this purpose, the authors in [52] proposed the "code multiplexer" defined as follows:

Definition 2. *The multiplexer is an intelligent switch that distributes turbo coded bits s_i over the D_{st} parallel sub-channels of the BO-channel.*

Actually, the multiplexer should be called "de-multiplexer" or equivalently "channel interleaver". We have chosen the word "multiplexer" in order to avoid any confusion with the interleaver denoted by $\mathbf{\Pi}$ used inside a turbo code. Fig. 2.12 shows two important multiplexing examples from [52] suite for a non-ergodic fading channel with $D_{st} = 2$ states. The two digits 1 and 2 represent the two states of the BO-channel. The symbol X represents a punctured parity bit. Note that in this chapter we will only consider half-rate codes multiplexed over two-state non-ergodic channels, but generalization to any rate codes on non-ergodic channels is straight-forward as long as $R_c \leq 1/D_{st}$.

Horizontal Multiplexer						
$\mathbf{s_1}$	1	1	1	1	1	1
$\mathbf{s_2}$	2	X	2	X	2	X
$\mathbf{s_3}$	X	2	X	2	X	2

H-π-diagonal Multiplexer						
$\mathbf{s_1}$	1	2	1	2	1	2
$\mathbf{s_2}$	2	X	2	X	2	X
$\pi^{-1}(\mathbf{s_3})$	X	1	X	1	X	1

Figure 2.12: Horizontal (top) and h-π-diagonal (bottom) multiplexers for a rate 1/2 parallel turbo code.

Proposition 1. *Let C be a rate 1/2 parallel turbo code transmitted on a 2-state channel and built from $RSC(g_1(x), g_2(x))$. Under horizontal state multiplexing and for any input weight ω, the number η of codewords in C with incomplete state diversity is*

$$\eta(\omega, d_{st} < 2) = 0 \quad \forall \ \ \omega \geq 2$$

Proof. For any non-zero turbo codeword, it is well-known that the Hamming weight of s_1 is $\omega \geq \omega_{min} = 2$ [61]. Also, the Hamming weight of both s_2 and s_3 must be positive despite puncturing. Hence, it is trivial that $d_{st} = 2$ since s_1 is always transmitted on the first channel state and (s_2, s_3) are transmitted on the second channel state. □

The recursive systematic convolutional constituent has constraint length $\nu + 1$. Its feedback generator polynomial is $g_1(x)$ and its forward generator polynomial is $g_2(x)$.

Definition 3. *A recursive systematic convolutional code is said to be a* full-span *convolutional code if the generators satisfy* $\deg(g_i(x)) = \nu$ *and* $g_i(0) = 1$*, for* $i = 1, 2$.

Trellis transitions outgoing from the 0-state and those incoming to the 0-state will be called *full-span transitions*, i.e. both bits are set to 1 on the transition label.

Proposition 2. *Let C be a rate 1/2 parallel turbo code transmitted on a 2-state channel and built from a full-span $RSC(g_1(x), g_2(x))$. Under h-π-diagonal state multiplexing and for any input weight ω, the number η of codewords in C with incomplete state diversity is*

$$\eta(\omega, d_{st} < 2) = 0 \quad \forall \ \ \omega \geq 2$$

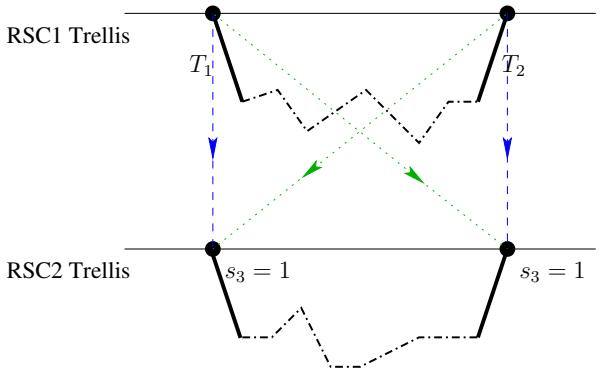

Figure 2.13: Trellis error events for input weight $\omega = 2$. The two interleaving configurations are indicated. Diversity is guaranteed by full-span transitions.

Proof. For $\omega = 2$ and $\omega = 3$: if a full-span transition is interleaved (via π) into a full-span transition, then state diversity is guaranteed. As shown in Fig. (2.13) and (2.15), one of the full-span transitions in RSC1 is converted into a full-span transition in RSC2.
For $\omega \geq 4$: Consider the case where $\omega = 4$. Except for the unique interleaving configuration depicted in Fig. (2.16), all turbo codewords exhibit $d_{st} = 2$ due to full-span transitions. Now, let $\chi_i(s_j) \in \{1, 2\}$ denote the BO-channel state over which the binary element s_j belonging to RSC_i is transmitted. We distinguish two cases when a critical configuration is transmitted on the channel.
Case 1: error event in RSC1 starts at state 1, $\chi_1(s_1) = 1$. Diversity is guaranteed by RSC1 because $\chi_1(s_2) = 2$.
Case 2: error event in RSC1 starts at state 2, $\chi_1(s_1) = 2$. Then, we distinguish two sub-cases:
Case 2.1: Information bit s_1 is set to 1 within the error event and hits state 1 yielding $\chi_1(s_1) = 1$. Hence, diversity is guaranteed by RSC1 without the help of RSC2.
Case 2.2: Information bit $s_1 = 1$ never hits state 1 in the trellis event of RSC1, $\chi_1(s_1) \neq 1$. This situation occurs because equality is not satisfied in (1.25) when $R_c = 1/2$ and $D_{st} = 3$, i.e. it is possible to create RSC1 codewords that never hit state 1. Thanks to the structure of the h-*pi*-diagonal multiplexer, at least one full-span transition in RSC2 has $\chi_2(s_3) = 1$ for $\chi_1(s_1) = 2$.
The same proof applies for $\omega > 4$. □

Example with RSC$(7, 5)_8$
A critical configuration is a configuration (or an event) in which the diversity is not

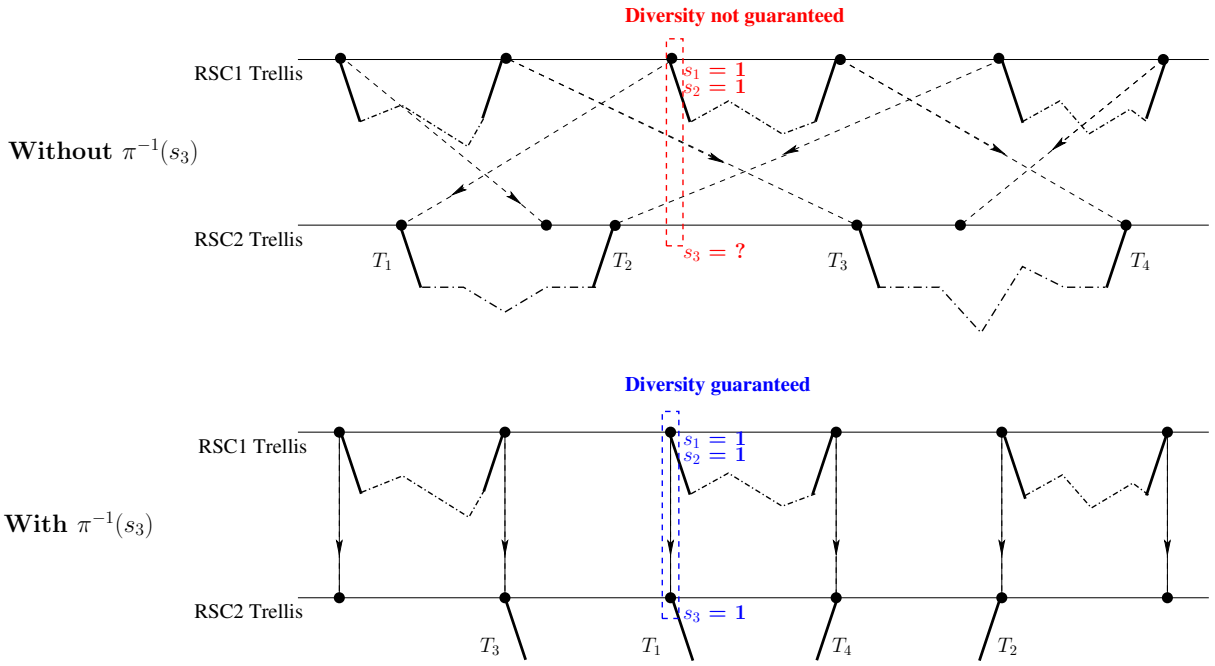

Figure 2.14: Effect of h-π-diagonal multiplexing on trellis events. Illustration for input weight $\omega = 6$ with and without de-interleaving of the second parity bit.

guaranteed by the first RSC alone, thus the receiver relies on the parity bit of RSC 2 to recover the diversity. Let us now give an example of critical configurations for $\omega = 4$ as defined in the proof of prop. 2. When $\chi_1(s_1) = 1$ and $\chi_1(s_2) = 2$, the RSC trellis is represented by the transition matrix

$$A_1 = \begin{bmatrix} 0 & 0 & D_1D_2LW & 0 \\ D_1D_2LW & 0 & L & 0 \\ 0 & D_1LW & 0 & D_2L \\ 0 & D_2L & 0 & D_1LW \end{bmatrix}$$

When $\chi_1(s_1) = 2$ and $\chi_1(s_2) = X$, the transition matrix is

$$A_2 = \begin{bmatrix} 0 & 0 & D_2D_3LW & 0 \\ D_2D_3LW & 0 & L & 0 \\ 0 & D_2LW & 0 & D_3L \\ 0 & D_3L & 0 & D_2LW \end{bmatrix}$$

The complete weight enumerator $T(W, D, L)$ of simple error events is given by the top left entry of the product $A_1A_2A_1A_2\ldots$ or $A_2A_1A_2A_1\ldots$ depending on the position of the outgoing transition. A critical configuration is given by a product of type $A_2(A_1A_2)^\ell$ for

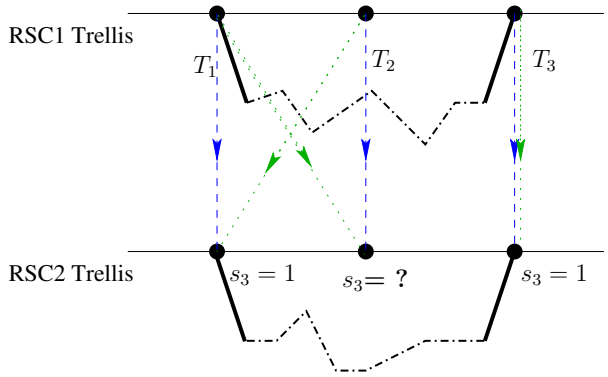

Figure 2.15: Trellis error events for input weight $\omega = 3$. The six interleaving configurations are equivalent to two distinct configurations.

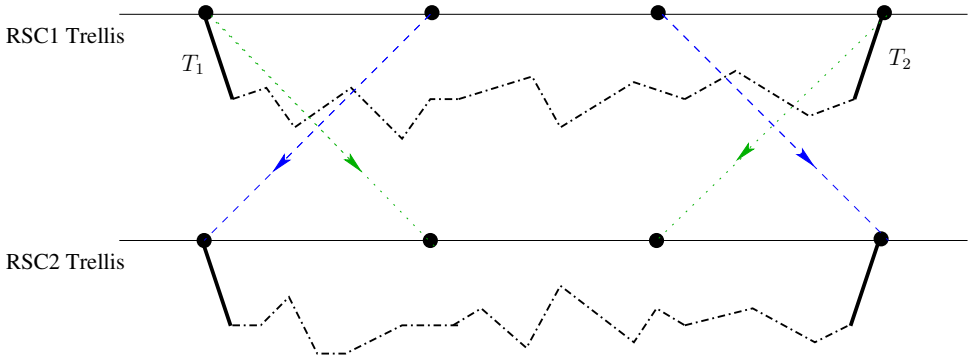

Figure 2.16: A critical configuration for full-span outgoing and incoming transitions. Input weight $\omega = 4$.

an event of length $2\ell + 1$. For $\ell = 1 \ldots 3$ no critical configurations are found. For $\ell = 4$, we have

$$T(W, D, L) = \ldots + (2D_1 D_2^5 D_3^4 + D_2^8 D_3^2) L^9 W^4 + \ldots$$

Therefore, the shortest critical event for $\omega = 4$ has length $L = 9$. It includes 4 information bits with $\chi_1(s_1 = 1) = 2$, 4 parity bits with $\chi_1(s_2 = 1) = 2$, and 2 punctured bits with $\chi_1(s_2 = 1) = X$. In this case, without a de-interleaver at the output of RSC 2, one cannot track the position of the parity bit s_3 at the output, as shown in Fig. 2.14. Therefore, we cannot make sure that full diversity is attained. However, a de-interleaver at the output of RSC 2 makes the coded bits of the turbo code synchronized within the trellis of the RSC constituents.

At this point, based on the study of η, the reader sees no difference between h-π-diagonal

and horizontal multiplexers. Indeed, propositions (1) and (2) state that both multiplexers achieve full state diversity. The error rate performance depends on the achieved diversity and on the so-called *coding gain* or *product distance* defined by the product $\omega_1\omega_2$ of partial Hamming weights. Now, it should be clear that horizontal multiplexing shows a great unbalance between ω_1 and ω_2. As an example, for input weight $\omega = 2$, consider RSC(7,5) error events of length $L = 4{+}3i$ and total Hamming weight $w_H = 6{+}2i$, $i = 0 \ldots (N{-}4)/3$. For horizontal multiplexing, $\omega_1 = 2$ and $\omega_2 = 4 + 2i$. Therefore, its coding gain behaves as $O(N)$. For h-π-diagonal multiplexing, $\omega_1 = \omega_2 = 3 + i$. Hence, the coding gain of h-π-diagonal multiplexing increases as $O(N^2)$. The loss is even more dramatic for $\omega = 3$. The latter is neglected on the Gaussian channel since its contribution to the error rate performance is $O(1/N)$. On non-ergodic fading channels, when $\omega = 3$, turbo codewords satisfying $w_H(s_2) >> 1$ and $w_H(s_3) >> 1$ will suffer from the unbalance of horizontal multiplexing. A comparison between h-π-diagonal and horizontal multiplexers is illustrated in Fig. 2.18 with 2 transmit antennas and a QPSK modulation.

2.8.3 Word error rate performance with $n_t = 2$

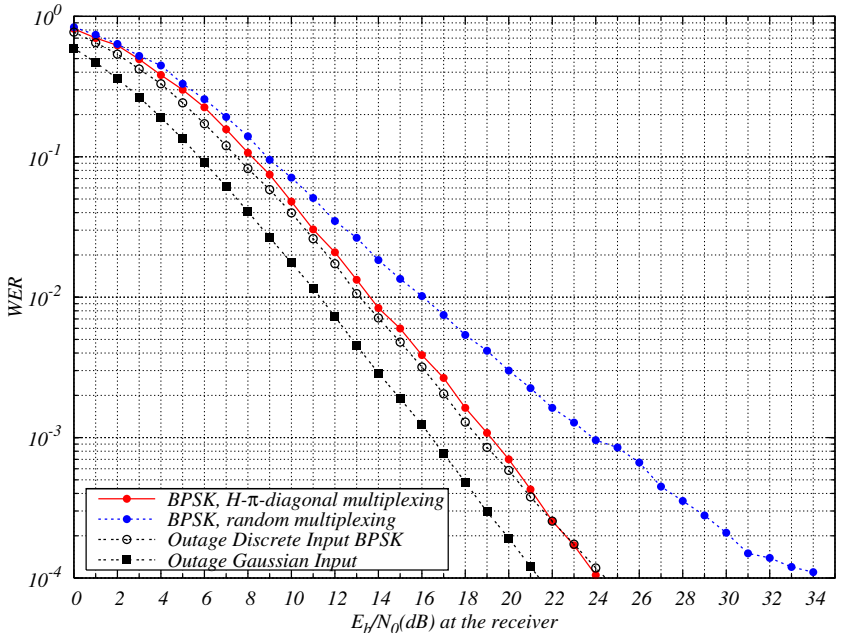

Figure 2.17: BPSK modulation, quasi-static channel, $n_t = 2$, $n_r = 1$, turbo code with $R_c = 1/2$, $(17, 15)_8$, $N = 400$.

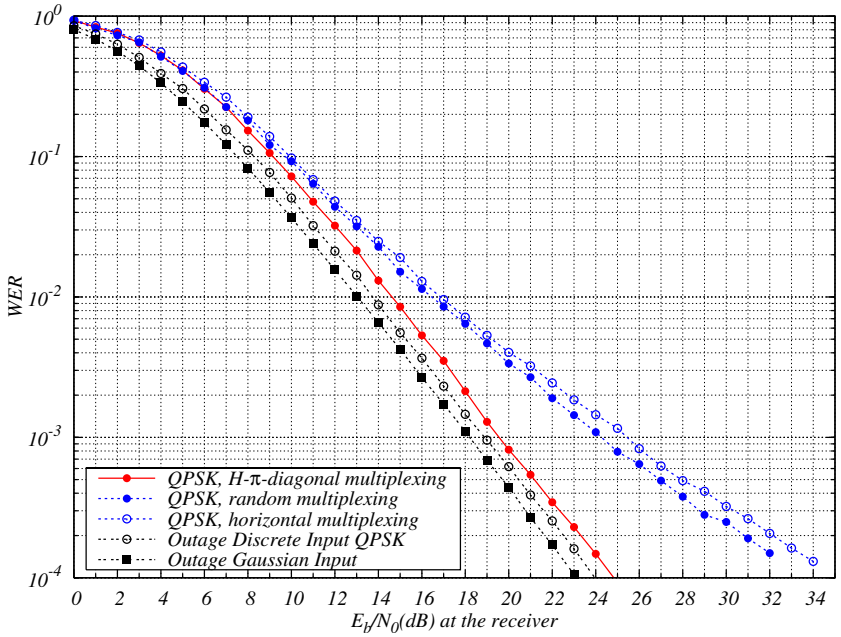

Figure 2.18: QPSK modulation, quasi-static channel, $n_t = 2$, $n_r = 1$, turbo code with $R_c = 1/2$, $(17, 15)_8$, $N = 400$.

In this section, computer simulations are made for $n_t = 2$ and without linear precoding ($s = 1$) on the quasi-static MIMO channel. The rate 1/2 turbo code is built from RSC$(17, 15)_8$ and a pseudo-random interleaver π of size N. All curves include word error rate versus signal-to-noise ratio per bit. Fig. 2.17 shows the performance of a BPSK modulation with 2 transmit and 1 receive antenna, and $N = 400$. Fig. 2.18 shows a similar situation with a QPSK modulation. The performance with 2 transmit and 2 receive antennas is given in Fig. 2.19. Notice that the word error rate is roughly the same for $N = 400$ and $N = 6400$. Finally, the performance of 8-PSK is illustrated in Fig. 2.20 and compared to both outage limits (discrete and Gaussian inputs).

2.8.4 Linear precoding via DNA rotations with $n_t = 4$

In the case of $n_t = 4$ transmit antennas, we have $D_{st} = 4$. Maximum state diversity in (1.25) cannot be attained with $R_c = 1/2$ if $D_{st} = 4$. Therefore, we add a linear precoder in order to downgrade D_{st} from 4 to 2. This does not affect the physical channel diversity D_{ch}. If the rotation has $s = 4$, i.e. a full spreading unitary precoder as usually studied in the literature, then D_{st} will reduce to 1. Also, MIMO detection complexity increases exponentially with s. The solution to maintain $D_{st} = 2$ is given by Dispersive Nucleo

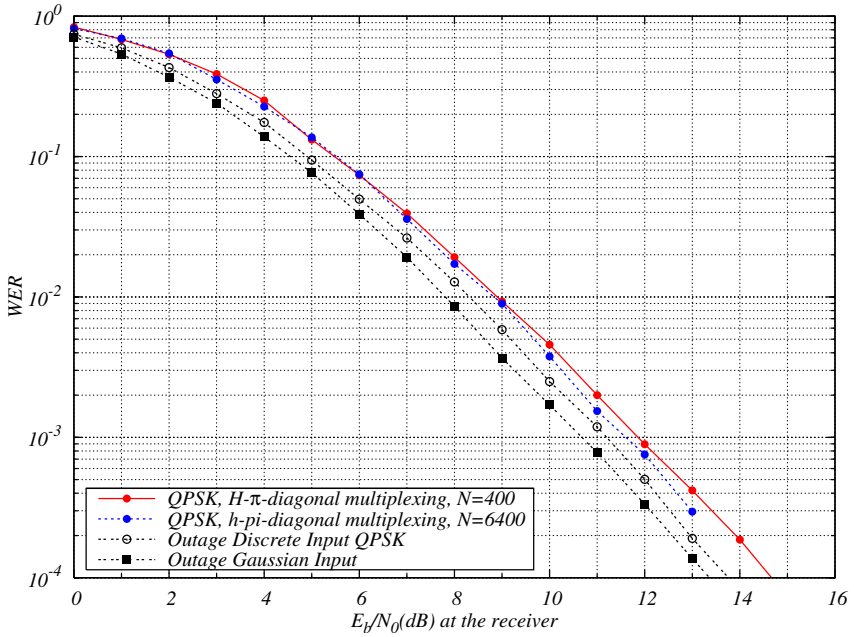

Figure 2.19: QPSK modulation, quasi-static channel, $n_t = 2$, $n_r = 2$, turbo code with $R_c = 1/2$, $(17, 15)_8$, $N = 400/6400$.

Algebraic (DNA) precoders discussed in section 2.6 for $s \leq n_t$. Now, let us observe the MIMO channel with $\mathbf{S_{DNA}}$ as in (2.30). The QAM vector $z = (z_1, z_2, \ldots, z_8)$ goes through the precoder before $\mathbf{H}$. Consider the lattice point $\mathbf{zSH}$ without adding Gaussian noise. One would notice that z_i is transmitted via the 1st and 2nd transmit antennas if i is odd, and via the 3rd and 4th transmit antennas if i is even. Consequently, the DNA precoder converts the $4 \times n_r$ MIMO channel onto two $2 \times n_r$ MIMO channels. Binary elements mapped to z_i when i is odd (resp. i is even) will be sent through the first BO-sub-channel (resp. the second BO-sub-channel). As a final illustration, Fig. 2.21 shows the error rate of BPSK modulation with 4 transmit and 2 receive antennas.

2.9 Conclusions

In this chapter, we proposed space-time bit-interleaved coded modulations for the multiple-antenna channel that perform close to outage limit. In [17], it was shown that cyclotomic rotations satisfying genie/DNA conditions are the best choice for precoding in space-time bit-interleaved coded modulations, due to their enhanced performance and their flexibility. These rotations are optimal in both algebraic and information theoretical senses. They

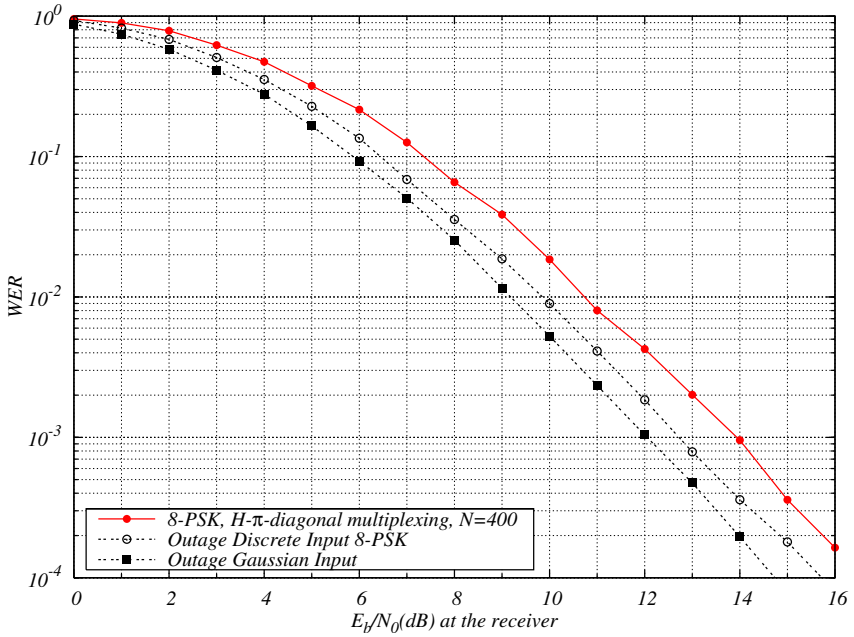

Figure 2.20: 8-PSK modulation, quasi-static channel, $n_t = 2$, $n_r = 2$, turbo code with $R_c = 1/2$, $(17, 15)_8$, $N = 1600$.

exist for any set of MIMO channel parameters, mainly the number of transmit antennas and the precoder time-spreading factor. However, the families of IOM linear precoders we presented in this chapter correct the failure of cyclotomic rotations to lead the system to reasonable performance since the first iteration in an iterative receiver when the system has delay constraints. They also exist whatever the MIMO system configuration is, with the difference in that their design requires Monte Carlo simulations. They can be designed by relaxing the genie constraints or by maintaining one constraint depending on the decoding technique we want to employ.

In addition, we proposed a low-complexity space-time coding scheme for $n_t = 4$ based on the Alamouti scheme. This low-complexity scheme ensures state diversity $D_{st} = 1$, which means it can be used with all coding rates $R_c \in [0, 1]$ while maintaining maximal channel diversity $d_{ch} = 4 \times n_r$. In addition to exponentially reducing the detection complexity, this scheme showed a slight degradation of the frame error rate over a quasi-static fading channel, that is more robust than classical ST-BICM. As configurations with $n_t = 4$ are particularly of interest in recent wireless communication systems (such as IEEE.802a/b/g standards), the low-complexity solution together with the high performance provided by this scheme are valuable.

Finally, we studied turbo-coded modulations for the MIMO channel based on the works in

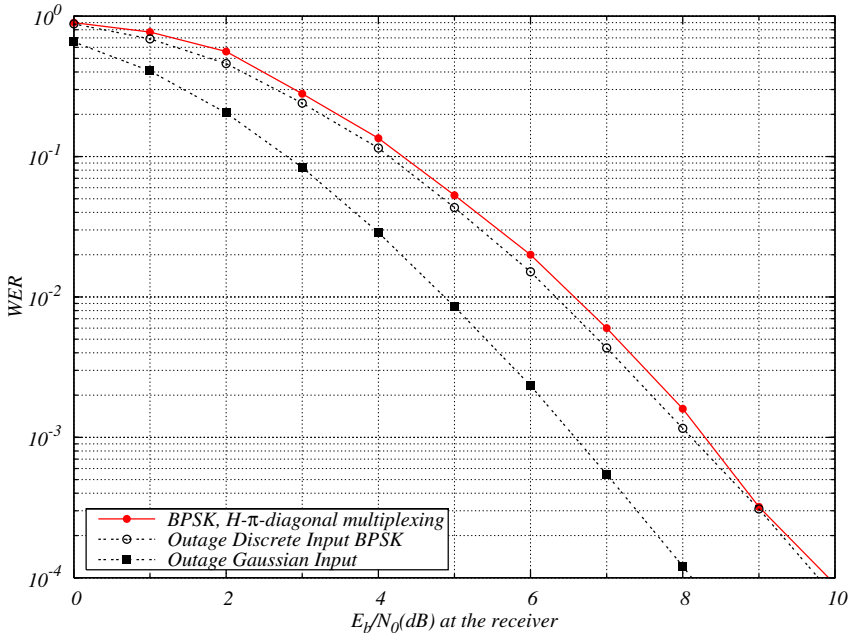

Figure 2.21: BPSK modulation, quasi-static channel, $n_t = 4$, $n_r = 2$, turbo code with $R_c = 1/2$, $(17, 15)_8$, $N = 1600$. Linear precoding via a cyclotomic DNA rotation

[52] on "code multiplexers". When the coding rate of the turbo-code satisfies $R_c \leq 1/D_{st}$, the use of multiplexers at the output of the encoder ensures low detection complexity and near-outage limit performance. Surprisingly enough, the frame error rate performance of turbo-coded modulations is insensitive to block length. This is probably due to the interleaving gain of the turbo-code on AWGN channels translated to non-ergodic fading channels, whereas the number of neighbors of a turbo-codeword increases linearly with the interleaver size [62]. Note that it was recently shown in [63] that LDPC codes have almost the same behavior over block-fading channels. However, the coding gain with regular turbo codes on block-fading channels is slightly better than that of regular LDPC codes.
To summarize, we can follow these strategies for low-complexity decoding of coded modulations over the MIMO channel:

- If $R_c \leq 1/D_{st}$ and an iterative receiver can be used, use turbo-codes with multiplexers for $n_t = 2$ antennas and turbo-codes with multiplexers along with DNA rotation for $n_t = 4$ as proposed in section 2.8.

- If $n_t = 4$ and an iterative receiver can be employed, use the Matrix-Alamouti scheme presented in section 2.7 whatever the channel coding rate is.

- Else, if $R_c > 1/D_{st}$, use cyclotomic rotations [17] with an iterative receiver.
- If no iterations are allowed at the receiver, use IOM rotations presented in section 2.6 with all channel configurations.

Chapter 3

Coded modulations for the amplify-and-forward cooperative channel

3.1 Introduction

As discussed in the previous chapter, multiple-antenna systems can provide reliable communication (through large diversity orders) and high data rates in block-fading environments. The advantages of such systems is widely recognized and they are proposed in many standards. However, due to size (and sometimes cost) limitations, the implementation of many antennas on a single terminal is unfeasible. This is the case of the uplink transmission in a cellular link for instance.

Since the early 1970s, the idea of the relay channel in information theory was proposed [64]. In [65], the authors proved the gain in capacity the relay channel has and sketched the rate regions for this channel under different hypothesis. Inspired by these works, the authors in [66, 67] proposed the concept of "user cooperation diversity", whereas user's terminals help each other to convey their signals to a destination. This allows for the signals to attain high spatial diversity orders by using the antennas of other terminals and thus by forming a virtual antenna array. Note that this is not a simple relaying problem, as users are responsible for the "partner's" signals as well as their own signals.

One main application is the cooperation of in-cell users in a cellular system. Reliable communication can be achieved through diversity and by relaying signals from terminals that are far from the base station. The drawback is the fact that the inter-user channel is noisy, thus imposing various cooperation protocols we will discuss later in this report. Another potential application is in wireless *ad hoc* networks, such as mesh networks for instance. A wireless *ad hoc* network does not depend on a central control unit, and it does not have a fixed infrastructure. The nodes communicate by forming a network based on

channel conditions and mobile locations.
The main problems in non-cooperative networks is their rigid infrastructure, whose blocking probability increases with the number of terminals that are sharing the network. Many service providers have experience dealing with temporary elevations in network traffic. COSMOTE, the Greek telecommunications company responsible for providing service to the 2004 Olympic games, had to deploy additional resources in the area surrounding the Olympic complex. This extra equipment allowed this system to successfully deliver over 100 million text messages during the 17 day duration of the games. Similarly, sporting events and large public gatherings in the United States regularly take advantage of the so-called Cell-on-Wheels (COW) services in order to account for location-dependent traffic spikes. With cooperative communications, networks will not experience such problems anymore, as the more users there are in a network, the more reliably one can communicate. In addition, the hardware implementation of multiple antennas on the same terminal that is difficult to realize is traded for protocol algorithms shared among terminals through the network, which is easily updatable and gains in flexibility.
In this chapter, we will start by recalling the communication protocols for the cooperative fading channel. We will then establish the system model for coded modulations over the amplify-and-forward protocol. Then we will discuss bounds on diversity for this type of protocol, that are followed by coding strategies and simulation results. The last part of this chapter discusses channel multiplexing issues for turbo-coded modulations over such protocols.

3.2 Cooperative communications protocols

After the authors in [66, 67] introduced the concept of cooperative diversity, many papers proposed cooperation protocols that define the way the cooperation between users is performed. These protocols can be classified into two major categories, that are amplify-and-forward (AF) and decode-and-forward (DF). Note that the large majority of the existing designs we will recall in the sequel are based on the so-called "Diversity-Multiplexing Tradeoff" (DMT) of the channel [68]. The DMT is a piece-wise linear function that represents, at very high signal-to-noise ratios, the tradeoff between the maximum achievable rate (as a function of the signal-to-noise ratio) and the maximal achievable diversity order over the wireless channel. Although the DMT bound gives an insight on the superiority of a given protocol (or a given antenna configuration for MIMO systems) and allows for the design of optimal space-time precoders for uncoded systems, its relevance as a design tool for coded modulations with iterative decoding is arguable.

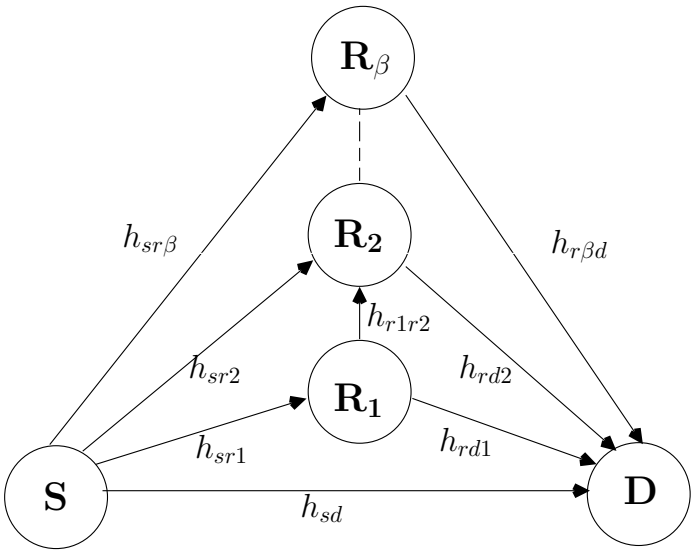

Figure 3.1: Cooperative fading channel.

3.2.1 Amplify-and-forward protocols

In these protocols, the relays scale the signals received from the source (or by other relays) and forward them to the destination (or to other relays) without other treatment. These protocols are easy to implement in practical communication systems, as the computational complexity they introduce at the relay is limited to the scaling operation. The orthogonal amplify-and-forward (OAF) protocol was first introduced in [69] for the single-relay case. By orthogonal we mean that the source and the relay do not send data simultaneously. The second major work concerning this family of protocols is the framework established in [70] for the single-relay case. The authors proposed three amplify-and-forward protocols that are:

- Protocol I: the source broadcasts a signal to both the relay and the destination in the first phase. In the second phase, the relay scales the signal and forwards it to the destination, while the source transmits another message to the destination. This protocol is also known as the non-orthogonal amplify-and-forward (NAF) protocol [71].

- Protocol II: the source broadcasts a signal to both the relay and the destination in the first phase like in Protocol I. In the second phase, only the relay scales the signal it received in the previous phase and forwards it to the destination. This protocol is the OAF protocol introduced in [69].

- Protocol III: the source sends a signal only to the relay in the first phase. The second phase is similar to the second phase in Protocol I.

In addition to introducing these protocols, the authors discussed and analyzed some information theoretical aspects of cooperative protocols that brought insight to the behavior of such systems. From these three protocol, Protocol I caught the attention of the researchers in the community as it allows for high data rates (the source always transmits). Indeed, in [71], it is shown that the NAF protocol outperforms the AF protocol for high data rates. However, for the case of more than one relay, the NAF protocol suffers from a limitation , as half of the symbols in the cooperation frame are protected. For this reason, the authors in [72] proposed the slotted amplify-and-forward (SAF) scheme; by allowing inter-relay communication (see Fig. 3.1), on can protect β out of $\beta + 1$ symbols. For this reason, the SAF scheme largely outperforms the β-relay NAF scheme for high data rates. Many space-time code design for uncoded fading channels for the AF protocols were proposed, among them [73] [74] [75, 76], but optimal space-time codes for uncoded systems can be found in [72] [77].

3.2.2 Decode-and-forward protocols

This class groups the protocols in which the relays operate on the signal they receive from the source (or from other relays) before forwarding it. The first protocol, the selection decode-and-forward, was introduced in [69] for the single-relay cooperative channel. In this protocol, the relay estimates the channel coefficient between the source and the relay, say h_{sr}, and it computes $|h_{sr}|^2$. If this value falls below a threshold, the relay remains idle. If not, the relay decodes the message and forwards it to the destination. This scheme was generalized to multiple relays in [78]. In [71], the authors introduced the dynamic decode-and-forward protocol wherein the time for which the relays listen to the source depends on the source-relay channel gain. In [79], the authors treated the compress-and-forward protocol and proved it to be optimal for the single-relay channel. Note that unlike the decode-and-forward protocol where the relays have to know the source-relay channel, the relays in the compress-and-forward protocol have to know all the channel coefficients of the incoming paths. In [80], the authors proposed an intuitive distributed turbo code that achieves high performance; it consists of broadcasting a convolutional codeword to both the relay and the destination, the relay decodes the codeword, interleaves it, and encodes it prior to forwarding to the destination that performs iterative decoding between the two codes. Similar constructions can be found in [81] for distributed turbo codes and in [82] for LDPC codes.

3.3 Space-time bit-interleaved coded modulations for the amplify-and-forward cooperative channel

As discussed in section 3.2.1, many distributed space-time codes for uncoded systems have been proposed in the literature. However, the optimal codes in [72] [77] that achieve the DMT frontier of the channel introduce delay in the cooperation frame of the NAF/SAF protocol, which means that the source broadcasts for several time slots before the cooperation at the relay starts. Indeed, as these codes were initially designed for MIMO systems, the spreading factor $s = n_t$ for such systems is translated into a delay $d = s - 1$ for the NAF/SAF protocols. This delay actually results in an exponential growth of the detection complexity at the receiver.
Nevertheless, in the presence of an error correcting code, it was shown in chapter 2 that one can trade diversity from the channel detector to the channel decoder over block-fading channels by using space-time rotations. In addition, for the SAF channel, unlike for the MIMO channel, the maximal diversity order $\beta + 1$ of the channel can be achieved using a rotation that does not lead additional complexity. This is a key point for our design framework in the rest of this chapter.
To our knowledge, no work has yet treated channel coding issues for AF cooperative protocols in general. In this chapter, we consider the problem of coding for the half-duplex non-orthogonal slotted amplify-and-forward (NAF/SAF) cooperative channel. We only consider a network with single-antenna nodes. We derive bounds on the diversity order of this protocol that are achieved by a distributed space-time bit-interleaved coded modulation (D-ST-BICM) scheme under iterative APP detection and decoding. These bounds lead to the design of space-time precoders that ensure maximum diversity and high coding gains.

3.4 System model and parameters

We consider the amplify-and-forward fading relay channel. We impose the half-duplex constraint, whereas terminals cannot transmit and receive signals simultaneously. We consider the TDMA-based Protocol I from [70] that is also known as the non-orthogonal amplify-and-forward (NAF) protocol. For the case of more than one relay, we use the "naive" slotted amplify-and-forward (SAF) cooperative protocol proposed in [83], where inter-relay communication is allowed; the source transmits in all time slots, and starting from the second slot, only one relay scales and transmits the message received in the previous time slot. By protecting β symbols out of $\beta + 1$, this protocol can achieve a diversity order of β with a length-$\beta + 1$ vector, whereas the classical β-relay NAF scheme

achieves the same diversity order with a length-2β vector. The main reason we use this protocol is because it induces low detection complexity. The "naive" SAF protocol gives the following signal model:

$$y_{d_i} = \sqrt{\mathcal{E}_i} h_{sd} x_i + \sqrt{1-\mathcal{E}_i} h_{r_i d} \gamma_{i-1} y_{r_{i-1}} + w_{d_i} \tag{3.1}$$

$$y_{r_i} = \sqrt{g_{sr_i}\mathcal{E}_i} h_{sr_i} x_i + \sqrt{g_{r_{i-1}r_i}\,(1-\mathcal{E}_i)} h_{r_{i-1}r_i} \gamma_{i-1} y_{r_{i-1}} + w_{r_i} \tag{3.2}$$

with $i = 1, ..., \beta+1$. Subscripts s, d, and r_i correspond to *source*, *destination*, and i^{th} *relay*. The unit variance complex symbol x_i is transmitted in the i^{th} slot, the received signal at the destination in the i^{th} time slot is y_{d_i}, while y_{r_i} is the signal received by the i^{th} relay. The coefficients $\mathcal{E}_i$ represent the energy transmitted by the source in the i^{th} slot. The geometric gain $g_{j\ell}$ is defined as $\mathbb{E}|h_{j\ell}|^2/\mathbb{E}|h_{s\ell}|^2$ [72]. The h_{kl} are the complex Gaussian fading coefficients that are constant for the duration of a codeword and w_{d_i} and w_{r_i} are AWGN noise components. The γ_i are the energy normalization coefficients at the i^{th} relay, subject to $\mathbb{E}|\gamma_i y_{r_{i-1}}|^2 \leq 1$, and $\gamma_0 = 0$. In matrix form, we can write for a system with β relays:

$$\mathbf{y}_d = \mathbf{x}\mathbf{H} + \mathbf{w}_c = \mathbf{z}\mathbf{S}\mathbf{H} + \mathbf{w}_c \tag{3.3}$$

where $\mathbf{y}_d$ is the length-$(\beta+1)$ vector of received signals and $\mathbf{z}$ is the length-$(\beta+1)$ vector of M-QAM symbols. S is a $(\beta+1)\times(\beta+1)$ precoding matrix, and $\mathbf{H}$ is given by:

$$\mathbf{H} = \begin{bmatrix} h_{11} & h_{12} & h_{13} & \cdots \\ 0 & h_{22} & h_{23} & \cdots \\ 0 & 0 & h_{33} & \cdots \\ \vdots & \vdots & \vdots & \ddots \end{bmatrix} \tag{3.4}$$

where

$$\begin{aligned} h_{ii} &= \sqrt{\mathcal{E}_i} h_{sd} \\ h_{12} &= \sqrt{g_{sr_1}\mathcal{E}_1(1-\mathcal{E}_2)}\gamma_1 h_{sr_1} h_{r_1 d} \\ h_{13} &= \sqrt{g_{sr_1} g_{r_1 r_2}\mathcal{E}_1(1-\mathcal{E}_2)(1-\mathcal{E}_3)}\gamma_1\gamma_2 h_{sr_1} h_{r_1 r_2} h_{r_2 d} \\ h_{23} &= \sqrt{g_{sr_2}\mathcal{E}_2(1-\mathcal{E}_3)}\gamma_2 h_{sr_2} h_{r_2 d} \end{aligned}$$

Finally, the vector $\mathbf{w}_c$ is a length-$(\beta+1)$ colored Gaussian noise vector whose entries are given by:

$$\begin{aligned} w_1 &= w_{d,1} \\ w_2 &= \sqrt{(1-\mathcal{E}_2)}\gamma_1 h_{r1d} w_{r,1} + w_{d,2} \\ w_3 &= \sqrt{(1-\mathcal{E}_2)(1-\mathcal{E}_3)}\gamma_1\gamma_2 h_{r1r2} h_{r2d} w_{r,1} + \sqrt{(1-\mathcal{E}_3)}\gamma_2 h_{r2d} w_{r,2} + w_{d,3} \end{aligned}$$

an so on. We set:

$$\mathbf{\Gamma} = \mathbf{E}\left[\mathbf{w}_c^{\dagger}\mathbf{w}_c\right] = 2N_0\mathbf{\Theta} \tag{3.5}$$

Where the † operator denotes transpose conjugate. By performing a Cholesky decomposition on $\mathbf{\Theta}$, we get:

$$\mathbf{\Theta} = \mathbf{\Psi}^{\dagger}\mathbf{\Psi} \tag{3.6}$$

Thus the equivalent channel model would become:

$$\mathbf{y}_d\mathbf{\Psi}^{-1} = \mathbf{zSH}\mathbf{\Psi}^{-1} + \mathbf{w} \tag{3.7}$$

where $\mathbf{w}$ is a white Gaussian noise vector.

3.5 The diversity of coded modulations over precoded SAF channels

The maximum diversity inherent to the SAF channel is $d_{max} = \beta + 1$, and it can be collected by an APP detector (at the destination) if linear precoding is used at the transmitter. In general, it is sufficient to use a linear precoder that mixes the $\beta+1$ constellation symbols being transmitted on the channel to achieve the full diversity with uncoded systems and without increasing the decoder complexity. However, using larger precoders can further improve the performance. From an algebraic point of view, a linear precoder of size $(\beta+1)^2 \times (\beta+1)^2$ is the minimal configuration to achieve the best coding gains (without channel coding) at the price of an increase in detection complexity (The complexity of an APP detector grows exponentially with the number of dimensions) [84].
On the other hand, for coded systems transmitted on block-fading channels, the channel decoder is capable of collecting a certain amount of diversity that is however limited by the Singleton bound [34]. As shown in [85], the lowest complexity solution is to first recover the channel code diversity and then collect the remaining diversity through linear precoding. For this purpose we derive hereafter an upper bound on the diversity order of a coded transmission through a precoded SAF channel, and deduce the precoding strategy to achieve the full diversity.

First, we will introduce a new model of block-fading channel that will be used in the following to compute the bounds on the diversity order of coded SAF channels.

3.5.1 Matryoshka block-fading channels

In this section we consider a block-fading channel model where the set of random variables of a higher diversity block always include the set of random variables of a lower diversity one, like Matryoshka dolls:

Definition 4. *Let us consider λ independent Rayleigh fading distributions. Let $\mathcal{M}(\mathcal{D},\mathcal{L})$ be a channel built from the concatenation of $|\mathcal{D}|$ blocks, where $\mathcal{D}$ and $\mathcal{L}$ are the sets of diversity order and lengths of each block, respectively. The integer $|\mathcal{D}|$ is the cardinality of $\mathcal{D}$. The i-th diversity block is defined by a linear combination of a subset $\mathcal{S}(i)$ of $\mathcal{D}(i) \leq \lambda$ Rayleigh distributions, such that $\mathcal{S}(i+1) \subset \mathcal{S}(i)$, i.e., the blocks are sorted such that $\forall i < j, \mathcal{D}(i) \geq \mathcal{D}(j)$ and we assume that $\mathcal{D}(1) = \lambda$ has the highest diversity order.*

Fig. 3.2 shows the representation of the Matryoshka block-fading channel. Notice that $n_{\mathcal{D}} = \lambda$ for the non-precoded channel.

$\mathcal{D}(1)$	$\mathcal{D}(2)$	$\cdots$	$\mathcal{D}(n_{\mathcal{D}})$
$\mathcal{S}(1) = \{\alpha_1, \cdots, \alpha_\lambda\}$	$\mathcal{S}(2) \subset \mathcal{S}(1)$		$\mathcal{S}(n_{\mathcal{D}}) \subset \mathcal{S}(n_{\mathcal{D}}-1)$
$\leftarrow \quad \mathcal{L}(1)$ bits $\quad \rightarrow$	$\leftarrow \mathcal{L}(2)$ bits $\rightarrow$		$\leftarrow \quad \mathcal{L}(n_{\mathcal{D}})$ bits $\quad \rightarrow$

Figure 3.2: Matryoshka block-fading channel model.

Let us now transmit a BPSK-modulated and interleaved codeword of a rate-R_c code on the channel $\mathcal{M}(\mathcal{D},\mathcal{L})$. First, let us focus on the pairwise error probability (PEP) of two given binary codewords c and c'. Due to the channel model, the diversity order of this PEP is equal to the diversity order of the lowest index block seeing a non null bit of $c - c'$. The performance of the coded modulation has a diversity order upper bounded by δ_{max} defined as follows:

Proposition 3. *The diversity observed after decoding a rate-R_c code transmitted over a $\mathcal{M}(\mathcal{D},\mathcal{L})$ channel is maximized by δ_{max} :*

$$\delta_{max} = \mathcal{D}(i) \text{ where } \sum_{k=1}^{i-1} \mathcal{L}(k) < R_c \sum_{k=1}^{|\mathcal{D}|} \mathcal{L}(k) \leq \sum_{k=1}^{i} \mathcal{L}(k) \tag{3.8}$$

and is achievable for any linear code.

Proof. This proof is inspired from the Singleton bound's one. The code has parameters (N, K), where $N = \sum_{k=1}^{|\mathcal{D}|} \mathcal{L}(k)$ and $K = R_c N$.

If $K > \sum_{k=1}^{i-1} \mathcal{L}(k)$, whatever the code, a puncturing of the last $\sum_{k=i}^{|\mathcal{D}|} \mathcal{L}(k)$ bits leads to a null minimal Hamming distance code. This means that there exists two codewords c and c' such that the first $\sum_{k=i}^{|\mathcal{D}|} \mathcal{L}(k)$ bits of $c - c'$ are null, and involves that $\delta_{max} \leq \mathcal{D}(i)$.

If the code is linear, there exists an interleaver that makes the code systematic. If the information bits are transmitted on the blocks of higher diversity order and $K \leq \sum_{k=1}^{i} \mathcal{L}(k)$, the Hamming distance after puncturing the last $\sum_{k=i+1}^{|\mathcal{D}|} \mathcal{L}(k)$ bits remains strictly positive and induces that $\delta_{max} \geq \mathcal{D}(i)$.□

□

As a remark, whatever the QAM modulation is, the log-likelihood ratio expression of the channel model at the output of the APP detector always takes equivalent BPSK modulations at its input. The bound on the diversity order applies then to any discrete modulation.

3.5.2 Precoded SAF channel models and associated bounds

Non-precoded SAF channels

The time periods of the SAF channel can be sorted into $\beta + 1$ blocks, the j-th block corresponding to the transmission through $0 \leq j - 1 \leq \beta$ relays. We will assume that the interleaver of the BICM is ideal, i.e., that for any pair of codewords (c, c'), the w non-null bits of $c - c'$ are transmitted in different blocks of $\beta + 1$ time periods. The interleaving, modulation and transmission through the channel transform the coded words c and c' into the points $\mathcal{C}$ and $\mathcal{C}'$ in an Euclidean space. For a fixed channel, the performance is directly linked to the Euclidean square distance $|\mathcal{C} - \mathcal{C}'|^2$, which can be rewritten as a sum of w square Euclidean distances associated to the non-null bits of $c - c'$.

The performance of a BPSK modulation transmitted through $j - 1$ relays during j time periods of a quasi-static SAF channel has a diversity order j. The square distance $|\mathcal{C} - \mathcal{C}'|^2$ is a function of the fading coefficients of the equivalent channel. It can be factorized as follows: $\sum_{k=1}^{\beta+1} d_k^2$ where d_k is the total Euclidean distance seen by the k-th block. Finally, the diversity order of a given pairwise error probability is equal to the maximal index k such that d_k is non-null. At very high SNR, the performance is lead by the worse pairwise error probability, the diversity order of the BICM is then the lower bound of all pairwise error probabilities diversity orders.

At the output of the APP detector, an equivalent block-fading channel is observed and the constituent blocks do not have the same intrinsic diversity order: A soft output belonging to the $\beta + 2 - j$-th block carries the attenuation coefficients $\{h_{sd}; h_{sr_1}h_{r_1d}; \ldots; h_{sr_1}h_{r_1r_2}\cdots h_{r_{j-2}r_{j-1}}h_{r_{j-1}d}\}$. As a remark, blocks are sorted such that the j-th block carries a diversity order $\beta+2-j$. Under perfect interleaving, the equivalent SAF channel at the output of the APP detector is a matryoshka $\mathcal{M}([\beta+1, \beta, \ldots, 1], [N/(\beta+1), \ldots, N/(\beta+1)])$ channel, where N is the number of coded bits per codeword. With this observation, we can conclude that the upper bound on the diversity order of a non-precoded SAF channel is

$$\delta_{max,1}(\beta, R_c) = 1 + \lfloor (1 - R_c)(\beta + 1) \rfloor \tag{3.9}$$

which is equal to the classical Singleton bound on the diversity order of block-fading channels [15].

Precoded SAF channels

Let us now introduce a linear precoder that rotates symbols of s different diversity order blocks together. First of all, let us focus on two different scenarios:

- The linear precoder size is lower than (or equal to) $\beta+1$. In this case, the dimension of the received vector $\mathbf{y}_d$ remains unchanged, thus there is no increase in detection complexity, and no delay is introduced to the protocol.
- The linear precoder size is lower than (or equal to) $(d+1)(\beta+1)\times(d+1)(\beta+1)$, where d is the delay (i.e. the source broadcasts for $d+1$ time slots before the relays start to cooperate). In this case, the complexity of the detector increases exponentially with d. As mentioned previously, these precoders are mandatory to achieve optimal performance for uncoded systems. However, in the presence of channel coding, they can be avoided.

We will now present two precoding strategies and compute the bound (3.8) for these two particular cases.

First strategy: a single precoder First, let us assume that s diversity blocks of size $N/(\beta+1)$ are linearly precoded together, then the diversity order of the new $sN/(\beta+1)$-length block is the maximum diversity order of the precoded blocks. As the other blocks keep their own diversity, it seems natural to maximize their diversity orders in a way to increase the coding gain at the output of the decoder (The best performance is achieved

for a block-fading channel with diversity orders as equal as possible.). The length of the precoder input vector is $\beta+1$. We propose to precode the first block with the $s-1$ last blocks, i.e., the highest diversity order with the $s-1$ lowest ones. At the output of the APP detector, the channel model is a matryoshka $\mathcal{M}(\mathcal{D},\mathcal{L})$ where $\mathcal{D}=[\beta+1,\beta,\ldots,s]$ and $\mathcal{L}=[sN/(\beta+1),N/(\beta+1),\ldots,N/(\beta+1)]$, which leads to the following upper bound on the diversity order:

$$\delta_{max,2}(\beta,R_c,s)=\min(s+\lfloor(1-R_c)(\beta+1)\rfloor,\beta+1) \tag{3.10}$$

Indeed, by replacing $\mathcal{D}=[\beta+1,\beta,\ldots,s]$ and $\mathcal{L}=[sN/(\beta+1),N/(\beta+1),\ldots,N/(\beta+1)]$ in (3.8), we observe that if $R_c\leq s/(\beta+1)$ then $R_c(\beta+1)\leq s+i-1<R_c(\beta+1)+1$, else we have that $i=1$ and $\delta_{max,2}(\beta,R_c,s)=\mathcal{D}(1)$. It is then easy to show that the upper bound on the diversity is given by (3.10). Note that, in the representation of Fig. 3.2, we have that $n_{\mathcal{D}}=\lambda-s+1$ with precoding.

If $s=1$, then $\delta_{max,2}(s)$ is equal to the Singleton bound on the diversity order of an uncorrelated block fading channel with equal per-block diversity. If $s\geq 1$, $\delta_{max,2}(s)$ is greater than the upper bound on the diversity order for block fading channels. For example, the full diversity order cannot be achieved for the transmission of a $s=2$-precoded BICM with rate 2/3 on a block fading with diversity order 3 (the diversity is upper bounded by 2). For the SAF channel, the full diversity order can be achieved in that case, as shown in Fig. 3.3.

As a remark, in order to achieve the upper bound on the diversity of a block fading channel, at least one non null bit of any word $c-c'$ should be placed in as many independent blocks as given by the singleton bound. For precoded SAF channels, the bound is achieved as soon as one non null bit of any word $c-c'$ is placed in a block of diversity higher than $\delta_{max,1}(s)$. The last problem has less constraint than the first one. Tables 3.1 and 3.2 show the values of $\delta_{max,2}(\beta,R_c,s)$ for different coding rates with respect to the number of relays and the value of s. We can notice that full diversity is obtained with $s\geq(\beta+1)R_c$ in all configurations.

Second strategy: $(\beta+1)/s$ precoders Let us assume that s divides $\beta+1$, we can then use $(\beta+1)/s$ precoders: The first precodes the highest diversity order block with the $s-1$ lowest ones. The second, if any, precodes the second highest diversity order block with the $s-1$ lowest non-precoded ones, and so on. By using this precoding strategy that includes several independent precoders, we further increase the diversity of the extrinsic probabilities at the input of the decoder, and consequently the diversity at the output of the decoder. Indeed, the equivalent $\mathcal{M}(\mathcal{D},\mathcal{L})$ channel has parameters

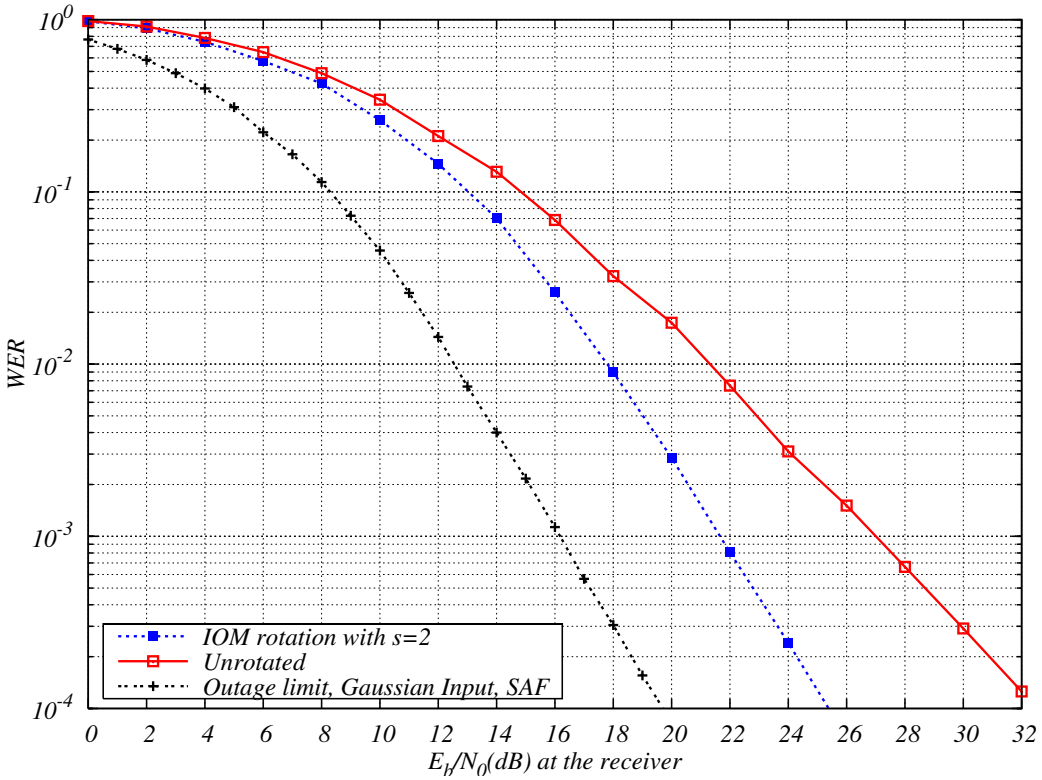

Figure 3.3: Two-relay SAF cooperative channel, R_c=2/3 RSC $(25,37,35)_8$ code, BPSK modulation, 1440 coded bits.

Table 3.1: $\delta_{max,2}(\beta, R_c, s)$ for $R_c = 1/2$

$\beta \setminus$ **s**	**1**	**2**	**3**	**4**	**5**
1	2	2			
2	2	3	3		
3	3	4	4	4	
4	3	4	5	5	5
5	4	5	6	6	6
6	4	5	6	7	7
7	5	6	7	8	8
8	5	6	7	8	9

$\mathcal{D} = [\beta+1, \beta, \ldots, \beta+2-(\beta+1)/s]$ and $\mathcal{L} = [sN/(\beta+1), \ldots, sN/(\beta+1)]$, which leads to the following upper bound on the diversity order:

Table 3.2: $\delta_{max,2}(\beta, R_c, s)$ for $R_c = 3/4$

$\beta \setminus \mathbf{s}$	**1**	**2**	**3**	**4**	**5**	**6**
1	1	2				
2	1	2	3			
3	2	3	4			
4	2	3	4	5		
5	2	3	4	5	6	
6	2	3	4	5	6	7
7	3	4	5	6	7	8

$$\delta_{max,3}(\beta, R_c, s) = min\left(\frac{(\beta+1)(s-1)}{s} + 1 + \left\lfloor \frac{(1-R_c)(\beta+1)}{s} \right\rfloor, \beta + 1\right) \tag{3.11}$$

It can be easily shown that

$$\delta_{max,2}(\beta, R_c, s) \leq \delta_{max,3}(\beta, R_c, s) \tag{3.12}$$

However, the maximum diversity order $\delta_{max,2}(\beta, R_c, s) = \delta_{max,3}(\beta, R_c, s) = \beta + 1$ is achieved for the same $s \geq (\beta+1)R_c$. The advantage of $\delta_{max,3}(\beta, R_c, s)$ over $\delta_{max,2}(\beta, R_c, s)$ is for non-full diversity schemes. In addition, it is important to note that the bounds in (3.10) and (3.11) have straight-forward applications to systems employing delay precoders.

3.6 Coding strategies

Based on the bounds on the diversity order derived in the previous section, one can choose a good coding strategy given the system parameters (i.e. number of relays, coding rate...). As for the coding gain, it is tedious to analytically compute the pairwise error probability for the NAF and SAF protocols, as it involves integrations over the product of two or more complex Gaussian variables representing the different channel gains $h_{j\ell}$. Now consider $\Delta^2 = \| \left(\mathbf{x} - \mathbf{x}'\right)\mathbf{SH} \|^2$ with $\mathbf{x} - \mathbf{x}' = \sum_{k=1}^{\beta+1} d_k^2$. Next, we look at the distribution of Δ^2 as an empirical tool that helps us in choosing the best coding strategy. Fig. 3.4 shows the distribution of Δ^2 for the single-relay NAF protocol. From the bounds on diversity of (3.10) and (3.11), we notice that if $R_c \leq 1/(\beta + 1)$, we do not need to precode for diversity purpose, as the channel decoder recovers the entire diversity of order $\beta + 1$. However, we can see that for unrotated QPSK input, there is a high number of small squared distances, thus we can eliminate the small values of Δ^2 by rotating the

QPSK vector. When the vector $\mathbf{z}$ has relatively small cardinality, it is useful to rotate the transmitted signal constellation with $s = s_{max} = \beta+1$ in a way to combine all the symbols together. A rotation plays the role of "smoothing" the distribution of the input vector $\mathbf{x}$, making it tend to the Gaussian distribution. However, unlike for MIMO systems (see Fig. 2.2), the rotation in this case keeps the length of the transmitted vector unchanged.

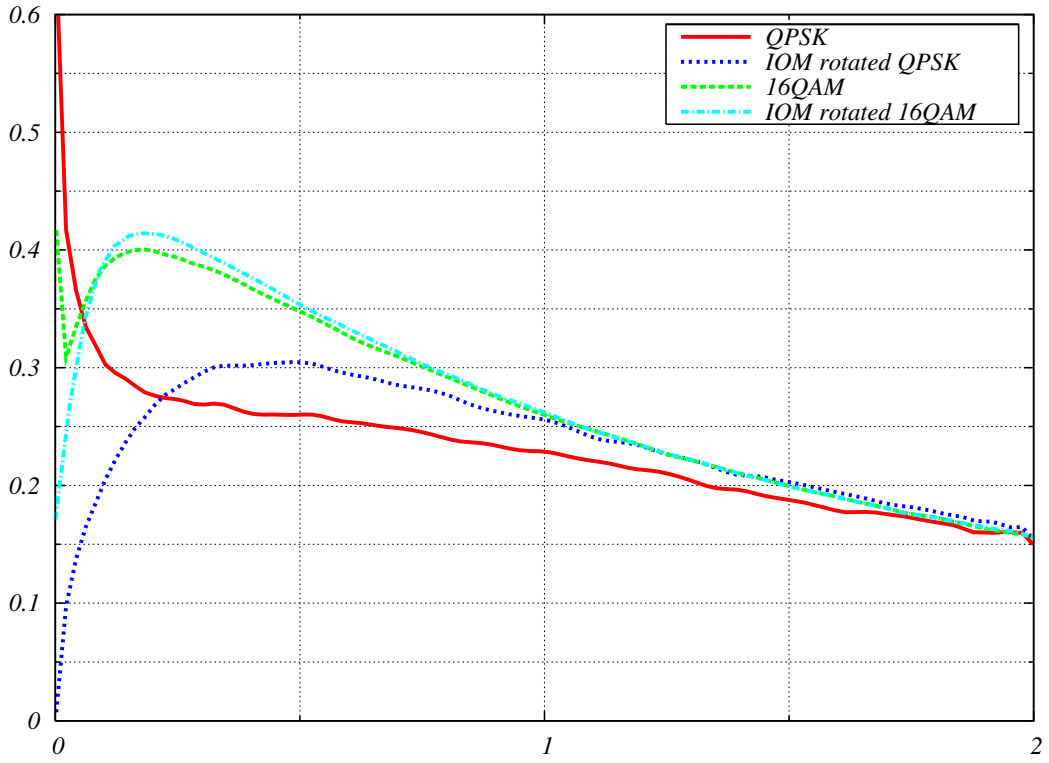

Figure 3.4: Distribution of Δ^2 for the single-relay NAF protocol.

With an increase in the constellation size, a rotation with s_{max} generates a dense vector space, making the extrinsics at the output of the detector suffer from interference between symbols. In this case, as the unrotated constellation generates a reasonable Δ^2 distribution with a small number of small distances, an optimized interleaver [17] that approaches the ideal interleaving condition is sufficient to provide high coding gains and maximum diversity. Now if $R_c > 1/(\beta + 1)$, rotations are mandatory to ensure full diversity at the receiver. For the same reasons as when $R_c \leq 1/(\beta + 1)$, we use rotations with s_{max} for small size constellations. With large size constellations, it is judicious to minimize the inter-symbol interference and choose a rotation with the minimum s that satisfies the bounds $\delta_{max,2}(\beta, R_c, s)$ or $\delta_{max,3}(\beta, R_c, s)$. We can then ensure full diversity and at the same time deliver better quality extrinsics (than with s_{max}) to the channel

decoder. Note that if no iterations are possible at the receiver, the s_{min} that allows for maximal diversity leads the optimal performance of the D-ST-BICM.
The threshold at which we can change the coding strategy (i.e. the value of s) cannot be computed analytically, but simulations showed that a rotation with s_{max} gives better performance with BPSK and QPSK modulations, while degrading the coding gain with 16-QAM constellations or higher. To conclude as to which strategy to follow in order to achieve high coding gains, we can say that:
I) With BPSK and QPSK modulations, always use precoders with s_{max} whatever the coding rate R_c is.
II) With 16-QAM modulations and higher:
1) If $R_c \leq 1/(\beta+1)$, do not precode, use optimized interleavers from [17].
2) If $R_c \geq 1/(\beta+1)$, precode with s_{min} that satisfies $\delta_{max,2}(\beta, R_c, s)$ or $\delta_{max,3}(\beta, R_c, s)$.
III) If no iterations are possible, precode with s_{min} that satisfies $\delta_{max,2}(\beta, R_c, s)$ or $\delta_{max,3}(\beta, R_c, s)$ whatever the coding rate R_c is.
These strategies will be illustrated in the next section. Finally, note that whatever the value of s is, there is no increase in the APP detection complexity.

3.6.1 Simulation results

In this section, word error rate performances are compared to information outage probability for different system configurations to illustrate the results presented in the previous sections. We consider the half-duplex SAF cooperative channels with different coding rates and constellation sizes. We set the values of $\mathcal{E}_1 = 1$, and $\mathcal{E}_2 = \mathcal{E}_3 = \mathcal{E}_1/2$ so that the received energy is invariant from slot to slot. The geometric gain coefficients g_{ij} are all set to 0 dB in this section. The space-time precoders are (IOM) as presented in section 2.6. They are selected from the ensemble of random rotations as:

$$P_{out}(\mathbf{S}) = P\left(\mathcal{I}_{SH} < (\beta+1)\,.m.R_c\right) \tag{3.13}$$

As an example, the 3×3 rotation $S_{IOM,s=2}$ that satisfies $\delta_{max,2}(\beta, R_c, s)$ obtained for the SAF protocol with two relays, 16-QAM input, and half-rate channel coding is given by:

$$\mathbf{S_{NAF-IOM,s=2}} = \begin{bmatrix} 0.69e^{-2.84} & 0 & 0.72e^{-0.12} \\ 0 & 1 & 0 \\ 0.72e^{-1.11} & 0 & 0.69e^{-1.29} \end{bmatrix} \tag{3.14}$$

Fig. 3.5 shows the outage probability for QPSK input, rotated QPSK input with an IOM rotation, and Gaussian input of the single-relay NAF protocol. Without rotation, the discrete input curve is about 2dB away from the Gaussian input. With IOM rotation, the curve roughly achieves the lower bound without any increase in detection complexity.

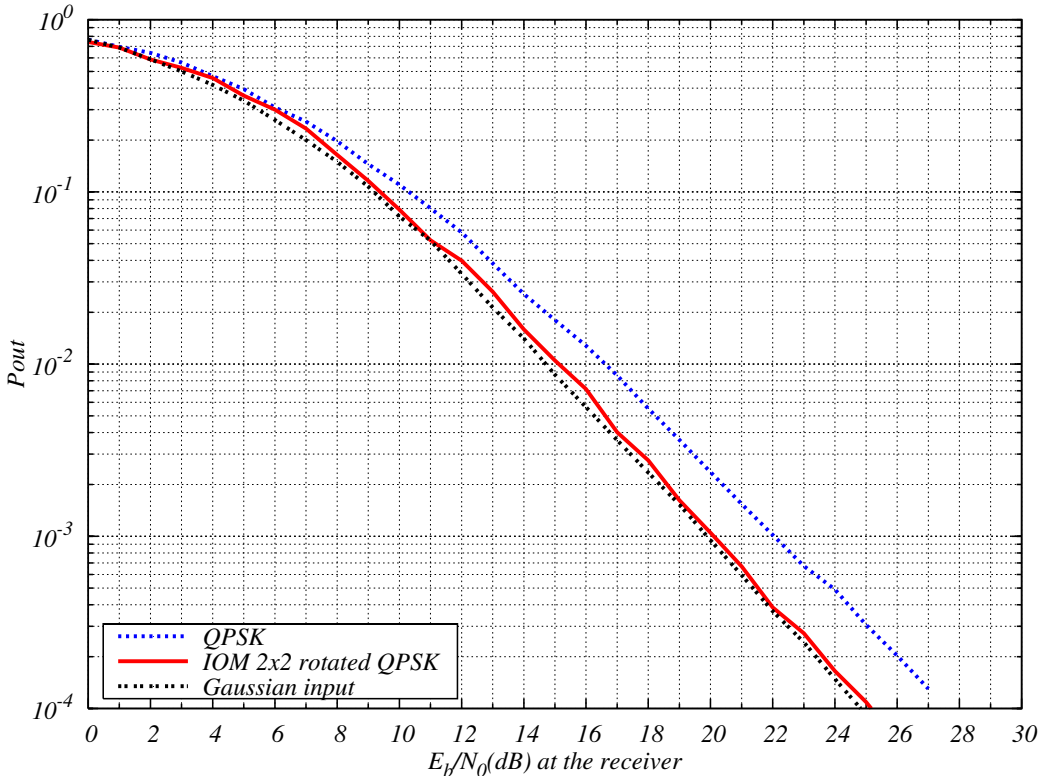

Figure 3.5: Outage probability comparison for the single-relay NAF protocol: QPSK input, rotated QPSK input with 2×2 IOM rotation, and Gaussian input.

In Fig. 3.6, we consider a 16-QAM modulation coded with half-rate codes over the two-relay SAF channel. Without rotation, the decoder is not capable of recovering the diversity as shown in (3.10). Adding a rotation with s_{max} ensures the diversity, but mixes three 16-QAM symbols which results in a dense signal space. We can achieve slightly better performance using a precoder with $s = 2$ as it creates less interference between signals, while ensuring maximum diversity. Note that this gain appears since the first iteration.

Finally, Fig. 3.7 shows the performance of QPSK constellation on a three-relay SAF cooperative channel using $R_c = 1/2$ and $R_c = 3/4$ codes. Diversity is provided in several ways; for $R_c = 3/4$ codes, a rotation with $s = 3$ is sufficient to provide diversity, while two $s = 2$ rotations are used for $R_c = 1/2$. However, to achieve optimal coding gains, a rotation with s_{max} has to be used.
For all these configurations, performance less than 2dB away from outage probability is achieved for codeword sizes in the range of 1000-1500 coded bits.

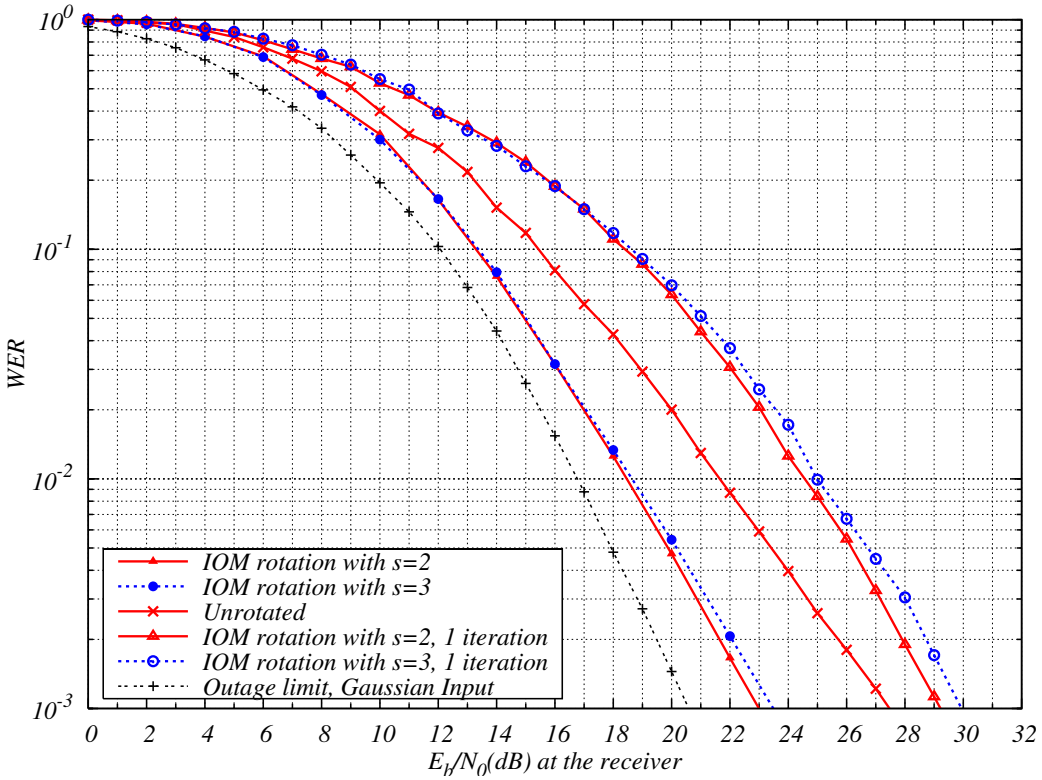

Figure 3.6: Two-relay SAF cooperative channel, R_c=1/2 NRNSC $(23,35)_8$ code, 16-QAM modulation, 1440 coded bits.

3.7 Code multiplexing over channel states for the half-duplex NAF cooperative channel

As discussed in section 2.8, channel multiplexers can ensure maximal diversity orders and optimal coding gains for turbo codes on block-fading channels provided the rate of the code respects $R_c \leq 1/D_{st}$, where D_{st} is number of states of the BO channel. For both the cases of single-input single-output block-fading channel with D_{st} blocks [52] and the MIMO channel with D_{st} channel states (see section 2.8), both the horizontal multiplexer and the h-π-diagonal multiplexer ensured maximal diversity for turbo codes. However, the h-π-diagonal multiplexer showed better coding gain as it helped to equalize the partial Hamming weights in (2.59). It is of great benefit to see what is the optimal channel multiplexer for turbo codes in the NAF protocol, as it was discussed in section 3.6 that for high spectral efficiencies a rotation degrades the performance of the code. In the sequel, we will only discuss the case of half-rate turbo codes over the single-relay half-duplex NAF cooperative channel. The generalization to the β-relay case is straight-forward as long as

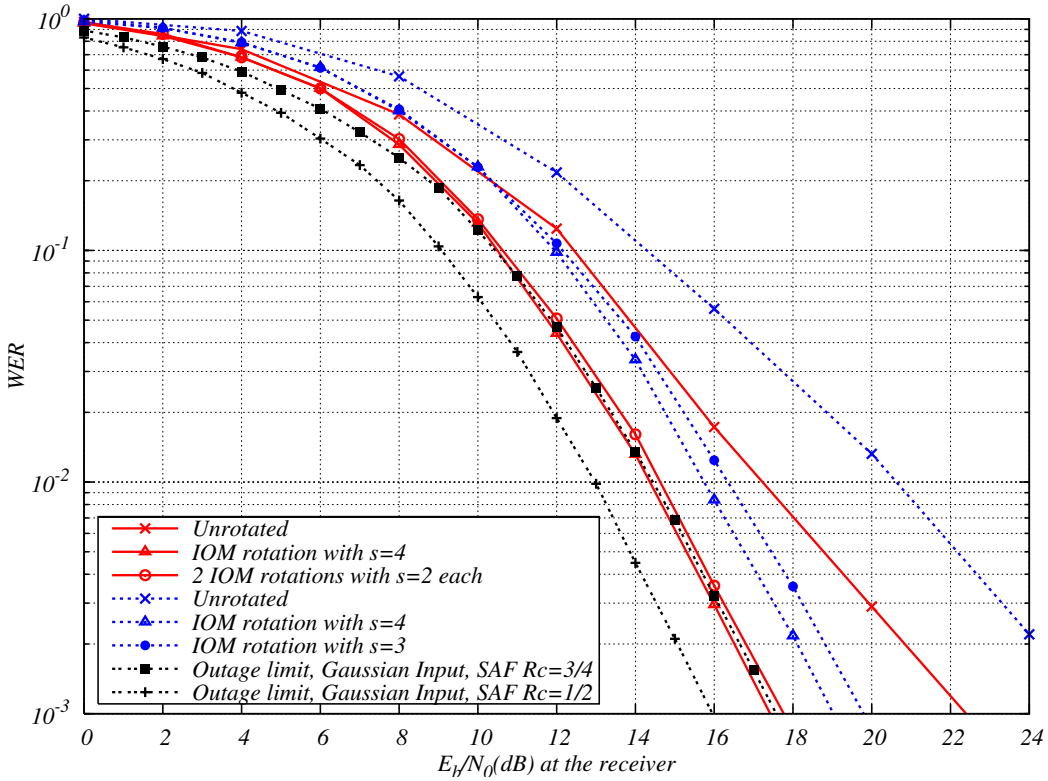

Figure 3.7: Three-relay SAF cooperative channel, R_c=1/2 $(23,35)_8$ (continuous red lines) and 3/4 $(13,25,61,47)_8$ (dashed blue lines) NRNSC codes, QPSK modulation, 1024 coded bits.

$R_c \leq 1/(\beta+1)$. We show in Fig. 3.8 the channel multiplexers for half-rate turbo codes over the NAF channel. Note that when the two channel states of the BO-channel are separated by a commas, this means that the binary element s_i is sent in the first time slot of the cooperation frame, and consequently it sees all the states of the matryoshka channel. The two multiplexers of Fig. 3.8 ensure maximal state diversity at the receiver over a two-state BO-channel as shown for MIMO channel with $n_t = 2$ (see section 2.8). The difference is that with horizontal multiplexing, diversity is always guaranteed by the first RSC code, as all the information bits see the two states of the BO-channel. With h-π-diagonal multiplexing, diversity is ensured through the two constituent codes as for the MIMO channel. However, the coding gains provided by the two multiplexers for the NAF protocol are different from that of the MIMO channel. To illustrate this issue, let us consider the product $\omega_1\omega_2$ of the partial Hamming weight in (2.59). Suppose that the constituent RSC codes are two half-rate $(7,5)_8$ codes, and that the input weight is $\omega = 2$. Consider now error events of length $L = 4+3j$ and total Hamming weight $w_H = 6+2j$,

Horizontal Multiplexer						
$\mathbf{s_1}$	1 , 2	1 , 2	1 , 2	1 , 2	1 , 2	1 , 2
$\mathbf{s_2}$	1	X	1	X	1	X
$\mathbf{s_3}$	X	1	X	1	X	1

H-π-diagonal Multiplexer						
$\mathbf{s_1}$	1 , 2	1	1 , 2	1	1 , 2	1
$\mathbf{s_2}$	1	X	1	X	1	X
$\pi^{-1}(\mathbf{s_3})$	X	1 , 2	X	1 , 2	X	1 , 2

Figure 3.8: Single-relay NAF channel: Horizontal (top) and h-π-diagonal (bottom) multiplexers for a rate 1/2 parallel turbo code.

$i = 0 \ldots (N-4)/3$. For horizontal multiplexing, $\omega_1 = 6 + 2j$ and $\omega_2 = 2$. For h-π-diagonal multiplexing, $\omega_1 = 6 + 2j$ and $\omega_2 = 3 + j$. Let ω_{1i}, ω_{2i}, ω_{1p}, and ω_{2p} be the partial weights of information and parity bits. For horizontal multiplexing, $\omega_{1i} = \omega_{2i} = 2$, $\omega_{1p} = 6 + 2j$, while $\omega_{2p} = 0$. For h-π-diagonal multiplexing, $\omega_{1i} = 2$, $\omega_{2i} = 2$ if j is odd, $\omega_{2i} = 1$ otherwise. $\omega_{1p} = 4 + 2j$, $\omega_{2p} = 1 + j$ if j is odd, $\omega_{2p} = 2 + j$ otherwise. Unlike the case of two-state BO-channel where information bits have diversity 1 with horizontal multiplexing, the horizontal multiplexer better protects the information bits than the h-π-diagonal multiplexer over the single-relay NAF channel. In fact, this interpretation joins the results on the bound on the diversity of Matryoshka block-fading channels under ideal interleaving derived in section 3.5, whereas an optimized interleaver makes the code systematic and places the information bits on the block carrying the maximal diversity order.

3.7.1 Simulation results

Fig. 3.9 and 3.10 shows the performance of half-rate turbo codes with different channel multiplexers and with 2×2 IOM rotations over the single-relay NAF protocol. As shown in section 3.6, IOM rotations are best performing for QPSK constellations, allowing the code to approach the outage probability by less than a dB. On the opposite, it is impossible for the code to manage the interference between QAM symbols created by IOM rotations for large constellations. In addition, horizontal multiplexing slightly outperforms the h-π-diagonal multiplexing in Fig. 3.9 for large constellations, as it better protects information symbols. The gain of horizontal multiplexing is even higher in Fig.

3.10 when the geometric gain g_{sr} between the source and the relay is considerable. Note that, like for MIMO systems, word error rate performance of turbo-coded modulations over the NAF protocol is insensitive to interleaver size.

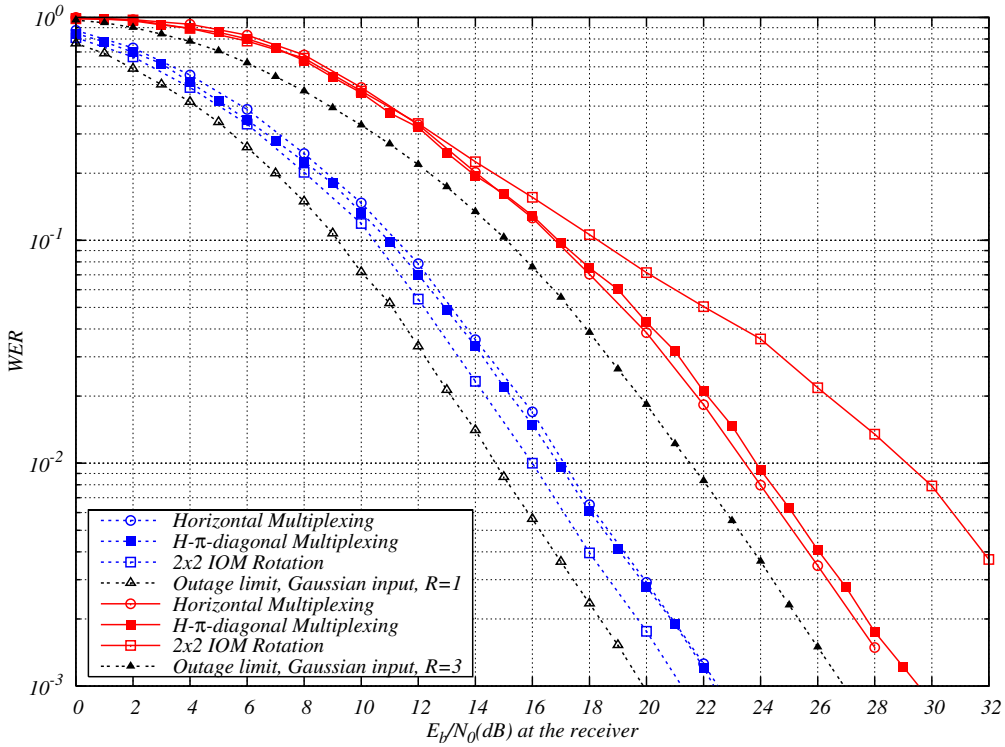

Figure 3.9: Single-relay NAF channel: Frame error rate comparison for QPSK (dashed blue lines) and 64-QAM (continuous red lines) modulations, turbo code with $R_c = 1/2$, $(17, 15)_8$. $g_{sr} = 0$ dB.

3.8 Conclusions

In this chapter, a framework for channel coding over the amplify-and-forward cooperative protocol with iterattive decoding was established. Bounds on the diversity orders for coded systems for the case where all terminal have a single antenna. It was shown that precoding without introducing time delay to the cooperation frame can lead the D-ST-BICM to achieve maximal diversity. The absence of delay is even more important in that it does not increase the detection complexity at the destination. It was also discussed that precoding all the symbols together, which might look as a reliable maximum diversity solution, is in fact harmful for the overall coding gain for large constellations. These coding

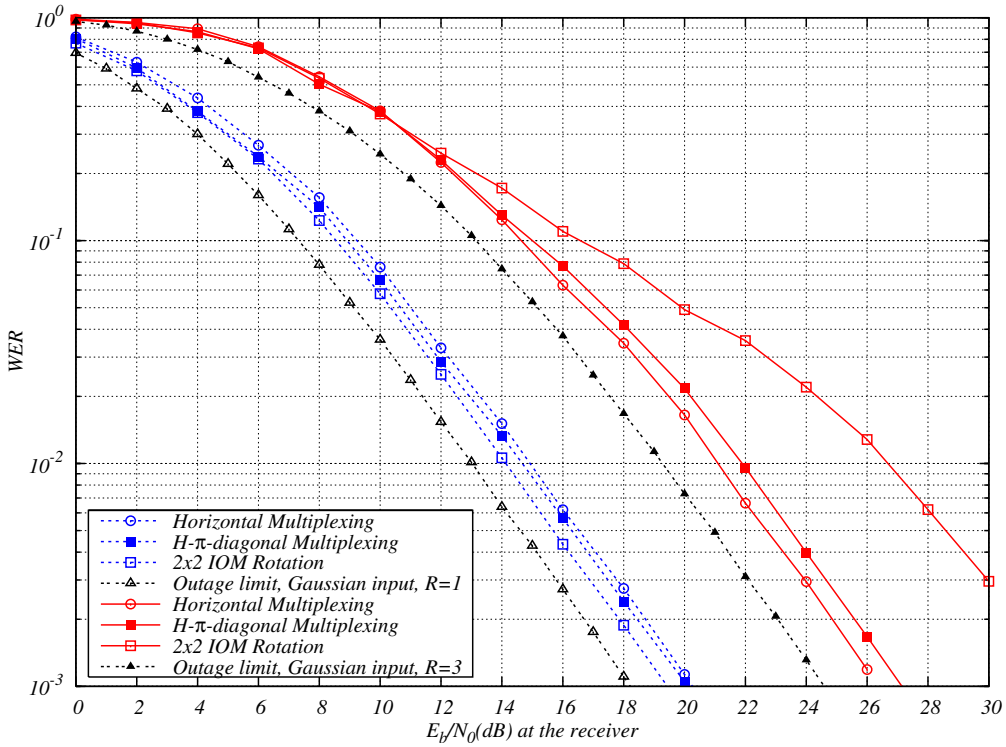

Figure 3.10: Single-relay NAF channel: Frame error rate comparison for QPSK (dashed blue lines) and 64-QAM (continuous red lines) modulations, turbo code with $R_c = 1/2$, $(17, 15)_8$. $g_{sr} = 20$ dB.

strategies also hold when no iterations are possible at the receiver. We also presented channel multiplexing issues for turbo codes over the AF protocol, and showed that we can closely approach the outage probability limit even for large constellations.

Chapter 4

Design of irregular turbo codes for block-fading channels

4.1 Introduction

The block-fading channel is a simplified channel model that characterizes delay-constrained communication over slowly-varying fading channels [2, 7, 54]. The received signal at block c is given by

$$\boldsymbol{y}_c = \alpha_c \boldsymbol{x}_c + \boldsymbol{w}_c \qquad c = 1, \ldots, n_c \tag{4.1}$$

where $\boldsymbol{x}_c, \boldsymbol{y}, \boldsymbol{w}_c \in \mathbb{R}^L$ are the input, output and noise vectors at block $c = 1, \ldots, n_c$, and L is the block length. The noise components have zero mean and variance N_0, and α_c is the Rayleigh fading coefficient of block c, assumed to be perfectly known to the receiver. Particular instances of the block-fading channel are orthogonal-frequency multiplexing modulation (OFDM) and frequency-hopping systems, such as mobile data communications in EDGE/3G and WiMax/LTE environments. Despite its simplification, it captures the essential characteristics of delay-constrained wireless communication and yields useful code design criteria. Since this channel is nonergodic, it has zero capacity and the fundamental limit is the outage probability [2, 7]. It has been shown in [15] that the diversity of binary codes of rate R_c over an n_c-block fading channel is given by the Singleton bound

$$\delta = 1 + \lfloor n_c(1 - R_c) \rfloor. \tag{4.2}$$

The design of binary linear codes for the block-fading channel has been studied in [34, 33, 15, 52, 51, 86]. However, these binary regular codes cannot perform closer than 1 dB from the outage probability. As shown in [51, 86], the effective design procedure for outage-approaching codes follows a two-step process:

1. Design block-wise maximum distance separable (MDS) codes, that achieve the largest possible diversity given by the Singleton bound in the block-erasure channel [87];

2. Reducing the decoding threshold in the AWGN channel.

In this chapter, we design irregular binary turbo codes [88] for block-fading channels. Based on the h-π-diagonal multiplexer [52] we design irregular turbo codes with full diversity. We then find irregular turbo codes with low decoding thresholds over the AWGN. We show that the resulting codes perform within 0.5 dB from the outage probability in both density evolution and finite-length cases, achieving the current best performance reported in the literature.

The organization of the chapter is as follows. In Section 4.2, we describe the structure and density evolution of irregular turbo codes. The specific block-fading design and density evolution are described in Section 4.3. Section 4.4 gives the concluding remarks.

4.2 Basics on Irregular Turbo Codes

In regular parallel turbo codes, the two constituent recursive systematic convolutional (RSC) encoders are identical (*i.e.* same constraint length and generator polynomials) [89]. This is equivalent to merging the two constituent encoders into a single one, and doubling the size of the interleaver. To do so, a 2-fold repeater is added before the interleaver Π, and we obtain a self-concatenated turbo code [90][91] as shown in Fig. 4.1. In this representation, each information bit is connected to the code trellis via two edges. We hence say that the *degree* of the information bits is $d = 2$ as shown in the propagation tree in Fig. 4.2, and that the turbo code is *regular*. Using this structure, one can create irregularity by repeating a certain fraction f_i of information bits i times, inducing larger protection for some bits than in the regular case [92]. Like for low-density parity check (LDPC) codes [93, 94], irregularity can enhance the performance of turbo codes for large block lengths [88, 92, 95, 96]. The encoder of an irregular turbo code is similar to that of Fig. 4.1, with the difference that the information bit stream is fed to a non-uniform repeater that divides the information bits into d classes with $d = 2, ..., d_{\max}$, where $d_{\max}$ is the maximum bit-node degree [88]. The number of bits in a class d is a fraction f_d of the total number of information bits at the turbo encoder input, knowing that bits in class d are repeated d times. Finally, the output of the non-uniform repeater is interleaved and fed to the RSC constituent code. In order to ensure a target rate, puncturing is used, and only a fraction $1 - f_p$ of parity bits are transmitted, where f_p is the fraction of punctured parity bits. Now let K denote the length of the information sequence, N the interleaver

size, ρ the rate of the RSC constituent code, and R_c the rate of the turbo code. We have the following

$$\sum_{d=2}^{d_{\max}} f_d = 1, \quad \sum_{d=2}^{d_{\max}} d \cdot f_d = \overline{d}, \tag{4.3}$$

$$N = \sum_{d=2}^{d_{\max}} d \cdot (f_d K) = K \cdot \overline{d}, \tag{4.4}$$

$$R_c = \frac{K}{K + \frac{N}{\rho} - N} = \frac{1}{1 + \left(\frac{1}{\rho} - 1\right)\overline{d}}, \tag{4.5}$$

$$\rho = \frac{1}{1 + (1 - f_p)\left(\frac{1}{\rho_0} - 1\right)}, \tag{4.6}$$

where $\rho_0 = k/n$ is the initial rate of the constituent RSC code before puncturing, and $\overline{d}$ is the average degree of information bits. Similar to LDPC codes, the degree distribution from an edge perspective is defined by

$$\lambda_d = \frac{d \cdot f_d}{\overline{d}}, \quad d = 2 \dots d_{\max}. \tag{4.7}$$

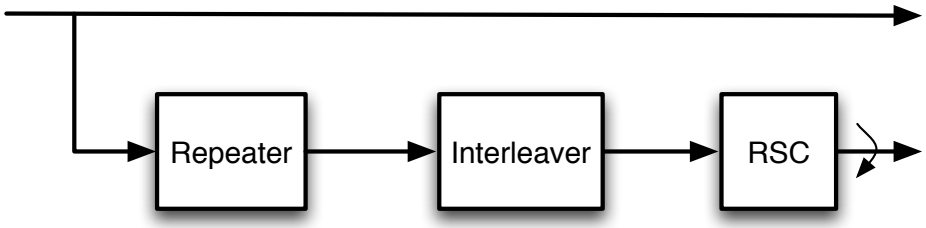

Figure 4.1: Systematic self-concatenated turbo encoder. Information bits are sent directly over the channel, and parity bits are generated by first repeating information bits, interleaving, and then recursive systematic convolutional (RSC) encoding.

4.2.1 Density Evolution in AWGN

We consider rate-R_c irregular turbo codes built from a rate-ρ RSC constituent code and degree profile $\{f_d\}_{d=2,\dots,d_{\max}}$. Due to the symmetry of the channel, we assume that the all-zero codeword is modulated into $\boldsymbol{x} = +1, +1, ..., +1$ and transmitted over an AWGN

channel with noise variance N_0. At the channel output, each received sample can be written as $y = x + w = 1 + w$, so the log-likelihood ratio (LLR) is given by the well-known expression:

$$\mathcal{M}_0 = \log \frac{p(y|x=+1)}{p(y|x=-1)} = \frac{2}{N_0} y = \frac{2}{N_0}(1+w). \tag{4.8}$$

We have $\mathcal{M}_0 \sim \mathcal{N}(\frac{2}{N_0}, \frac{4}{N_0})$, the associated probability density function will be denoted by $p_0(x)$.

The local neighborhood tree for an information bit belonging to an acyclic asymptotically large irregular turbo code is shown in Fig. 4.2. The index i refers to the decoding iteration number. A bitnode of degree d has $d-1$ incoming extrinsic probabilities ξ_i and one outgoing *a priori* probability $\pi_{d,i}$ which also plays the role of a partial *a posteriori* probability (APP). The total APP may be obtained by combining $\pi_{d,i}$ with an extra extrinsic probability. The message associated to ξ_i is $\mathcal{M}_i = \frac{\log(\xi_i(\text{bit}=0))}{\log(\xi_i(\text{bit}=1))}$ and its probability density function is $p_{\mathcal{M}_i}(x)$. Given d and i, the probability density function of log-ratio messages associated to $\pi_{d,i}$ will be denoted by $p_{d,i}(x)$. Following [96] we have that

$$p_{d,i}(x) = \mathcal{F}^{-1}\left[\mathcal{F}\left[p_0(x)\right]\mathcal{F}^{d-1}\left[p_{\mathcal{M}_i}(x)\right]\right] \tag{4.9}$$

where $\mathcal{F}$ denotes the Fourier transform operator. Based on partial a posteriori probabilities, the average bit error probability at iteration i is defined as

$$P_b(i) = \sum_{d=2}^{d_{\max}} f_d P_b(d,i) \tag{4.10}$$

where $P_b(d,i)$ is the bit error probability of class d given by the area under the tail of $p_{d,i}(x)$.

At an RSC checknode level as illustrated in Fig. 4.2, based on a priori input π_{i-1} with pdf $p_{i-1}(x)$, an accurate estimation of $p_{\mathcal{M}_i}(x)$ is made via a forward-backward algorithm [97] applied on a sufficiently large trellis window of size W centered around the information bit. Since we are dealing with random ensembles of irregular turbo codes, we have

$$p_i(x) = \sum_{d=2}^{d_{\max}} \lambda_d \; p_{d,i}(x). \tag{4.11}$$

Given an irregular turbo ensemble, its decoding *threshold* is the minimal signal-to-noise ratio E_b/N_0 for which $P_b(i)$ vanishes with i. The threshold can be determined via Density Evolution (DE) [96], a procedure where $p_i(x)$ is updated from $p_{i-1}(x)$ by propagating probabilistic densities through the tree graph of Fig. 4.2.

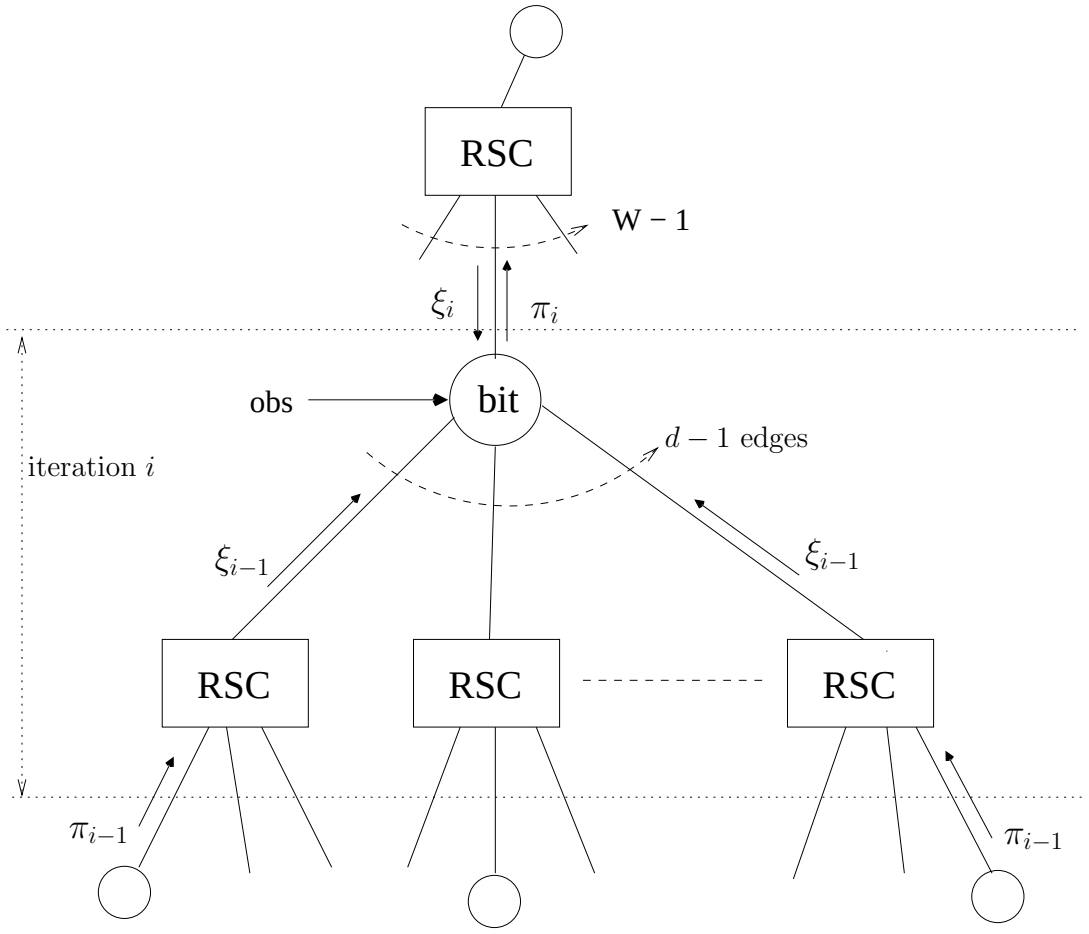

Figure 4.2: Propagation tree used in density evolution for an irregular turbo code. The π_i represents *a priori* probability, and the ξ_i the extrinsic probability. Circles represent bitnodes, and rectangles are local neighborhood RSC trellis constraints.

4.2.2 Numerical results for AWGN

The DE method gives the limiting convergence behavior of capacity-approaching codes, and it is used to find optimal degree profiles for LDPC codes in [93, 96, 98]. By setting the average degree to be $\overline{d} = 3$ and using the RSC $(13, 15)_8$ constituent code, we obtained powerful half-rate irregular turbo codes with different degree profiles; for example by taking $f_2 = 0.9$, $f_9 = 0.04$, and $f_{15} = 0.06$, the threshold is 0.31 dB. The distributions $f_2 = 0.923$ and $f_{15} = 0.077$ or $f_2 = 0.9$ and $f_{12} = 0.1$, yield a 0.36 dB threshold. Recall that Shannon limit for half-rate coding over the AWGN channel is approximately 0.18 dB. The irregular turbo code defined by $f_2 = 0.9$ and $f_{12} = 0.1$ is used later in section 4.3

over the block-fading channel.

4.3 Irregular Turbo Codes over Block-Fading Channels

In [52], the authors proposed multiplexer design for regular parallel turbo codes that ensure full diversity and optimal coding gain. However, as the self-concatenated structure of the code involves only one constituent code, the generalization of the so-called h-π-diagonal multiplexers initially designed for regular parallel turbo codes is not straightforward. Without loss of generality, we restrict our design to irregular turbo codes over block-fading channels with $n_c = 2$ blocks and rate $R_c = 1/2$. The extension to block-fading channels with more fading blocks follows similar arguments but it is not discussed in this manuscript. Special care should be taken when designing a turbo code that achieves the Singleton bound without attaining full diversity, i.e., $n_c > \delta \geq 1/R_c$.

In an irregular turbo code with average degree $\overline{d}$, a bit is connected to the trellis of the code via $\overline{d}$ edges on average. Following the identity $N = K\overline{d}$, this can be seen as a "parallel" turbo code with β constituent codes, where:

$$\beta = \lceil\ \overline{d}\ \rceil \tag{4.12}$$

In order to achieve high coding gains, the h-π-diagonal multiplexer should be extended to irregular turbo codes. We consider constituent RSC codes with initial coding rate $\rho_0 = 1/2$. To keep the structure of the multiplexer, only half of the parity bits of the first RSC constituent code should be punctured, knowing that the overall rate R_c should remain fixed. Now let ϕ_p be the fraction of parity bits to be punctured from every RSC constituent code starting from the second one. We have that:

$$\phi_p = \frac{\beta f_p - \frac{1}{2}}{\beta - 1} \tag{4.13}$$

The general h-π-diagonal multiplexer is shown in Fig. 4.3, where b is the information bit, and s_j is the parity bit of constituent code j. As an example, we consider a half-rate irregular turbo code with $\beta = \overline{d} = 3$. This gives $f_p = 0.66$ and $\phi_p = 0.75$, so 3 parity bits out of 4 are punctured from both RSC 2 and RSC 3. Again, we consider a half-rate irregular turbo code with $\overline{d} = 2.727$. We get $f_p = 0.63$ and $\phi_p = 0.7$. The puncturing pattern is then slightly different from that of the previous example, as in a period of length 20, there is one more bit that is sent over the channel.

RSC 1 (information)	b	1	2	1	2
RSC 1 (parity)	s_1	2	X	2	X
RSC 2 (parity)	$\pi^{-1}(s_2)$	X	1/X	X	1/X
$\vdots$	$\vdots$	$\vdots$	$\vdots$	$\vdots$	$\vdots$
RSC β (parity)	$\pi^{-1}(s_\beta)$	X	1/X	X	1/X

Figure 4.3: H-π-diagonal multiplexer of a half-rate irregular turbo code built from $\rho_0 = 1/2$ constituent RSC code. The number of rows is $\beta + 1$ where $\beta = \lceil\, \bar{d}\, \rceil$. One parity bit out of two is punctured from RSC 1. There is a fraction ϕ_p of punctured parity bits per row (represented by an X) starting from RSC 2.

4.3.1 Density evolution on BF channel

In this section we study the word error rate performance of half-rate irregular turbo codes over a two-state block-fading channel via density evolution. As with the AWGN channel, we assume that the all-zero codeword is modulated into $x = +1, +1, ..., +1$ and transmitted over a block-fading channel with n_c states ($n_c = 2$ in our case).

For a given fading instance $\boldsymbol{\alpha} = (\alpha_1, \alpha_2)$, the irregular turbo code ensemble is observing two types of channel messages, $\mathcal{M}_{0,1} \sim \mathcal{N}(\frac{2\alpha_1}{N_0}, \frac{4\alpha_1^2}{N_0})$ and $\mathcal{M}_{0,2} \sim \mathcal{N}(\frac{2\alpha_2}{N_0}, \frac{4\alpha_2^2}{N_0})$, as in (4.8). DE is performed in a similar fashion as described in Section 4.2.A after taking into account the multiplexing of bits (i.e. which channel assigned to which bit) as defined in Fig. 4.3. At a fixed SNR, it is possible to determine via DE whether the average bit error probability $P_b(i)$ vanishes with i or not. When $P_b(i) \nrightarrow 0$ as $i \to +\infty$, we say that a density evolution outage (DEO) occurs.

Now, let us define the following indicator function:

$$\mathbf{1}_{\text{DEO}}(\alpha) = \begin{cases} 0, & P_b(i) \to 0, \\ \\ 1, & P_b(i) \nrightarrow 0. \end{cases} \tag{4.14}$$

The probability of a DEO is then given by

$$P_{\text{DEO}} = \int_{\boldsymbol{\alpha} \in \mathbb{R}^2} \mathbf{1}_{\text{DEO}}(\boldsymbol{\alpha}) p(\boldsymbol{\alpha}) d\boldsymbol{\alpha} = \int_{\boldsymbol{\alpha} \in V_o} p(\boldsymbol{\alpha}) d\boldsymbol{\alpha}, \tag{4.15}$$

where V_o is the outage region for the irregular turbo code ensemble under DE, i.e.,

$$V_o = \left\{ \boldsymbol{\alpha} \in \mathbb{R}_+^{n_c} \mid \mathbf{1}_{\text{DEO}}(\boldsymbol{\alpha}) = 1 \right\}. \tag{4.16}$$

The $(n_c - 1)$-dimensional surface separating V_o from its complementary in $\mathbb{R}_+^{n_c}$ is called the outage boundary. Thus, DE on a block-fading channel is a method to determine the outage

boundary for a given turbo code ensemble at a given SNR. The information-theoretical boundary related to the outage probability is defined by the equality $C(\boldsymbol{\alpha}, E_b/N_0) = R_c$, where C is the channel capacity (or mutual information) under a certain type of input alphabet.

For an infinite-length code ensemble, it is easy to show that the word error probability P_{ew} satisfies [86]

$$P_{\text{DEO}} \leq P_{ew}. \tag{4.17}$$

Consequently, the outage probability found by DE is a lower bound for the word error probability and can be compared to the information outage probability. Equality in (4.17) occurs if the block threshold is equal to the bit threshold [99].

4.3.2 Numerical results on BF channel

Fig. 4.5 compares the outage boundary of regular and irregular turbo codes with the 8-state RSC$(13, 15)_8$ constituent code and h-π-diagonal multiplexing at $E_b/N_0 = 8$dB. The irregular turbo code is the best one from Section 4.3.1, with a threshold of 0.31dB on the AWGN channel. The boundaries are computed by picking points orthogonal to the BPSK input outage. Although irregular and regular codes have similar performance for largely unbalanced fading pairs, the irregular turbo code performs better in the neighborhood of the ergodic line. It actually approaches the BPSK input outage border over a large range of fading pairs.

Fig. 4.6 shows the word error rate performance of the same codes and h-π-diagonal multiplexing under both density evolution and Monte Carlo simulation with $K = 6000$ bits. As we observe, both DE performance and finite-length are very close to the outage probability (within 0.5 dB). Note that, as observed in [15, 52, 51, 86], irregular turbo codes are good for the block-fading channel, in the sense that their performance is insensitive to the block length.

For finite length simulations, the repeater should be designed in a special way, as shown in Fig. 4.4. Bits are divided into two groups, and only the information bits of the first RSC are transmitted over the channel: circled bits are transmitted over the 1^{st} channel state, and non-circled bits are sent over the 2^{nd} channel state. To guarantee full diversity, the decoder should always find its way through the trellis of the code, thus bits corresponding to the same trellis transition should not be sent over the same channel state [52]. In order to ensure this property, bits of degree greater than 2 are placed in the H positions in the multiplexer of Fig. 4.4. Repetition is thus done in a way that if the 2nd channel state is unreliable, decoding can be successful through RSC 2 and RSC 3, and if the 1st channel state is unreliable, RSC 1 can decode the received codeword.

	RSC 1						RSC 2						RSC 3					
I	(1)	2	(3)	4	(5)	6	(1)	2	(H)	(H)	(5)	6	(H)	(H)	(3)	4	(H)	(H)
P	p_1	X	p_3	X	p_5	X	X	(p_2)	X	X	X	(p_6)	X	X	X	(p_4)	X	X

Figure 4.4: H-π-diagonal multiplexer of a half-rate irregular turbo code with $\overline{d} = 3$ transmitted on a 2-state block-fading channel using a punctured half-rate constituent RSC code. The irregular turbo encoder is built using 3 constituent encoders, where only the information bits (on the line labeled with I) of RSC 1 are transmitted over the channel. The bits p_i correspond to parity bits, the X represents punctured parity bits, and the bits labeled H correspond to bits with degree higher than 2. The circled bits are sent over the the 1^{st} channel state, the other bits are sent over the 2^{nd} state. In order to achieve full diversity, some of the circled information bits should be repeated more than twice and fed to RSC 2 and RSC 3.

Note that although the density evolution convergence criterion is based on bit error probability, it is relevant to assume that the word error probability of irregular turbo codes has an equivalent decoding threshold under density evolution. In fact, it was shown in [99] that the word and bit error probability of certain LDPC codes, among which the class of Irregular Repeat-Accumulate (IRA) codes [100], have identical thresholds. Irregular turbo codes can be seen as IRA codes that are decoded iteratively using a different scheduling, that results from the difference between forward-backward and belief-propagation decoding.

4.4 Conclusions

In this chapter, we presented irregular turbo codes that are capable of closely approaching the outage probability of the block-fading channel, both in terms of density evolution (infinite length) and finite length. The design method is based on two steps. First, a suitable full-diversity multiplexer was designed. Second, codes were optimized over the AWGN channel through density evolution. This represents the best family of codes over the block-fading channel reported in the literature.

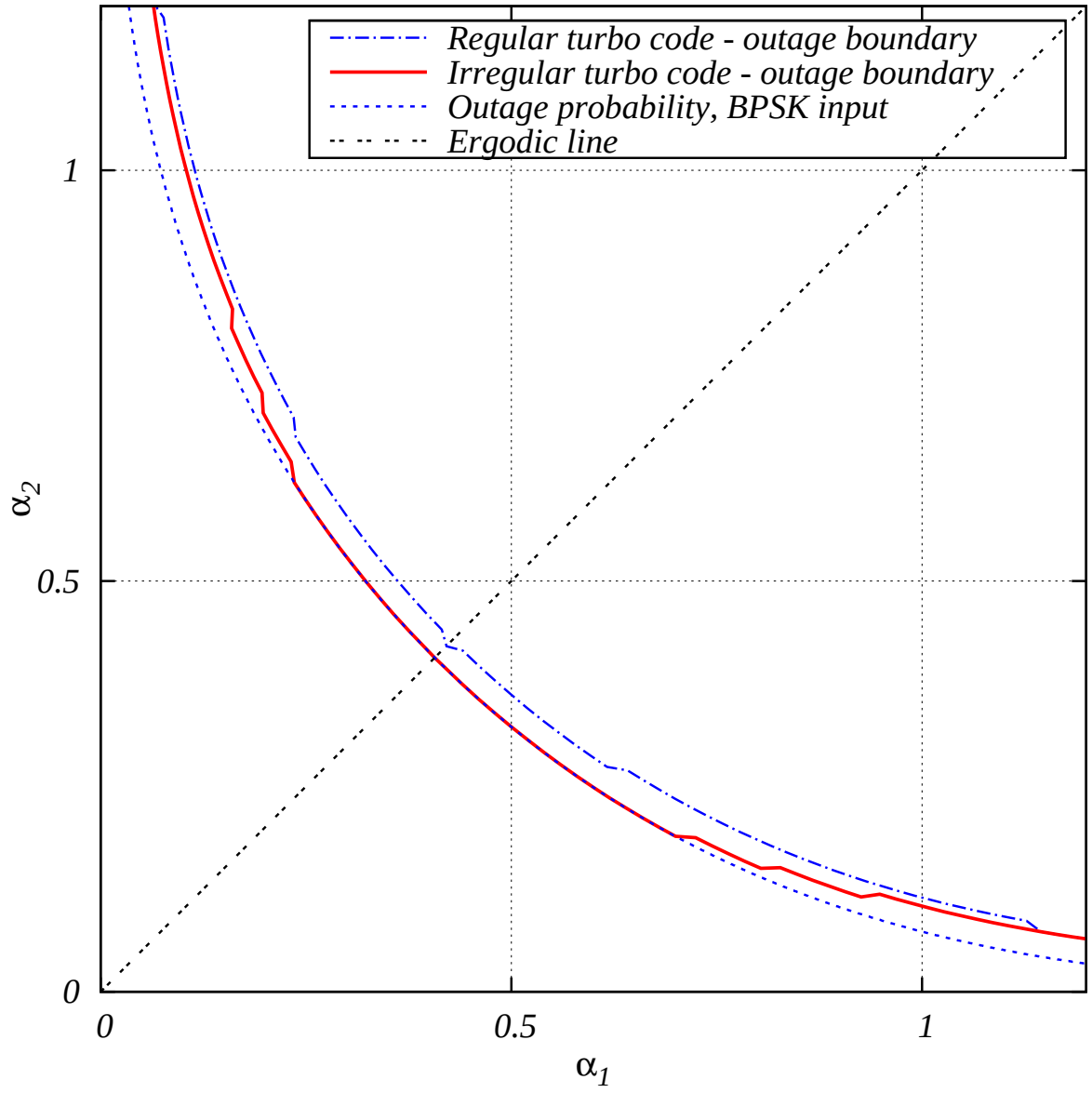

Figure 4.5: Outage boundary of regular and irregular turbo codes under h-π-diagonal multiplexing and with the RSC $(13, 15)_8$ constituent code at $E_b/N_0 = 8$dB. Circles filled with crosses correspond to the fading pairs in which irregular turbo codes outperform regular codes. Although the two codes have similar performance with largely unbalanced fading pairs, the irregular code outperforms the regular code in the vicinity of the ergodic line.

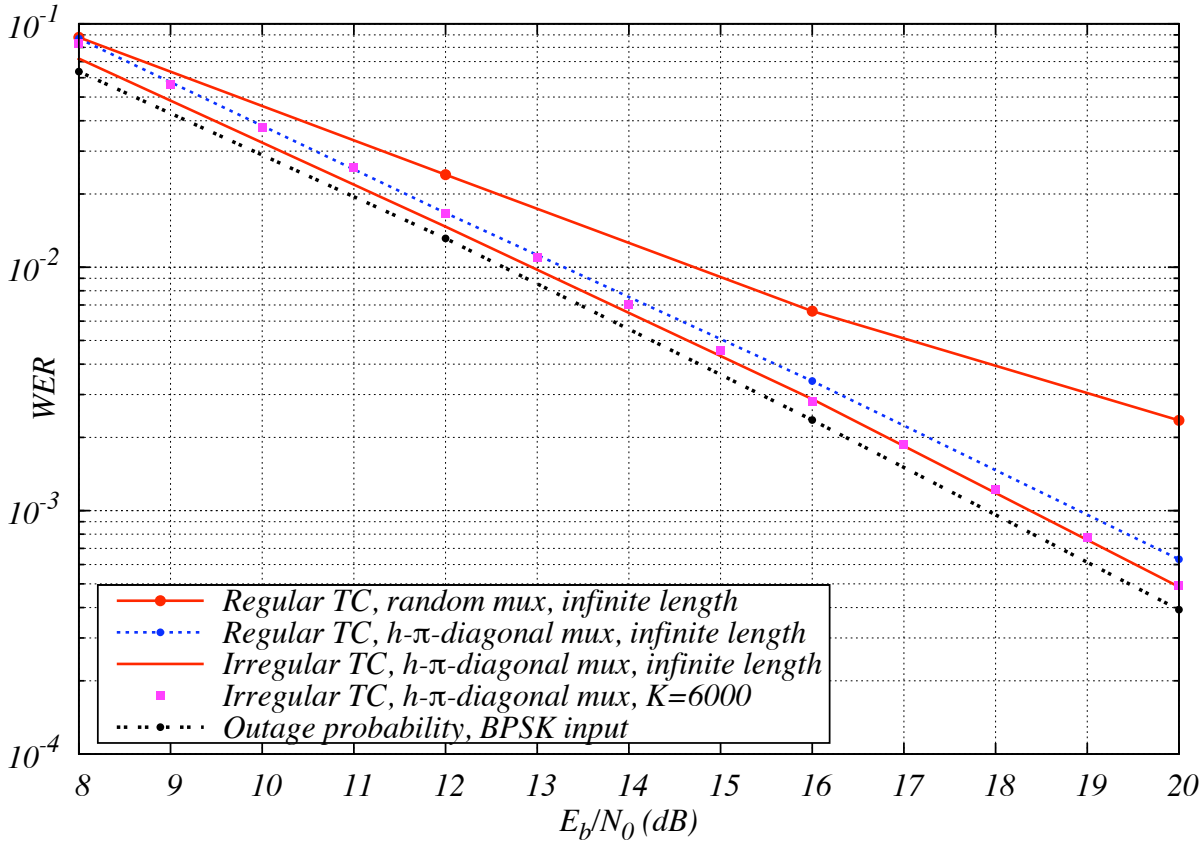

Figure 4.6: Word error rate for $R_c = \frac{1}{2}$ turbo codes over the block-fading channel with $n_c = 2$, RSC $(13, 15)_8$ constituent code and BPSK modulation. Performance of codes is invariant with codeword length, and it was estimated using both the density evolution algorithm and Monte Carlo simulations.

Conclusions

This manuscript presented space-time bit-interleaved coded modulations for both the multiple-antenna block-fading channel and the amplify-and-forward cooperative fading channel with single-antenna nodes. What these schemes have in common is that they were capable of achieving the maximal diversity orders the block-fading channels -they were designed for- allowed and they provided high coding gains with relatively low decoding complexity at the receiver.

For the multiple-antenna channel, we proposed the following:

- *Information Outage Minimizing* (IOM) space-time precoders: these precoders allow for optimal performance of the ST-BICM if no iterations are possible at the receiver. They can also be adapted so that they become optimal for both "one-shot" decoding and iterative decoding

- Matrix-Alamouti space-time precoder: application of the Alamouti scheme with two transmit antennas to four transmit antennas. With proper signal decoupling and iterative interference cancellation/decoding, frame error rate robust with respect to the frame size was achieved.

- Turbo-code design for multiple-antenna systems: these systems achieved optimal word error rate performance insensitive to the interleaver size by using a special multiplexer that places the binary elements at the output of the code "intelligently" on the channel states. This performance is achieved at no additional cost in complexity.

For the amplify-and-forward cooperative fading channel, the following results were carried out:

- Bounds on the diversity order of coded systems over the Matryoshka block-fading channel representing the slotted amplify-and-forward protocol were derived. These bounds can be achieved by judicious precoding without affecting the decoding complexity.

- Coding strategies based on the bounds on diversity that allow to achieve high coding gains depending on the coding rate, modulation size, and number of relays.
- Turbo-code design for the amplify-and-forward cooperative fading channel: the code multiplexer that suits the Matryoshka block-fading channel model proved to be optimal. Again, word error rate performance insensitive to block size at no increase in complexity is achieved.

Finally, we proposed irregular turbo codes that exhibit a vanishing gap with the outage probability for large block lengths over the single-input single-output block-fading channel. This is done through an adapted channel multiplexer that suits the self-concatenated structure of the code. This result can be applied to any block-fading channel type. The material elaborated in this report opens the way for the following perspectives:

- Study of sub-optimal receivers for the SAF protocol: indeed, the upper-triangular structure of the channel matrix can allow for the implementation of sub-optimal detectors such as the Successive Interference Cancellation (SIC) or the SISO-Minimum Mean-Square Error (MMSE) detectors that can provide a drastic complexity reduction with respect to the exhaustive APP detector.
- Derive bounds on the diversity order of the MIMO-SAF channel: investigate on what diversity orders a D-ST-BICM can achieve in the case where the nodes have multiple antennas.
- Study of Decode-and-Forward protocols from the D-ST-BICM point-of-view.
- Study of the schemes proposed in this manuscript for Multi-Carrier (MC)-CDMA systems and OFDM systems.

Bibliography

[1] J. G. Proakis, *Digital communications*, McGraw-Hill New York, 1989.

[2] L.H. Ozarow, S. Shamai, and A.D. Wyner, "Information theoretic considerations for cellular mobile radio," *IEEE Transactions on Vehicular Technologies*, vol. 43, no. 2, pp. 359–378, May 1994.

[3] C.E. Shannon, "The Mathematical Theory of Communication," *Bell System Technical J*, vol. 27, pp. 379–423, 1948.

[4] I.E. Telatar, "Capacity of Multi-Antenna Gaussian Channels," *European Transactions on Telecommunications*, vol. 10, no. 6, November 1999.

[5] G.J. Foschini and M.J. Gans, "On Limits of Wireless Communications in a Fading Environment when Using Multiple Antennas," *Wireless Personnal Communications*, vol. 6, no. 3, pp. 311–335, March 1998.

[6] S. Verdu and Te Sun Han, "A general formula for channel capacity," *IEEE Transactions on Information Theory*, vol. 40, no. 4, pp. 1147–1157, July 1994.

[7] E. Biglieri, J. Proakis, and S. Shamai, "Fading channels: information-theoretic and communications aspects," *IEEE Transactions on Information Theory*, vol. 44, no. 6, pp. 2619–2692, October 1998.

[8] G. Caire, G. Taricco, and E. Biglieri, "Optimum power control over fading channels," *IEEE Transactions on Information Theory*, vol. 45, no. 5, pp. 1468–1489, July 1999.

[9] A. Guillén i Fàbregas, *Concatenated Codes for Block-Fading Channels*, Ph.D. thesis, EPFL, Lausanne, 2004.

[10] Z. Wang and G.B. Giannakis, "Outage mutual information of space-time MIMO channels," *IEEE Transactions on Information Theory*, vol. 50, no. 4, pp. 657–662, April 2004.

[11] T.M. Cover and J.A. Thomas, *Elements of Information Theory*, Wiley New York, 1991.

[12] G. Ungerboeck, "Channel coding with multilevel/phase signals," *IEEE Transactions on Information Theory*, vol. 28, no. 1, pp. 55–67, 1982.

[13] E. Zehavi, "8-PSK trellis codes for a Rayleigh channel," *IEEE Transactions on Communications*, vol. 40, no. 5, pp. 873–884, 1992.

[14] G. Caire, G. Taricco, and E. Biglieri, "Bit-interleaved coded modulation," *IEEE Transactions on Information Theory*, vol. 44, no. 3, pp. 927–946, May 1998.

[15] A. Guillén i Fàbregas and G. Caire, "Coded modulation in the block-fading channel: coding theorems and code construction," *IEEE Transactions on Information Theory*, vol. 52, no. 1, pp. 91–114, Jan. 2006.

[16] J.J. Boutros, N. Gresset, and L. Brunel, "Turbo coding and decoding for multiple antenna channels," *International Symposium on Turbo Codes & Related Topics*, 2003.

[17] N. Gresset, *New space-time coding techniques with bit-interleaved coded modulations*, Ph.D. thesis, ENST, Paris, 2004.

[18] D.J. Costello Jr and G.D. Forney Jr, "Channel Coding: The Road to Channel Capacity," *Arxiv preprint cs.IT/0611112*, 2006.

[19] P. Elias, "Coding for noisy channels," *IRE Conv. Rec*, vol. 4, no. S 37, pp. 47, 1955.

[20] P. Elias, "Error-free Coding," *IEEE Transactions on Information Theory*, vol. 4, no. 4, pp. 29–37, 1954.

[21] G.D. Forney Jr, *Concatenated codes*, Cambridge MA, MIT Press, 1966.

[22] R. Gallager, "Low-density parity-check codes," *IEEE Transactions on Information Theory*, vol. 8, no. 1, pp. 21–28, 1962.

[23] D. Divsalar and F. Pollara, "Turbo codes for PCS applications," *IEEE International Conference on Communications, 1995*, vol. 1, 1995.

[24] S. M. Alamouti, "A simple transmit diversity technique for wireless communications," *IEEE Journal on Selected Areas in Communications*, vol. 16, no. 8, pp. 1451–1458, October 1998.

[25] V. Tarokh, N. Seshadri, and A.R. Calderbank, "Space-Time Codes for High Data Rate Wireless Communication: Performance Criterion and Code Construction," *IEEE Transactions on Information Theory*, vol. 44, no. 2, March 1998.

[26] J.J Boutros, N. Gresset, L. Brunel, and M. Fossorier, "Soft-input soft-output lattice sphere decoder for linear channels," *IEEE Global Telecommunications Conference*, vol. 3, 2003.

[27] H. V. Poor, "Iterative Multiuser Detection," *IEEE Signal Processing Magazine*, pp. 81–88, January 2004.

[28] M. Sudan, "Decoding of Reed-Solomon codes beyond the error-correction bound," *Journal of Complexity*, vol. 13, no. 1, pp. 180–193, 1997.

[29] R. Koetter and A. Vardy, "Algebraic soft-decision decoding of Reed-Solomon codes," *IEEE Transactions on Information Theory*, vol. 49, no. 11, pp. 2809–2825, 2003.

[30] A. Viterbi, "Error bounds for convolutional codes and an asymptotically optimum decoding algorithm," *IEEE Transactions on Information Theory*, vol. 13, no. 2, pp. 260–269, 1967.

[31] R. Silverman and M. Balser, "Coding for constant-data-rate systems," *IEEE Transactions on Information Theory*, vol. 4, no. 4, pp. 50–63, 1954.

[32] G. Battail, "Pondération des symboles décodés par l'algorithme de Viterbi," *Annales des télécommunications*, vol. 42, no. 1-2, pp. 31–38, January-February 1987.

[33] E. Malkamaki and H. Leib, "Evaluating the performance of convolutional codes over block fading channels," *IEEE Transactions on Information Theory*, vol. 45, no. 5, pp. 1643–1646, July 1999.

[34] R. Knopp and P.A. Humblet, "On coding for block fading channels," *IEEE Transactions on Information Theory*, vol. 46, no. 1, pp. 189–205, Jan. 2000.

[35] G.J. Foschini, "Layered space-time architecture for wireless communication in a fading environment when using multielement antennas," *Bell Labs Technical Journal*, pp. 41–49, October 1996.

[36] J.-C. Guey, M.P. Fitz, M.R. Bell, and W.-Y. Kuo, "Signal design for transmitter diversity wireless communication systems over Rayleigh fading channels," *IEEE Vehicular Technology Conference*, 1996.

[37] G. Battail, "Rotating a redundant constellation in signal space against channel fluctuations," *International Conference on Communications Technology, Beijing, China, July. Also ENST, Paris, France, internal report*, 1989 (postponed until 1990).

[38] K. Boulle and J.-C. Belfiore, "Modulation scheme designed for the Rayleigh fading channel," *Conference on Information Sciences and Systems (CISS 1992), Princeton University, March 1992.*, pp. 288–293, 1992.

[39] V. M. DaSilva and E.S. Sousa, "Fading-resistant modulation using several transmitter antennas," *IEEE Transactions on Communications*, vol. 45, no. 10, pp. 1236–1244, Oct. 1997.

[40] J.J. Boutros and E. Viterbo, "Signal space diversity: a power-and bandwidth-efficient diversitytechnique for the Rayleigh fading channel," *IEEE Transactions on Information Theory*, vol. 44, no. 4, pp. 1453–1467, July 1998.

[41] D. Rainish, "Diversity Transform for Fading Channels," *IEEE Transactions on Information Theory*, vol. 44, no. 12, pp. 1653–1661, December 1996.

[42] C. Lamy and J. Boutros, "On Random Rotations Diversity and Minimum MSE Decoding of Lattices," *IEEE Transactions on Information Theory*, vol. 46, pp. 1584–1589, July 2000.

[43] H. El Gamal and M. O. Damen, "Universal space-time coding," *IEEE Transactions on Information Theory*, vol. 49, no. 5, pp. 1097–1119, May 2003.

[44] B.A. Sethuraman, B.S. Rajan, and V. Shashidhar, "Full-diversity, high-rate space-time block codes from division algebras," *IEEE Transactions on Information Theory*, vol. 49, no. 10, pp. 2596–2616, October 2003.

[45] M.O. Damen, A. Tewfik, and J.-C. Belfiore, "A construction of a space-time code based on number theory," *IEEE Transactions on Information Theory*, vol. 48, no. 3, pp. 753–760, March 2002.

[46] J.-C. Belfiore, G. Rekaya, and E. Viterbo, "The Golden code: a 2×2 full-rate space-time code with nonvanishing determinants," *IEEE Transactions on Information Theory*, vol. 51, no. 4, pp. 1432–1436, April 2005.

[47] P. Dayal and M. K. Varanasi, "An Optimal Two-Transmit Antenna Space-Time Code and its Stacked Extensions," *IEEE Transactions on Information Theory*, vol. 51, no. 12, pp. 4348–4355, Dec. 2005.

[48] Yao and G.W. Wornell, "Achieving the full MIMO diversity-multiplexing frontier with rotation-based space-time codes," *41st Allerton Conf. Commun., Control and Computing, Monticello, IL.*

[49] F. Oggier, G. Rekaya, J.-C. Belfiore, and E. Viterbo, "Perfect Space-Time Block Codes," *IEEE Transactions on Information Theory*, vol. 52, no. 9, pp. 3885–3902, April 2005.

[50] B. Hassibi and B.M. Hochwald, "High-rate codes that are linear in space and time," *IEEE Transactions on Information Theory*, vol. 48, no. 7, pp. 1804–1824, July 2002.

[51] J.J. Boutros, E. Calvanese Strinati, and A. Guillén i Fàbregas, "Analysis of coding on non-ergodic block-fading channels," *43nd Allerton Conference on Communications, Control and Computing, Monticello, IL*, September 2005.

[52] J.J. Boutros, E. Calvanese Strinati, and A. Guillén i Fàbregas, "Turbo code design for block fading channels," *42nd Allerton Conference on Communications, Control and Computing, Monticello, IL*, September 2004.

[53] J.J. Boutros, F. Boixadera, and C. Lamy, "Bit-interleaved coded modulations for multiple-input multiple-output channels," *IEEE International Symposium on Spread Spectrum Techniques and Applications*, 2000.

[54] E. Biglieri, *Coding for Wireless Channels*, Springer, 2005.

[55] N. Gresset, J.J. Boutros, and L. Brunel, "Optimal linear precoding for BICM over MIMO channels," *IEEE International Symposium on Information Theory*, 2004.

[56] P.J. Smith and M. Shafi, "On a Gaussian approximation to the capacity of wireless MIMO systems," *IEEE International Conference on Communications*, 2002.

[57] O. Tirkkonen, A. Boariu, and A. Hottinen, "Minimal non-orthogonality rate 1 space-time block code for 3+ Tx antennas," *IEEE Sixth International Symposium on Spread Spectrum Techniques and Applications*, vol. 2, 2000.

[58] J. J. Boutros and G. Caire, "Iterative multiuser joint decoding: unified framework and asymptotic analysis," *IEEE Transactions on Information Theory*, vol. 48, pp. 1772–1793, July 2002.

[59] "Double-STTD scheme for HSDPA systems with four transmit antennas: Link Level Simulation Results," *TSGR1-20(01)-0458, TSG-RAN Working Group 1 meeting no. 20*, May 21-25, 2001, Busan, Korea.

[60] C. Berrou and A. Glavieux, "Near Shannon limit error-correcting coding and decoding: Turbo-codes.," *IEEE Transactions on Information Theory*, vol. 44, no. 6, pp. 2619–2692, October 1996.

[61] S. Benedetto and G. Montorsi, "Unveiling turbo codes: some results on parallel concatenated coding schemes," *IEEE Transactions on Information Theory*, vol. 42, no. 2, pp. 409–428, March 1996.

[62] L.C. Perez, J. Seghers, and D.J. Costello Jr, "A distance spectrum interpretation of turbo codes," *IEEE Transactions on Information Theory*, vol. 42, no. 6 Part 1, pp. 1698–1709, 1996.

[63] J.J. Boutros, A. Guillén i Fàbregas, E. Biglieri, and G. Zemor, "Design and analysis of low-density parity-check codes for block-fading channels," *Information Theory and Applications Workshop, UCSD, California.*

[64] E.C. van der Meulen, "Three-terminal communication channels," *Adv. Appl. Prob*, vol. 3, pp. 120–154, 1971.

[65] T. Cover and A. El Gamal, "Capacity theorems for the relay channel," *IEEE Transactions on Information Theory*, vol. 25, no. 5, pp. 572–584, 1979.

[66] A. Sendonaris, E. Erkip, and B. Aazhang, "User cooperation diversity. Part I. System description," *IEEE Transactions on Communications*, vol. 51, no. 11, pp. 1927–1938, November 2003.

[67] A. Sendonaris, E. Erkip, and B. Aazhang, "User cooperation diversity. Part II. Implementation aspects and performance analysis," *IEEE Transactions on Communications*, vol. 51, no. 11, pp. 1939–1948, November 2003.

[68] L. Zheng and D.N.C. Tse, "Diversity and multiplexing: a fundamental tradeoff in multiple-antenna channels," *IEEE Transactions on Information Theory*, vol. 49, no. 5, pp. 1073–1096, 2003.

[69] J.N. Laneman, D.N. Tse, and G.W. Wornell, "Cooperative diversity in wireless networks: Efficient protocols and outage behavior," *IEEE Transactions on Information Theory*, vol. 50, no. 12, pp. 3062–3080, December 2004.

[70] R.U. Nabar, H. Bolcskei, and F.W. Kneubuhler, "Fading relay channels: performance limits and space-time signal design," *IEEE Journal on Selected Areas in Communications*, vol. 22, no. 6, pp. 1099–1109, August 2004.

[71] K. Azarian, H. El Gamal, and P. Schniter, "On the achievable diversity-multiplexing tradeoff in half-duplex cooperative channels," *IEEE Transactions on Information Theory*, vol. 51, no. 12, pp. 4152–4172, December 2005.

[72] S. Yang and J.-C. Belfiore, "Towards the Optimal Amplify-and-Forward Cooperative Diversity Scheme," *Arxiv preprint cs.IT/0603123*, 2006.

[73] Y. Jing and B. Hassibi, "Distributed space-time coding in wireless relay networks-Part I: basic diversity results," *IEEE Transactions Wireless Communications*, 2005.

[74] Y. Ding, J.-K. Zhang, and K. M. Wong, "The amplify-and-forward half-duplex cooperative system: pairwise error probability and precoder design," *IEEE Transactions on Signal Processing*, vol. 55, no. 2, pp. 605–617, Feb. 2007.

[75] G.S. Rajan and B.S. Rajan, "A Non-orthogonal distributed space-time protocol, Part-I: Signal model and design criteria," *IEEE International Workshop on Information Theory, Chengdu, China*, pp. 22–26, October 2006.

[76] G.S. Rajan and B.S. Rajan, "A Non-orthogonal distributed space-time protocol, Part-II: Code construction and DM-G Tradeoff," *IEEE International Workshop in Information Theory, Chengdu, China*, pp. 488–492, October 2006.

[77] S. Yang and J.-C. Belfiore, "Optimal space-time codes for the MIMO amplify-and-forward cooperative channel," *Arxiv preprint cs.IT/0509006*, 2005.

[78] J.N. Laneman and G.W. Wornell, "Distributed space-time-coded protocols for exploiting cooperative diversity in wireless networks," *IEEE Transactions on Information Theory*, vol. 49, no. 10, pp. 2415–2425, October 2003.

[79] M. Yuksel and E. Erkip, "Cooperative Wireless Systems: A Diversity-Multiplexing Tradeoff Perspective," *Arxiv preprint cs.IT/0609122*, 2006.

[80] B. Zhao and M.C. Valenti, "Cooperative diversity using distributed turbo codes," *Virginia Tech Symposium on Wireless Personal Communications, Blacksburg, VA*, June 2003.

[81] Z. Zhang and T.M. Duman, "Capacity-approaching turbo coding and iterative decoding for relay channels," *IEEE Transactions on Communications*, vol. 53, no. 11, pp. 1895–1905, 2005.

[82] A. Chakrabarti, E. Erkip, A. Sabharwal, and B. Aazhang, "Code Designs for Cooperative Communication," .

[83] S. Yang and J.-C. Belfiore, "On Slotted Amplify-and-Forward Cooperative Diversity Schemes," *IEEE International Symposium on Information Theory, Seattle, WA*.

[84] S. Yang and J.-C. Belfiore, "Optimal Space-Time Codes for the Amplify-and-Forward Cooperative Channel," *43rd Allerton Conf. Commun., Control and Computing, Monticello, IL*.

[85] N. Gresset, J.J. Boutros, and L. Brunel, "Linear precoding under iterative processing for multiple antenna channels," *IEEE International Symposium on Control, Communications and Signal Processing*, 2004.

[86] J.J. Boutros, A. Guillén i Fàbregas, E. Biglieri, and G. Zemor, "Low-Density Parity-Check Codes for Nonergodic Block-Fading Channels," *submitted to the IEEE Trans. Inf. Theory, October 2007*, revised Nov. 2009.

[87] A. Guillén i Fàbregas, "Coding in the Block-Erasure Channel," *IEEE Transactions on Information Theory*, vol. 52, no. 11, pp. 5116–5121, 2006.

[88] J.J. Boutros, G. Caire, E. Viterbo, H. Sawaya, and S. Vialle, "Turbo code at 0.03 dB from capacity limit," *IEEE International Symposium on Information Theory ISIT, 2002*, p. 56.

[89] C. Berrou, A. Glavieux, and P. Thitimajshima, "Near Shannon limit error-correcting coding and decoding: Turbo-codes.," *IEEE International Conference on Communications, 1993, Geneva*, vol. May, 1993.

[90] S. Benedetto, G. Montorsi, D. Divsalar, and Pollara F., "Soft-input soft-output modules for the construction and distributed iterative decoding of code networks," *European Transactions on Telecommunications*, vol. 9, March-April 1998.

[91] Loeliger H.A., "New turbo like codes," *IEEE Int. Symp. on Inf. Theory, Ulm*, June-July 1997.

[92] B. Frey and MacKay D., "Irregular turbo codes," *Proc. 37th Allerton Conference, Illinois*, September 1999.

[93] T.J. Richardson, M.A. Shokrollahi, and R.L. Urbanke, "Design of capacity-approaching irregular low-density parity-check codes," *IEEE Transactions on Information Theory*, vol. 47, no. 2, pp. 619–637, 2001.

[94] M.G. Luby, M. Mitzenmacher, M.A. Shokrollahi, and D.A. Spielman, "Improved low-density parity-check codes using irregular graphs," *IEEE Transactions on Information Theory*, vol. 47, no. 2, pp. 585–598, 2001.

[95] G.M. Kraidy and V. Savin, "Capacity-approaching irregular turbo codes for the binary erasure channel," *IEEE Trans. Comm.*, to appear.

[96] T. Richardson and R. Urbanke, *Modern coding theory*, Cambridge University Press, 2008.

[97] F. Jelinek J. Raviv L. Bahl, J. Cocke, "Optimal decoding of linear codes for minimizing symbol error rate," *IEEE Transactions on Information Theory*, vol. 20, no. 2, pp. 284–287, March 1974.

[98] S.Y. Chung, G.D. Forney Jr, T.J. Richardson, and R. Urbanke, "On the design of low-density parity-check codes within 0.0045 dB ofthe Shannon limit," *IEEE Communications Letters*, vol. 5, no. 2, pp. 58–60, 2001.

[99] H. Jin and T. Richardson, "Block error iterative decoding capacity for LDPC codes," *Proc IEEE Int. Symp. Inf. Theory*, pp. 52–56, 2005.

[100] H. Jin, A. Khandekar, and R. McEliece, "Irregular repeat-accumulate codes," *Proc. 2nd Int. Symp. Turbo Codes and Related Topics*, pp. 1–8, 2000.